AFT Impulse™

Verification Cases

AFT Impulse Version 10

Waterhammer Modeling in Piping Systems

Published: October 24, 2023

Applied Flow Technology

Dynamic solutions for a fluid world ™

Contents

AFT Impulse Verification Overview

There are a number of aspects to the verification process employed by Applied Flow Technology to ensure that AFT Impulse provides accurate solutions to waterhammer and surge transient problems in pipe flow systems. These are discussed in Verification Methodology. A listing of all of the verified models is given in Summary of Verification Models. The verification models are taken from numerous References.

Verification References

1. Brown, R.J., Water-Column Separation at Two Pumping Plants, Journal of Basic Engineering, 1968
2. Chaudhry, M. Hanif, Ph.D., Applied Hydraulic Transients, 3rd Ed., 2014, Springer
3. Karney, Bryan W and McInnis, Duncan, Efficient Calculation of Transient flow in Simple Pipe Networks, 1992, Journal of Hydraulic Engineering, Vol. 118, No. 7, No. 26648, July
4. Karney, Bryan W and McInnis, Duncan, Transient Analysis of Water Distribution Systems, Journal AWWA, July 1990, pp. 62-70
5. Kamemura, Toshihiko, et. al., Fluid Transients in Pipeline, 1988, Nippon Kokan Technical Report Overseas, No. 52, pp. 42-49
6. Kaplan M., Streeter V., and Wylie E.B., Oil Pipeline Transients, The University of Michigan, Industry Program of the College of Engineering, August 1966, IP-743
7. Liou, Jim C. P., Understanding Line Packing in Frictional Water Hammer, ASME, Journal of Fluids Engineering, August 2016, Vol. 138
8. Parmakian, John, Waterhammer Analysis, Dover Publishing, 1963
9. Watters, Gary Z., PE, Modern analysis and Control of Unsteady Flow in Pipelines, 1979, Ann Arbor Science
10. Wylie, E. Benjamin, Fluid Transients in Systems, 1993, Prentice-Hall

Verification Reference - Brown Cover Page

List of All Verification Models

R. J. BROWN
General Engineer,
Technical Engineering Analysis
Branch, Bureau of Reclamation,
Denver, Colo.

Water-Column Separation at Two Pumping Plants

Results of field measurement of transients in two pump discharge lines show that the pressures were greater than had been predicted during design, and a theory and method of analysis are developed which explains the time-history of the transients measured. The field measurements were undertaken because of the complexity of the phenomena and because very little measured data were available. Results are presented graphically along with analytical solutions. Conclusions drawn were: (a) The inherent difficulty of prediction of water-column separation effects is further complicated by the uncertainty about complete pump operating characteristics and actual moment of inertia of pumps and motors; (b) the effects of air and gases entrained in solution in the water must be considered in the analytical solution; and (c) entrained air can have a detrimental effect on the water-hammer transient, i.e., larger pressure surges in the discharge line and higher reverse speeds of the pumps can be caused by its presence.

Introduction

An important consideration in the design of a pump discharge line is the possible occurrence of water-column separation during a water-hammer transient. Following a power outage at the pumping units, negative pressure waves will be propagated throughout the discharge line. Water-column separation will appear when the transient hydraulic gradient drops to the vapor pressure of water at any point in the line. These phenomena can be visualized as two individual water columns separated by a vapor pocket at the low pressure point. In general, the water-hammer pressure created when the two liquid water columns rejoin is of a destructive nature, being very large in magnitude.

In 1946, the Bureau of Reclamation designed Mile 7.2 and Mile 22.5 Pumping Plants [1][1] with the knowledge that water-column separation would occur during operation of the systems. These pumping plants were selected as ideal trial cases because both of the discharge lines had distinct "knees" in their profiles, and, therefore, the exact locations of the points of separation were predetermined. Water-column separation is a complicated phenomenon and after the pumping plants were built, the accuracy and completeness of the theory used to predict the transient pressures were questioned.

To check the theoretical approach, field tests were performed and pressure-time histories were recorded at various test stations on the line. In general, the measured transient pressures were greater than had been predicted.

In the following sections, the original design for water-column separation in the pump discharge lines will be reviewed. The results of the recorded pressure-time histories from the field tests will be explained and presented in graphical forms. A modified theoretical approach devised to more accurately predict the phenomena will be discussed.

Original Design Criteria

The original methods used in designing the discharge line for water-hammer pressures will be briefly outlined. The basic data for both systems are listed in Table 1 and Fig. 1. The water-column separation criteria have been described [2, 3] but a brief résumé of that subject is in order. Basically, the analytic procedure was a graphical solution on a pump char-

[1] Numbers in brackets designate References at end of paper.

Contributed by the Fluids Engineering Division and presented at the Fluids Engineering Conference, Philadelphia, Pa., May 6–9, 1968, of The American Society of Mechanical Engineers. Manuscript received at ASME Headquarters, February 15, 1968. Paper No. 68—FE-23.

Nomenclature

A = cross-sectional area of the pipeline, ft²
a = velocity of pressure wave, ft/sec
C = total volume of air and entrained gases, at an absolute pressure head of 34 ft, in the discharge line, ft³
$\bar{C}$ = air volume/inner volume of discharge pipe
C_i = air volume at gas pocket at location i, ft³
D = inside diameter of pipeline, ft
f = Darcy's friction factor
H = head between hydraulic grade line and forebay elevation, ft
H_0 = head across the unit, ft
H_{Li} = head from forebay elevation to absolute zero pressure head level for the gas at location i, ft
H_{ui} = head from forebay elevation to an upper effective pressure head level at gas pocket location i, ft
H_P = pumping head, ft
H_R = rated head, ft
$h = \frac{H_P}{H_R}$
L = length of discharge line, ft
L_i = length of line between gas pocket locations, ft
N = speed of unit, rpm
N_R = rated speed of unit, rpm
N_s = specific speed of unit, gpm units
Q = discharge at a point in the pipeline, cfs
Q_R = rated discharge, cfs
q = discharge/rated discharge
T = torque on the unit, lb-ft
t = time, sec
V = velocity at a point in the pipeline, fps
V_R = rated velocity, fps
$v = V/V_R$
WR^2 = flywheel effect of the rotating parts of the pump and motor, lb-ft²
α = speed of unit/rated speed
β = torque on unit/rated torque
$\rho = \frac{aV_R}{2g\,H_R}$ = pipeline constant

Verification Reference - Chaudhry Cover Page

List of All Verification Models

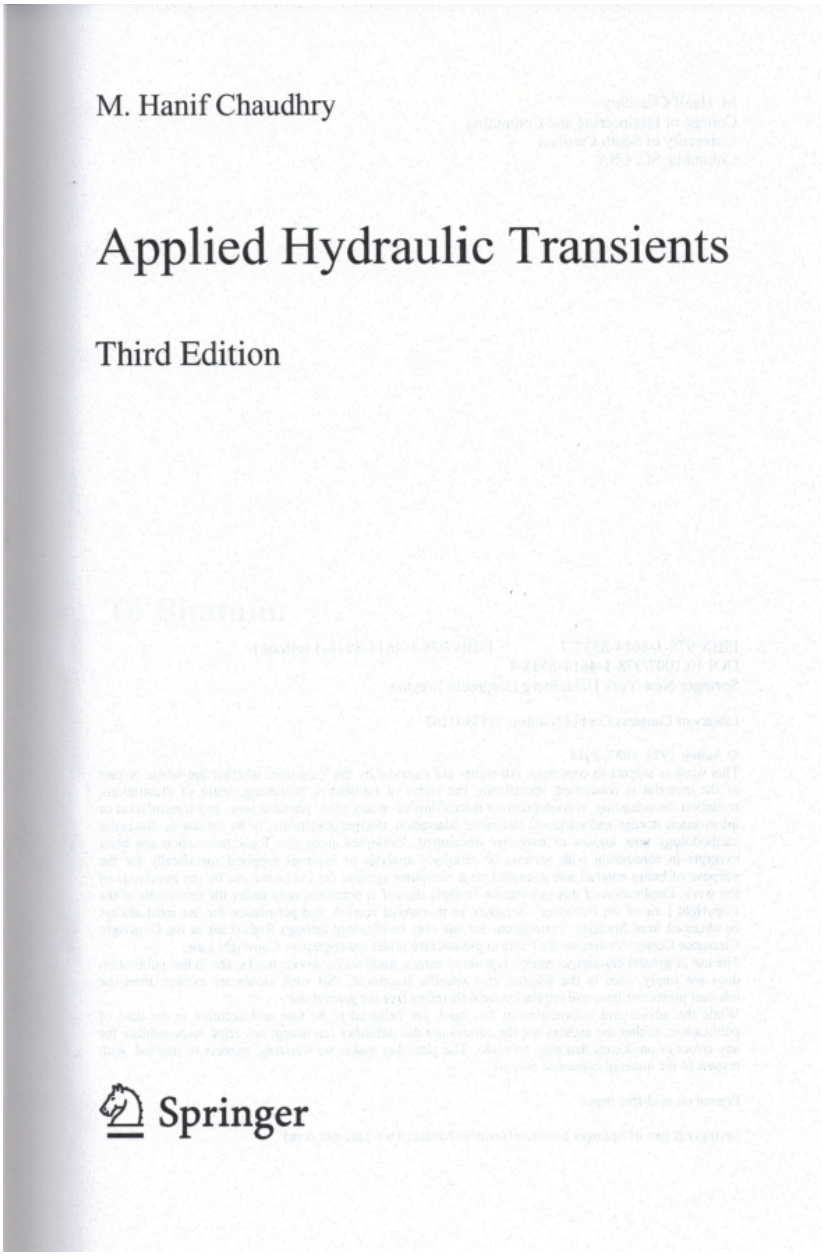

M. Hanif Chaudhry
College of Engineering and Computing
University of South Carolina
Columbia, SC, USA

ISBN 978-1-4614-8537-7 ISBN 978-1-4614-8538-4 (eBook)
DOI 10.1007/978-1-4614-8538-4

Verification Reference - Kamemura Cover Page

List of All Verification Models

NIPPON KOKAN TECHNICAL REPORT
Overseas No. 52 (1988)

Fluid Transients in Pipeline

—Liquid Column Separation and Development of Comprehensive Program—

Toshihiko Kamemura*, Kazuo Jyowo**,
Teruhiko Hata***, Hideo Hayashi****,
Tatsuki Yoshikai***** and Munetaka Kondo******

NKK has developed a computer program, SURGE 2, to simulate transient phenomena in liquid pipeline. SURGE 2 can analyze any piping systems, however complicated they may be. Furthermore this program can simulate liquid column separation. For numerical analysis, the characteristics method which is introduced air release method is adopted. Liquid column separation experiments were conducted using 15.2mm in diameter and 200m long test pipeline. Experimental data were compared with calculated results to find out good agreement in respect to change of flow rate and pressure.

1. Introduction

In planning and designing a pipeline, fluid transients phenomena cause problems of significant engineering concern especially in two aspects. The first problem is the high and low pressure caused by the transients phenomena. High pressure brings about destructive damage to pipes and devices, while low pressure causes cavitation, resulting in various troubles such as breakdown of pumps and others. Liquid column separation phenomenon resulting from low pressure also brings about destructive high pressure with the collapse of vapor cavity. The second problem is the effect of fluid transients phenomena to various control systems and conversely, the effect of control systems to the pipeline system.

In recent years, as a result of active pursuit of safety and total efficiency of plants and pipelines, the piping system is becoming complicated. In a complicated piping system, adverse effects from fluid transients phenomena frequently occur, the effects spreading to many directions. Under these circumstances, in 1974, NKK developed SURGE 1, a computer program to simulate fluid transients phenomena. Since then, SURGE 1 has been applied to analysis of fluid transportation in many pipelines and has demonstrated its power. However, SURGE 1 had problems; that it could not analyze liquid column separation phenomenon, influence of trapped air in pipe, and transients phenomena of looped piping. Also, it could not deal with equipment such as surge tanks, air valves and others.

Consequently, a comprehensive program, SURGE 2, to analyze the above phenomena was completed in 1986, after three years of development. The feature of SURGE 2 is that it can calculate both the steady and unsteady flow problems of the piping system, however complicated they may be, and also analyze liquid column separation phenomenon. In addition, experiments were conducted on a 15.2mm diameter, 200m length test pipeline, the results of which were compared with analytic results to examine the reliability of the program.

In this paper, the analytic theory, function, and experimental verification of SURGE 2 are presented.

2. Analytic theory

2.1 Steady flow calculation

Various reports have been made for solution of steady flow piping network, but in SURGE 2, Newton-Raphson's solution was adopted in view of its applicability under diverse conditions.

A piping network is modeled with flow paths and joints. Section points, branch and confluence points, and boundary points of piping are treated as the joints, and connecting these joints are the flow paths. A flow path consists of pipes, valves, and pumps.

Generally, the relationship between pressure, P, and the flow rate, Q, are expressed as:

* Manager, Pipeline Design Sec., Engineering & Design Dept.
** Team Manager, Pipeline Design Sec., Engineering & Design Dept.
*** Pipeline Design Sec., Engineering & Design Dept.
**** General Manager, No. 1 Research Dept., Kawasaki Research Labs., Engineering Research Center
***** Manager, Information Systems Dept.
****** Manager, Pipeline Inspection Services

Verification Reference - Kaplan Cover Page

List of All Verification Models

THE UNIVERSITY OF MICHIGAN

INDUSTRY PROGRAM OF THE COLLEGE OF ENGINEERING

OIL PIPELINE TRANSIENTS

Michel Kaplan
Victor L. Streeter
E. Benjamin Wylie

August, 1966

IP-743

Verification Reference - Karney Cover Page - Efficient Calculation...

List of All Verification Models

.SHE '92 July Vol 118 #7

EFFICIENT CALCULATION OF TRANSIENT FLOW IN SIMPLE PIPE NETWORKS

By Bryan W. Karney[1] and Duncan McInnis[2]

ABSTRACT: Extensions to the conventional method of characteristics allow transient conditions in simple pipe networks to be efficiently calculated. In particular, treating both boundary conditions and network topology in a general and comprehensive fashion simplifies the solution of many combinations of hydraulic devices. The algebraic framework presented includes a flexible integration of the friction loss term that reduces to previous linear approximations as special cases. In addition, an explicit algorithm is derived for a general hydraulic element called an external energy dissipator. This boundary condition conveniently represents surge tanks, relief valves, storage reservoirs, valves discharging to the atmosphere, and many other common devices. Significantly, the solution remains explicit even if friction losses and inertia effects are present in both the storage element and a connecting pipe. This comprehensive approach to transient analysis simplifies control logic, encourages accurate reporting of field data, and improves execution times. The procedure is illustrated by analyzing transient conditions in a small network containing a variety of devices.

INTRODUCTION

Although water distribution networks have existed for hundreds of years, transients have not always been explicitly considered in design calculations. Early networks were fed by gravity from high-elevation reservoirs or water towers, and nearly steady conditions prevailed in the system. In addition, the number, length, and diameter of pipes were typically small and pressures low. The most significant problem was to predict the equilibrium distribution of flow under assumed demand conditions. Thus, the lack of attention given to transient considerations in these networks was usually well-justified.

Modern water distribution systems, by contrast, are usually fed by numerous pumping stations discharging directly into the system. In addition, flow disturbances are common. The automatic stopping of pumps, the adjustment of control valves and the influence of accidential events, such as power outages, all generate transient conditions. These disturbances are superimposed on a network that has large pipes and high discharge rates. The result is a highly dynamic system that should be analyzed as such (Sharp 1981; Karney and McInnis 1990).

This paper is intended to facilitate calculation of transient conditions in pipe networks. Although a general algebraic and conceptual framework applicable to any network is presented, special attention is given to combinations of simple devices. No attempt is made to treat all boundary conditions comprehensively (an impossible task in a single paper). Rather, the purpose is to show how significant gains in efficiency and accuracy can be achieved for a class of boundary conditions called external energy dissipators. An explicit equation is presented for this composite storage element that accounts for losses in a short conduit connecting a reservoir to a j .tio of any number of pipes. Such a solution is useful in itself and serves as model for solving more complex boundary conditions. The versatility ar efficiency of the approach are demonstrated by analyzing a small test ne work.

[1]Asst. Prof., Dept. of Civ. Engrg., Univ. of Toronto, M5S 1A4, Canada.
[2]Grad. Student, Dept. of Civ. Engrg., Univ. of Toronto, Toronto, M5S 1A4, Canada.

Note. Discussion open until December 1, 1992. To extend the closing date one month, a written request must be filed with the ASCE Manager of Journals. The manuscript for this paper was submitted for review and possible publication on May 23, 1990. This paper is part of the *Journal of Hydraulic Engineering*, Vol. 118, No. 7, July, 1992. ©ASCE, ISSN 0733-9429/92/0007-1014/$1.00 + $.15 per page. Paper No. 26648.

GOVERNING EQUATIONS AND THEIR SOLUTION

This section extends the conventional method of characteristics for ne work applications. The key result is a linear equation that accounts for ar number of interacting pipes at a network node. Although a similar relatic is developed in Wylie and Streeter (1982), the equation developed here algebracially simpler while being computationally more flexible, particular in relation to the linearization of the friction term.

Two equations, a momentum equation and a relation of mass conse vation, are used to model transient flow in closed conduits [e.g., Chaudh (1987), Wylie and Streeter (1982)]. If x is distance long the centerline the conduit, t is time, and partial derivatives are represented as subscript these equations can be written as

$$V_t + gH_x + \frac{f_p V|V|}{2D_p} = 0 \quad \ldots\ldots (1)$$

$$H_t + \frac{a^2}{g} V_x = 0 \quad \ldots\ldots (2)$$

in which $H = H(x,t)$ = piezometric head; $V = V(x,t)$ = fluid velocity; D = inside pipe diameter; f_p = Darcy-Weisbach friction factor; a = celerity of the shock wave; and g = acceleration due to gravity. To be compatible x and V must be positive in the same direction. Eqs. (1) and (2) are valid if the flow is one-dimensional, the conduit properties (diameter, wave speed temperature, etc.) are constant, the convective and slope terms are small and the friction force can be approximated by the Darcy-Weisbach formula for steady flow. In addition, it is usually assumed that the friction factor is either constant or weakly dependent on Reynolds number.

The popular method of characteristics (MOC) is a simple and numerically efficient way of solving the unsteady flow equations (Wylie and Streeter 1982; Chaudhry 1987). In essence, the MOC combines the momentum and continuity expressions to form the following compatibility equation in discharge Q and head H:

$$dH \pm B\, dQ \pm \frac{R}{\Delta x} Q|Q|\, dx = 0 \quad \ldots\ldots (3)$$

in which A_p = cross-sectional area of the pipe; $B = a/gA_p$; and $R = f_p\Delta x/2gD_pA_p^2$. Eq. (3) is valid only along the so-called C^+ and C^- characteristic lines defined by $dx/dt = \pm a$. To satisfy these characteristic relations, the x-t grid is usually chosen to ensure $\Delta x = \pm a\Delta t$ (see Fig. 1).

Once initial conditions and the space-time grid have been specified, (can be integrated along AP and BP in Fig. 1. Although the first two term are easily computed, the third integral requires the variation of Q with to be known. In practice, the flow component has usually been approximate as either $Q_A|Q_A|$ or $Q_P|Q_A|$ (Wylie 1983; Wylie and Streeter 1982; Chaudh

Verification Reference - Karney Cover Page - Transient Analysis...

List of All Verification Models

Transient Analysis of Water Distribution Systems

Bryan W. Karney and Duncan McInnis

The pressures generated by transient (water hammer) conditions in pipe systems are frequently three or more times the value of normal operating pressures. Thus, transient pressures must be known if the size and strength of the required pipe is to be rationally selected, if surge-suppression equipment is to be logically sized, and if system operating rules are to be intelligently specified. In practice, however, analysts frequently neglect transient conditions, particularly in complex systems such as distribution networks. With modern computer techniques it is possible to analyze distribution systems under a wide range of flow conditions and with relatively few restrictions. Examples are presented of the dangers of oversimplifying either the physical system or the operating conditions.

Pressure pipe systems are subject to a wide range of physical loads and operational requirements. For example, underground piping systems must withstand internal and external corrosion, various forms of bedding stresses, differential settlement, construction damage, local stresses at connections, as well as other external and internal forces. As a result of this ongoing chemical and physical attack, both the hydraulic and structural capacities of the pipe are reduced over time until some kind of failure occurs. The failure may be physical in nature, such as a break that causes loss of water and pressure, or it may be economic, arising from increased fluid friction with its associated reduced flow capacity, increased power costs, or both. In Canada alone, the estimated cost of repairing water main breaks exceeds Can$100 million annually.

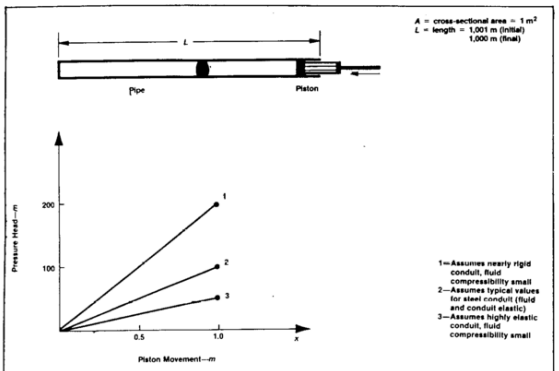

Figure 1. Relation between fluid compressibility and pressure head in a closed conduit

One source of loading that is commonly neglected in water distribution system analysis is due to water hammer or transient conditions. Although it is well known that the pressures generated during transient conditions should be an important consideration when simple pipeline systems are being designed, there is widespread belief that transient conditions are intrinsically less severe in network applications. In fact, several examples in this article demonstrate that the maximum transient pressure in some branched and looped systems may exceed the corresponding pressure rise in a simple system. Thus, if the size and strength of the required pipe are to be rationally selected, if the surge-suppression equipment is to be logically sized, and if system operating rules are to be intelligently specified, reliable transient analysis is essential.

One source of loading commonly neglected in system analysis is due to water hammer or transient conditions.

In the past few years, many refinements and improvements have been made in the accuracy and efficiency of transient analysis. More attention, however, has frequently been given to how the analysis is performed than to what is being modeled. Many articles have been written on the relative accuracy and computational merits of various numerical procedures; few have considered the sensitivity of transient conditions to the assumed initial state or what kind of interaction between automatic control

Verification Reference - Liou Cover Page

List of All Verification Models

Understanding Line Packing in Frictional Water Hammer

Jim C. P. Liou
Mem. ASME
Department of Civil Engineering,
University of Idaho,
Moscow, ID 83844-1022
e-mail: liou@uidaho.edu

For valve closure transients in pipelines, friction attenuates the amplitude of water hammer wave fronts and causes line packing. The latter is a sustained head increase behind the wave front. Line packing can lead to overpressure. Because of the nonlinearity of the friction term in the governing equations of water hammer, a satisfactory analytical explanation of line packing is not available. Although numerical methods can be used to compute line packing, an analytical explanation is desirable to better understand the phenomenon. This paper explains line packing analytically and presents a formula to compute the line packing that leads to the maximum pressure at the closed valve.
[DOI: 10.1115/1.4033368]

Introduction

In pipeline transients, frictional resistance to flow generates line packing, which is a sustained pressure rise in the pipeline behind the water hammer wave front after the closure of a discharge valve. This phenomenon is of interest to cross-country oil pipelines and long water transmission mains because the sustained pressure rise can be very significant relative to the initial sudden pressure rise by water hammer and can result in unacceptable overpressures.

For a highly frictional pipeline, where the length is large and/or the diameter is small, the effective closure time of a discharge valve is much shorter than its physical closure time [1]. For such pipelines, line packing can be analyzed in terms of an instantaneous closure of a discharge valve. Figures 1 and 2 contrast the valve closure transients with and without friction.

Depicted in Fig. 1 is the water hammer without friction, with H_U = head at the reservoir end, H_V = head at the valve end, V_0 = steady-state discharge velocity, V = velocity immediately behind the wave front, a = wave speed, t = time, and dt = a time increment. The head and velocity profiles at t (solid lines) and $t + dt$ (dotted lines) are indicated. The profiles represent the head and velocity waves of water hammer. The initial hydraulic grade line is horizontal. The head rise at the closed valve propagates upstream unattenuated. The velocity behind the head wave is stopped completely. Before the waves are reflected back to the valve, the head at the closed valve remains constant and equals the reservoir head plus the head rise due to stopping the initial velocity.

Depicted in Fig. 2 is the water hammer with friction. In this figure, L = pipe length and x = distance measured from the reservoir toward the valve. The head wave attenuates as it travels upstream. The velocity is not stopped fully by passage of the head wave. There is a sustained head rise behind the wave front as more and more fluid is packed into the closed end. If the wave front is sufficiently attenuated, the head at the closed valve will rise over time almost monotonically toward H_U. If the attenuation is less, the head wave reflected from the reservoir will reverse the head rise at the closed valve $2L/a$ s after the valve closure. For the latter case, the peak head at the closed end at $2L/a$ s may significantly exceed H_U. This peak pressure, hereafter referred to as line packing, is addressed in this paper.

In fluid mechanics and hydraulics textbooks that discuss water hammer, the friction effect is either not addressed or only briefly mentioned about the extent of its damping effect [2,3, for example]. To the knowledge of the author, the only exception is Ref. [4], which gives an approximation formula for line packing. Phenomenological explanations of attenuation and line packing are found in textbooks on water hammer [5,6]. Because friction influences water hammer in a complicated way, quantification of the phenomenon is accomplished through numerical solution of the governing equations in academic research, and through commercial software in practice.

In the early literature on water hammer, the friction factor of the initial steady-state flow was used during transient flow. This simple approach was discussed and improved upon with unsteady friction in a large body of literature from 1968 [7] to present [8–10]. Several studies [10–13] contain comparisons between results of steady and unsteady friction models and the assessment

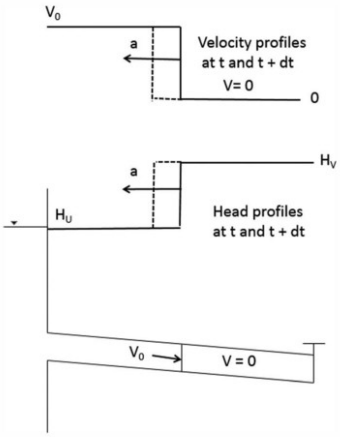

Fig. 1 Head and velocity profiles at two instants in a frictionless pipe

Contributed by the Fluids Engineering Division of ASME for publication in the JOURNAL OF FLUIDS ENGINEERING. Manuscript received November 10, 2015; final manuscript received March 21, 2016; published online June 8, 2016. Assoc. Editor: Praveen Ramaprabhu.

Verification Reference - Parmakian Cover Page

List of All Verification Models

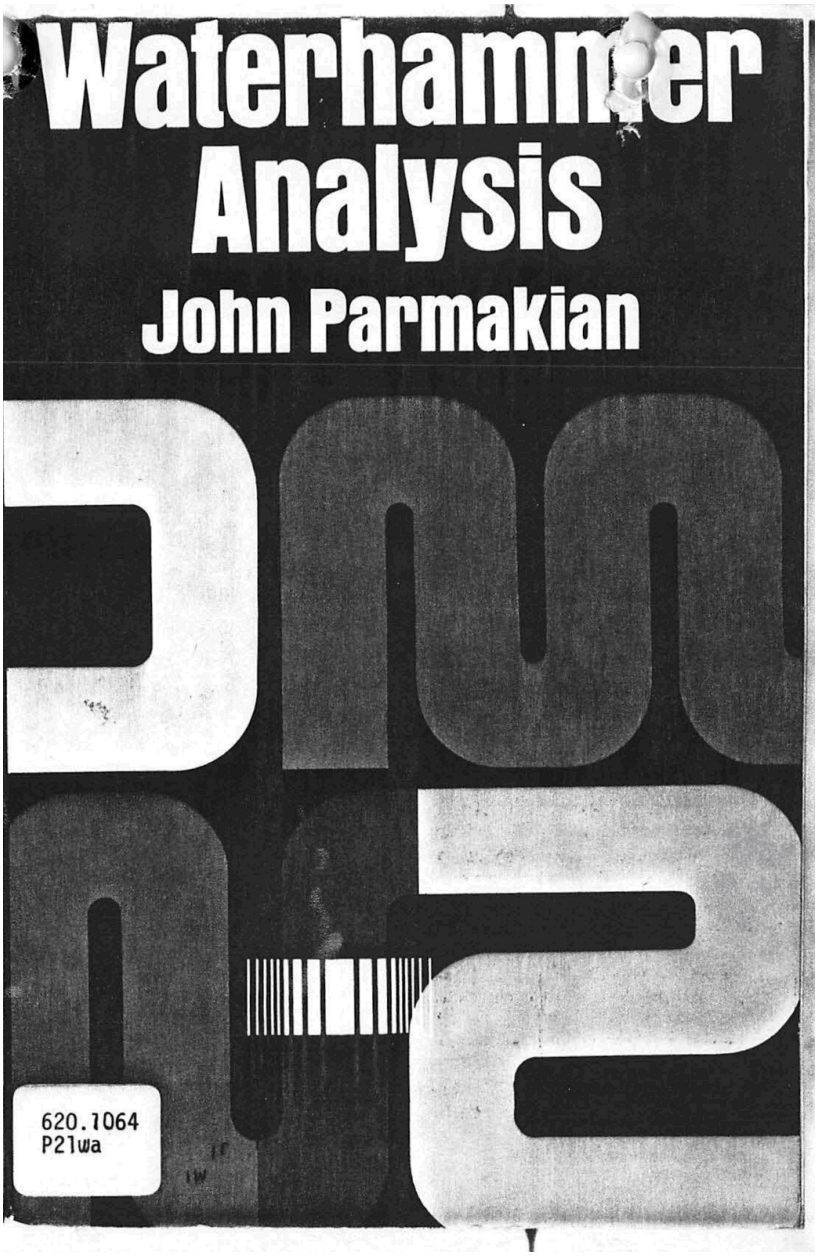
Waterhammer
Analysis
John Parmakian
620.1064
P21wa

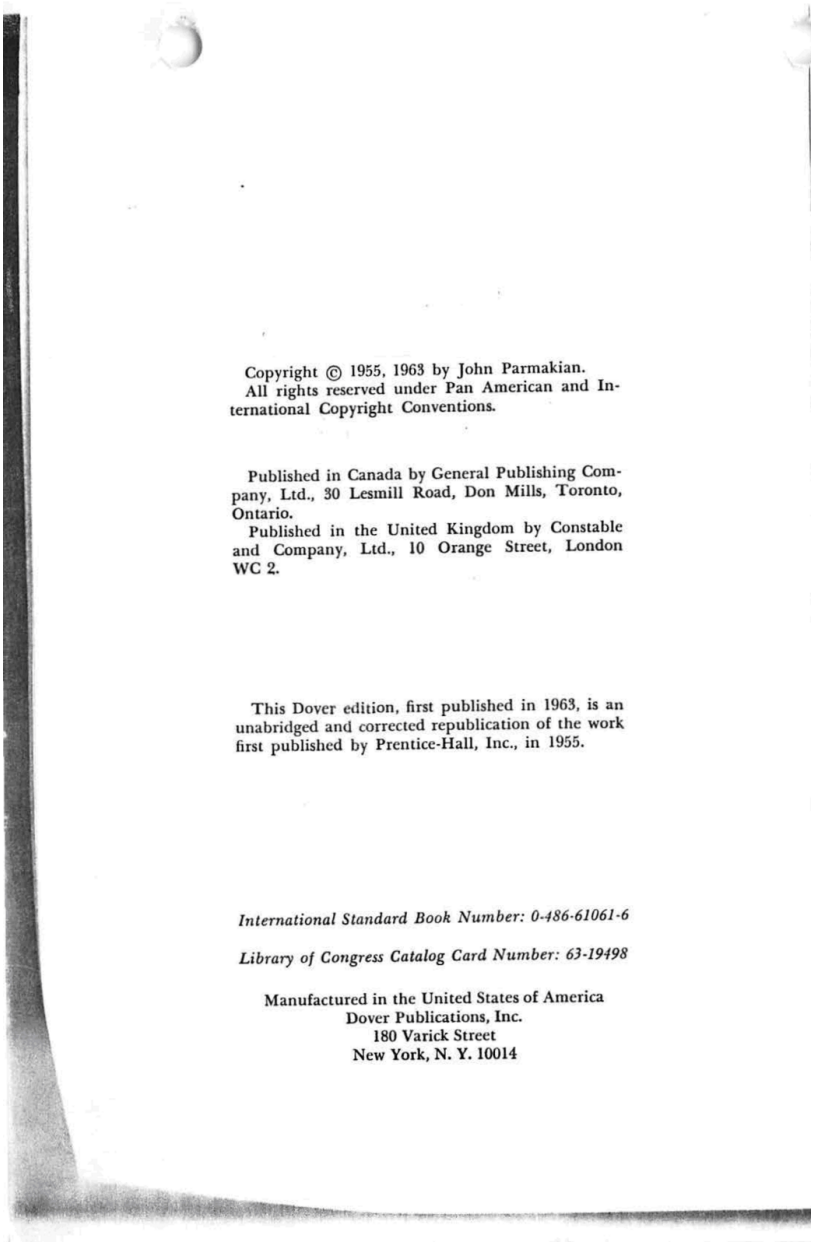

Published in Canada by General Publishing Company, Ltd., 30 Lesmill Road, Don Mills, Toronto, Ontario.
Published in the United Kingdom by Constable and Company, Ltd., 10 Orange Street, London WC 2.

This Dover edition, first published in 1963, is an unabridged and corrected republication of the work first published by Prentice-Hall, Inc., in 1955.

International Standard Book Number: 0-486-61061-6

Library of Congress Catalog Card Number: 63-19498

Manufactured in the United States of America
Dover Publications, Inc.
180 Varick Street
New York, N. Y. 10014

Verification Reference - Watters Cover Page

List of All Verification Models

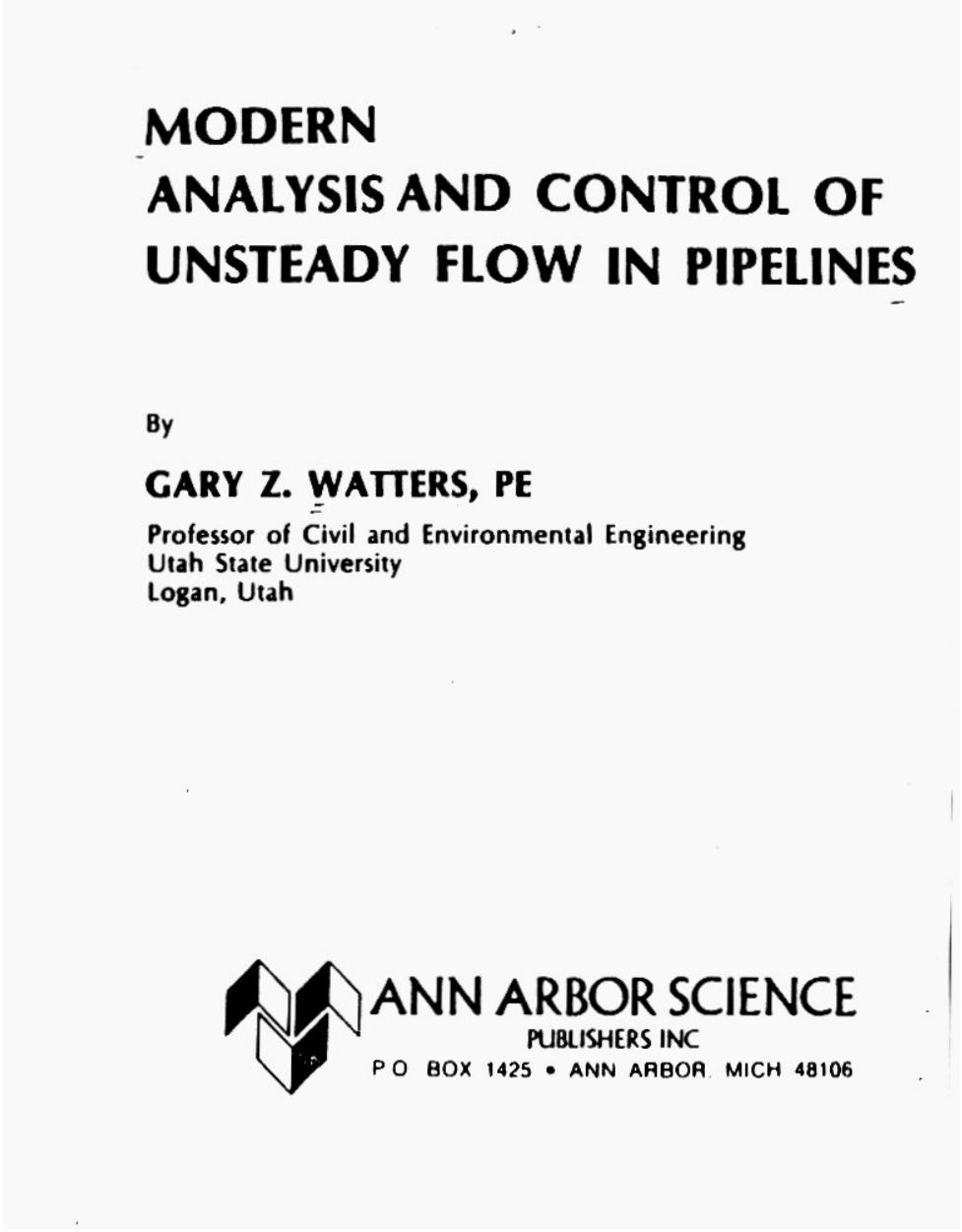

MODERN
ANALYSIS AND CONTROL OF
UNSTEADY FLOW IN PIPELINES

By

GARY Z. WATTERS, PE

Professor of Civil and Environmental Engineering
Utah State University
Logan, Utah

ANN ARBOR SCIENCE
PUBLISHERS INC
P O BOX 1425 • ANN ARBOR MICH 48106

Verification Reference - Wylie Cover Page

List of All Verification Models

Fluid Transients in Systems

by

E. Benjamin Wylie

Professor of Civil and Environmental Engineering
University of Michigan

and

Victor L. Streeter

Professor Emeritus of Hydraulics
University of Michigan

with

Lisheng Suo

Associate Professor of Hydropower Engineering
Hohai University; Nanjing, China

PRENTICE HALL, Englewood Cliffs, NJ 07632

Verification Methodology

The *AFT Impulse* software is a waterhammer and surge transient analysis product intended for use by trained engineers. As a technical software package, issues of quality and reliability of the technical data generated by the software are important. The following description summarizes the steps taken by Applied Flow Technology to ensure the high quality of the technical data.

1. Comparisons with open literature examples

Numerous examples of waterhammer and surge transient analysis in pipe flow systems are available in the open literature which include published results. AFT Impulse results have been compared against many open literature systems. AFT Impulse predictions compare favorably in all cases.

2. Transient solver checks for artificial transient to ensure true steady initial conditions

Before running the transient solution, AFT Impulse always runs the transient solver for a single time step with no transient boundary conditions in effect. It then compares the initial conditions to the single step calculation to see if significant differences exist. If so, a warning is generated.

3. Steady-state and transient solution at time zero are self checking

AFT Impulse has two Solvers – one for the steady-state and one for the transient. They use two entirely different solution algorithms. First the steady-state state solver is run, and then the results are used to initialize the transient solver. Before the transient solver is actually run, a sanity check is performed (as discussed in Item 2 above). If the two solvers disagree, a warning is generated. Thus is if there were fundamental calculation errors in either method then an artificial transient would be generated and the user warned. This does not ensure all transient calculations afterwards are correct, but does ensure that the fundamental transient equations are being properly represented.

Summary of Verification Models

Comparison of AFT Impulse predictions to the published calculation results is included herein for twenty-two cases from ten sources.

Below is a summary of the cases:

Case	Fluid	Pipes	Pumps	Reference
Case 1	Water	1	0	Wylie
Case 2	Water	2	0	Wylie
Case 3	Water	2	1	Chaudhry
Case 4	Water	1	0	Wylie
Case 5	Water	1	0	Wylie
Case 6	Water	1	0	Wylie
Case 7	Water	1	0	Wylie
Case 8	Water	1	0	Wylie
Case 9	Water	1	0	Wylie
Case 10	Water	1	0	Wylie
Case 11	Water	8	0	Karney (1992)
Case 12	Water	8	0	Karney (1992)
Case 13	Water	2	1	Watters
Case 14	Water	2	1	Wylie
Case 15	Water	5	0	Kamemura
Case 16	S.G. 1.155	1	1	Parmakian
Case 17	Water	3	1	Watters
Case 18	Water	1	0	Chaudhry
Case 19	Oil	1	0	Kaplan
Case 20	Water	2	0	Karney (1990)
Case 21	Water	7	0	Karney (1990)
Case 22	Oil	2	0	Liou

Verification Case 1

View Model Problem Statement

PRODUCT: AFT Impulse

TITLE: ImpVerify1.imp

REFERENCE: Fluid Transients in Systems, 1993, Prentice-Hall, E. Benjamin Wylie, Victor L. Streeter, Page 46, Example 3.1

FLUID: Water

ASSUMPTIONS: N/A

RESULTS:

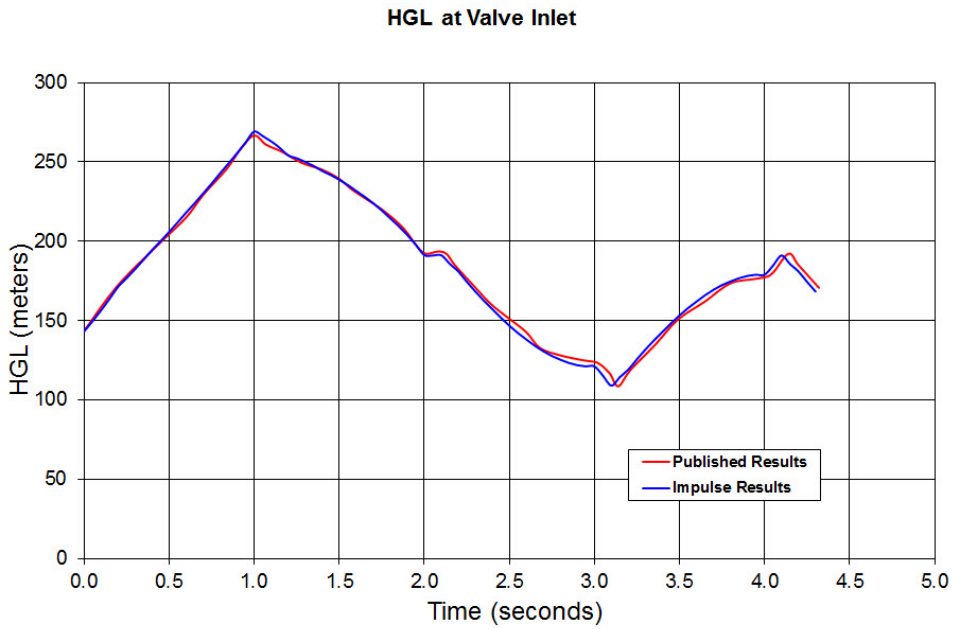

DISCUSSION:

The results from AFT Impulse are compared to a simulation run by Wiley. Full details of the problem statement can be seen by clicking the link above. Close agreement can be observed in the results.

List of All Verification Models

Verification Case 1 Problem Statement

Verification Case 1

Fluid Transients in Systems, 1993, Prentice-Hall, E. Benjamin Wylie, Victor L. Streeter, Page 46, Example 3.1

Wylie's Title Page

3-4 Single-pipeline Applications

The procedure to solve a transient fluid flow problem numerically involves a number of repetitious calculations. A computer program to solve a problem involving a single pipe leading from a reservoir to a valve (Fig. 3-4) has the following elements:

1. Read in values of data that describe the system and the character of the particular transient.
2. Calculate constants and initial steady-state conditions, and store initial values of Q_i and H_i for $t = 0$.
3. Print out values of Q_i and H_i at each section, plus printout time and valve opening.
4. Increment time by $2\Delta t$, and at intermediate time Δt calculate interior points at even-numbered sections Q_2, H_2 to Q_N, H_N.
5. Calculate interior points at odd-numbered sections Q_3, H_3 to Q_{N-1}, H_{N-1}, and then calculate the boundary values Q_1, H_1, Q_{NS}, and H_{NS}.
6. Transfer back to the print statement (No. 3), or to increment time (No. 4), and check to see if T_{max}, the duration of the transient, has been exceeded. If not, continue with the calculations.

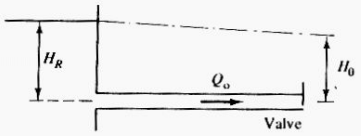

Figure 3-4 Single pipeline.

Example 3-1

The valve closure relationship for the pipeline shown in Fig. 3-4 is given by the equation

$$\tau = \tau_i - (\tau_i - \tau_f)\left(\frac{t}{t_c}\right)^{E_m}$$

in which t_c is the time of operation, τ_i the initial value of valve opening, and τ_f the final value. The steady-state open position of the valve is defined by a value of $(C_d A_G)_0$ in Eq. (3-35). The initial valve opening may be zero or any positive number, in this case $\tau_i = 1$. The input data for the problem are: $L = 600$ m, $a = 1200$ m/s, $D = 0.5$ m, $f = 0.018$, $H_R = 150$ m, $t_c = 2.1$ s, $\tau_i = 1$, $\tau_f = 0$, $T_{max} = 4.3$ s, $E_m = 0.75$, $(C_d A_G)_0 = 0.009$, $g = 9.806$ m/s^2, and $N = 10$.

Figure D-1 in Appendix D presents a FORTRAN listing of a program for use with MS-DOS on a PC to solve for the pressure head and flow response as a result of a specified valve motion. The input data are listed at the end of the program and are read from a separate file named SINGLE.DAT. In addition to all input data listed above, two new parameters are included. These are IPR, a control parameter that controls the number of time increments, $\Delta T = 2\Delta t$, between each printout of calculated results, and IGRAF, a section number at which pressure head data are stored for later graphing if desired.

Steady-state discharge, Q_0, is calculated in the program to balance the pipe friction and valve losses corresponding to $(C_d A_G)_0$ with the energy available in the reservoir. The initial flow, Q_i, for the specific problem is calculated for the given initial valve opening, τ_i.

The computer output is shown in Fig. D-1b, and a graphical display of head at the valve, discharge at the reservoir, and valve opening as a function of time are shown in Fig. 3-5.

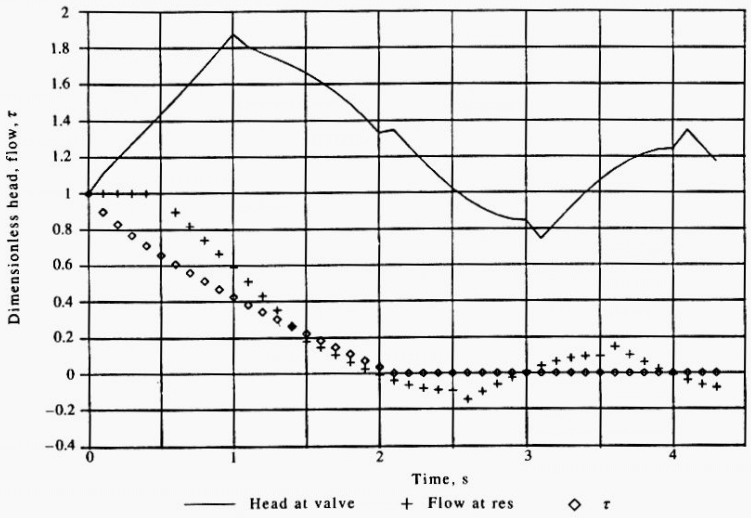

Figure 3-5 Response in single pipeline due to valve closure.

Included in the FORTRAN program is a collection of variables to store transient information to graph if desired. These data are stored in the file attached to device 8. They include the initial pipe profile and hydraulic grade line, transient head profiles along the pipeline at each successive pair of time steps, and a time history of pressure head at section IGRAF. A separate program written in BASIC for the IBM-PC is provided in Fig. D-2, Appendix D, to read and graph these data with IBM GRAPHICS. It is a fairly primitive and simple graphics package and is provided only as a useful tool to examine transient results, not as an exposition of recommended graphic displays. The same program, called GRAF, will be available for use by other programs in this book.

Example 3-2

Consider a single horizontal pipeline as shown in Fig. 3-4 with the valve closed at the downstream end. Assume that a series of sinusoidal waves passes over the reservoir

View Verification Case 1 Model

Verification Case 1

Valve Downstream of Reservoir, Wylie, Pg 46, Example 3.1

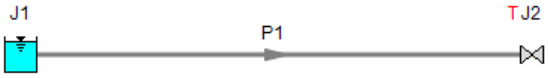

Verification Case 2

View Model Problem Statement

PRODUCT: AFT Impulse

TITLE: ImpVerify2.imp

REFERENCE: Fluid Transients in Systems, 1993, Prentice-Hall, E. Benjamin Wylie, Victor L. Streeter, Page 121

FLUID: Water

ASSUMPTIONS: N/A

RESULTS:

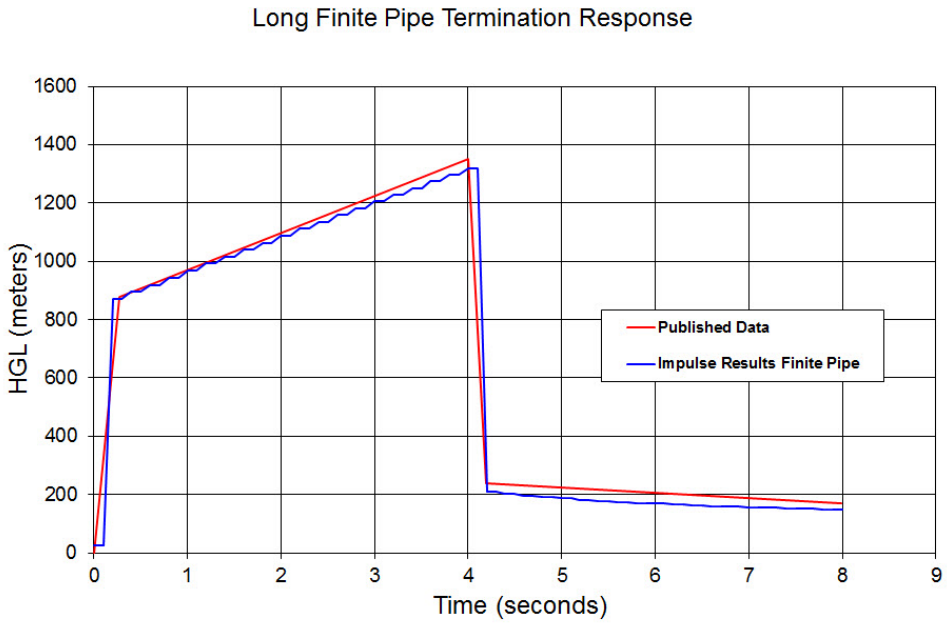

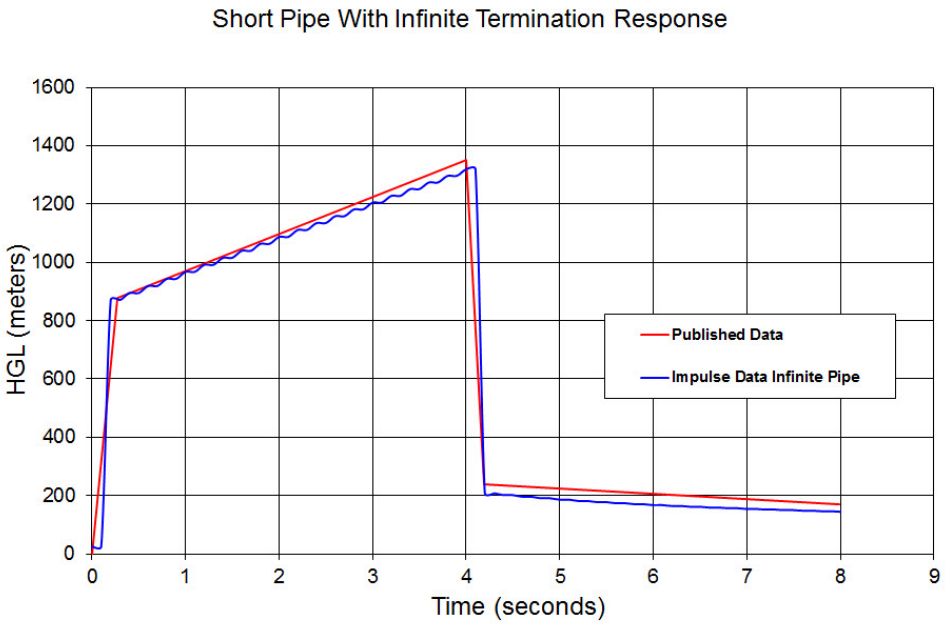

DISCUSSION:

A long pipeline is modeled using two methods, one where the full length of the pipe is modeled, and one where two sections of the pipe are modeled with the infinite pipe method applied. It can be seen in the two graphs above that similar to Wylie, AFT Impulse gives nearly identical results for the pipe with each of the methods applied. As noted by Wylie, the infinite pipe feature can only be used up to the time when a reflection would return from the end of the pipeline.

List of All Verification Models

Verification Case 2 Problem Statement

Verification Case 2

Fluid Transients in Systems, 1993, Prentice-Hall, E. Benjamin Wylie, Victor L. Streeter, Page 121

Wylie Title Page

6-2 Infinite Pipeline

In a long pipeline system the analyst may be interested in the transient details locally and not in the long-term behavior of the extended system. Under these conditions it is helpful to use an alternative model,[16] but one that will respond similarly to the long pipe. This substitute element, which is to respond like the long pipe, is useful only up until a reflection would return from the other extremity of the long pipe (i.e., until $2L/a$ seconds), where L and a refer to the actual long line.

Conceptually, the characteristic impedance of the pipeline should provide the desired termination. However, the impedance B in the relationship $\Delta H = \pm B\Delta Q$ is valid only for frictionless systems. Figure 6-8 provides a sketch in which the desired termination would be located at point U, two distance intervals upstream from the exciter in the system. For illustration purposes a valve has been used for the exciter in this high-friction system, although it could be a pump or any other dynamic element.

Inasmuch as the only reflections in the system are from the friction gradient, any disturbances created at the exciter, point D, pass upstream only. Therefore, values of the variables at point I (Fig. 6-8), are extrapolated along a characteristic line beyond the modeled pipe termination one Δx. Although a linear extrapolation produces reasonable results, second order is better and is recommended:

$$H_I = 3H_1 - 3H_2 + H_3 \qquad Q_I = 3Q_1 - 3Q_2 + Q_3 \tag{6-11}$$

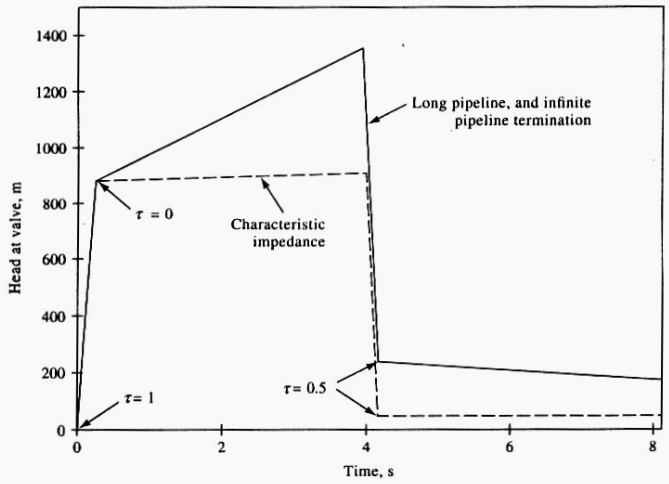

Figure 6-9 Infinite pipe termination response.

With values of the variables at point I available, a standard C^+ compatibility equation can be used, and a typical interior point calculation can be performed at section i.

Figure 6-9 shows results from an example with a rapid valve closure at $t = 0.2$ s and rapid opening to $\tau = 0.5$ at $t = 4.2$ s in the pipe in Fig. 6-8. The data are $L = 4800$ m, $D = 0.2$ m, $f = 0.018$, $a = 1200$ m/s, $Q_0 = 0.210$ m^3/s, $H_0 = 27.88$ m, $N = 40$. Three different results at the valve are shown in Fig. 6-9: the actual values from the long pipe simulation, the values with the infinite pipe model as described above, and the values from use of the characteristic impedance termination. The latter two terminations were located at point U, 240 m upstream from the valve.

This represents a high-friction system, $f\,\Delta x\,Q_0/2DAa = 0.03$, and it is seen that the results from the infinite pipe termination are indistinguishable in the sketch. The largest discrepancy, of approximately 2.9 m, occurred at the end of the simulation. For slower transients or lower-friction cases the results would be considerably better. Use of the pipeline impedance, although perfect in the frictionless case, is seen to be unacceptable in this high-friction rapid transient.

View Verification Case 2 Model

Verification Case 2

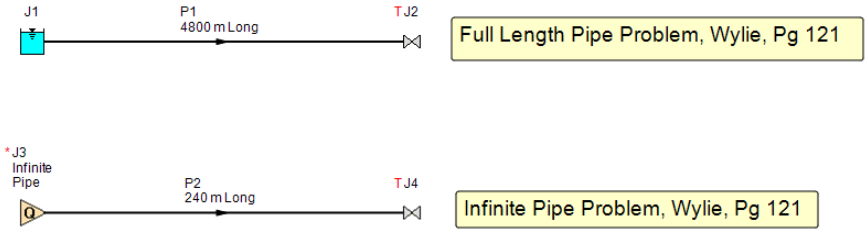

Verification Case 3

View Model Problem Statement

PRODUCT: AFT Impulse

TITLE:ImpVerify3.imp

REFERENCE: M. H. Chaudhry, *Applied Hydraulic Transients*, 3rd ed. Springer, pp. 131, 535-543.

FLUID: Water

ASSUMPTIONS: N/A

RESULTS:

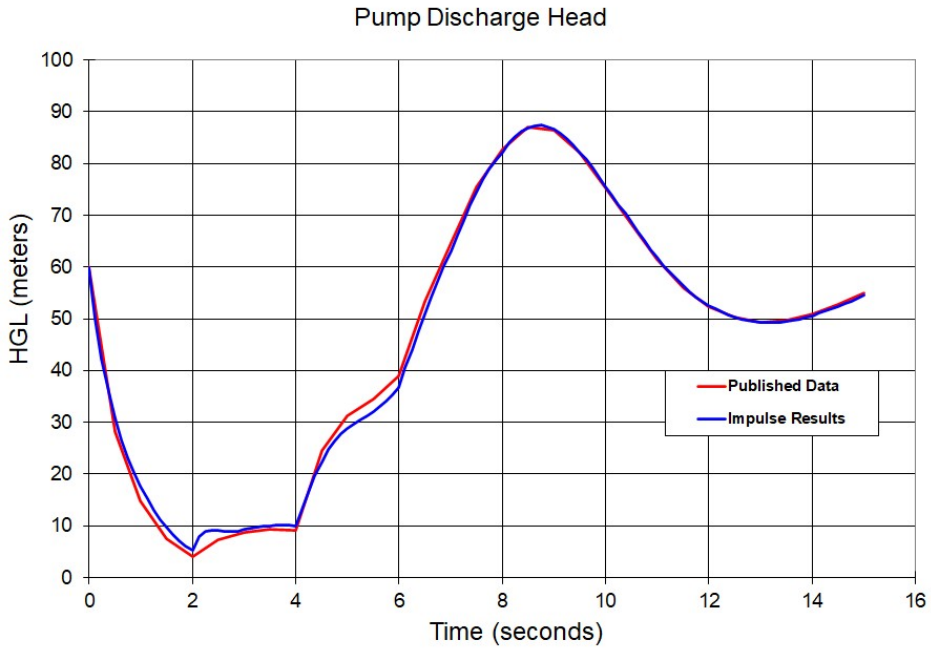

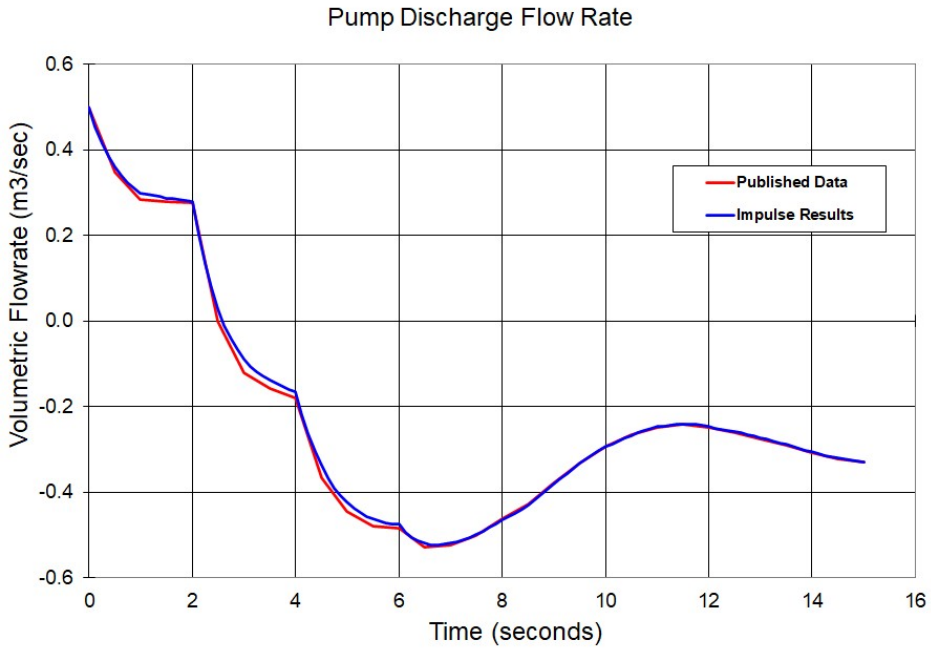

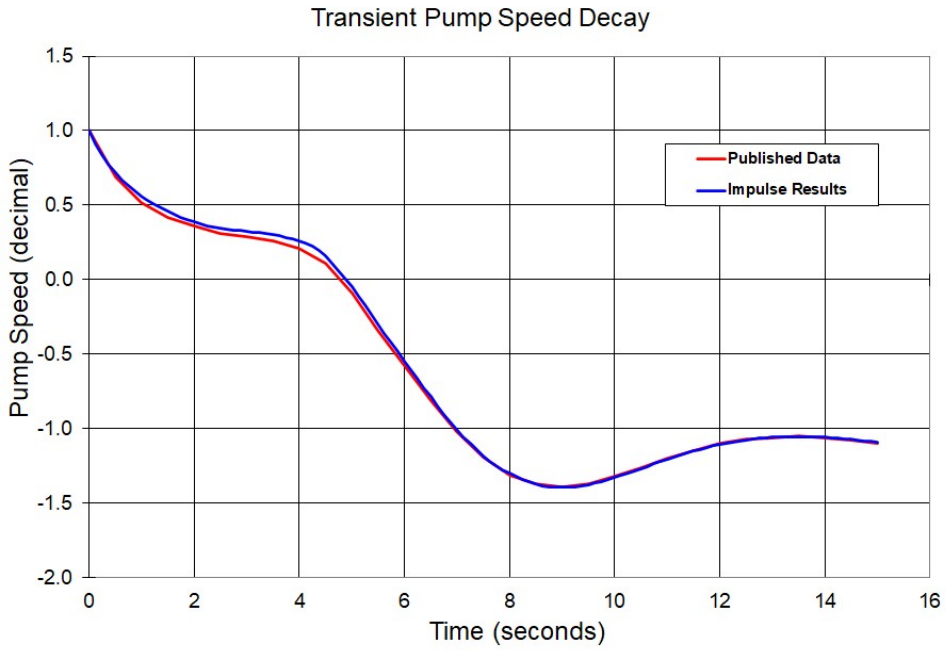

DISCUSSION:

The results from AFT Impulse are compared to a simulation run by Chaudhry. Full details of the problem statement can be seen by clicking the link above. Close agreement can be observed in the results.

List of All Verification Models

Verification Case 3 Problem Statement

Verification Case 3

M. H. Chaudhry, *Applied Hydraulic Transients*, 3rd ed. Springer, pp. 131, 535-543.

Chaudhry Title Page


```
      VE=VE+DV
      IF (ABS(DV).LE.0.001.AND.ABS(DALPHA).LE.0.001) GO TO 50
      IF (JJ.GT.30) GO TO 70
      GO TO 8
50    TH=ATAN2(ALPHAE,VE)
      TH=57.296*TH
      IF (TH.LT.0.0) TH=TH+360.
      CALL PARAB(TH,2,BETA)
      MB=TH/DTH+1
      BETA= BETA * (ALPHA*ALPHA+V*V)
      IF (MB.EQ.M) GO TO 60
      GO TO 8
60    DALPHA=ALPHAE-ALPHA
      DV=VE-V
      ALPHA=ALPHAE
      V=VE
      RETURN
70    Write(2,80) T,ALPHAE,VE
80    FORMAT(8X,'***ITERATIONS IN PUMP SUBROUTINE FAILED'/8X,'T=',F8.2
     2/8X,'ALPHAE =',F6.3/8X,'VP =',F6.3)
      STOP
      END
      SUBROUTINE PARAB(X,J,Z)
      COMMON /PAR/FH,FB,DX
      DIMENSION FH(60),FB(60)
      I=X/DX
      R=(X-I*DX)/DX
      IF(I.EQ.0) R=R-1.
      I=I+1
      IF(I.LT.2) I=2
      GO TO (10,20) ,J
10    Z=FH(I)+0.5*R*(FH(I+1)-FH(I-1)+R*(FH(I+1)+FH(I-1)-2.*FH(I)))
      RETURN
20    Z=FB(I)+0.5*R*(FB(I+1)-FB(I-1)+R*(FB(I+1)+FB(I-1)-2.*FB(I)))
      RETURN
      END
```

C-2 Input Data

```
2,2,2,2,9.81,0.5,1100.0,15.0

55,5.0,0.250,60.0,1100.0,0.84,16.85

-0.53,-0.476,-0.392,-0.291,-0.150,-0.037,0.075,0.200,0.345,

0.500,0.655,0.777,0.9,1.007,1.115,1.188,1.245,1.278,1.290,1.287,

1.269,1.240,1.201,1.162,1.115,1.069,1.025,0.992,0.945,0.908,0.875,

0.848,0.819,0.788,0.755,0.723,0.690,0.656,0.619,0.583,0.555,0.531,

0.510,0.502,0.500,0.505,0.520,0.539,0.565,0.593,0.615,0.634,0.640,

0.638,0.630

-0.350,-0.474,-0.180,-0.062,0.037,0.135,0.228,0.320,0.425,0.500,0.548,

0.588,0.612,0.615,0.600,0.569,0.530,0.479,0.440,0.402,0.373,0.350,0.34,

0.34,0.35,0.38,0.437,0.52,0.605,0.683,0.75,0.802,0.845,0.872,0.883,0.878,

0.86,0.823,0.78,0.725,0.66,0.58,0.49,0.397,0.31,0.23,0.155,0.085,0.018,

-0.052,-0.123,-0.22,-0.348,-0.49,-0.68

450.0,0.75,900.0,0.01

550.0,0.75,1100.0,0.012
```


C-3 Program Output

```
 NUMBER OF PIPES =  2
 NUMBER OF REACHES ON LAST PIPE =  2
 STEADY STATE DISCH. =  .500 M3/S
 STEADY STATE  PUMP SPEED =1100.0 RPM
 TIME FOR WHICH TRANS. STATE COND.  ARE TO BE COMPUTED = 15.0 S
 NUMBER OF PARALLEL PUMPS =  2

 NUMBER OF POINTS ON CHARACTERISTIC CURVE =  55
 THETA INTERVAL FOR STORING CHARACTERISTIC CURVE =  5.
 RATED DISCH. =  .25 M3/S
 RATED HEAD =  60.0 M
 RATED PUMP SPEED =1100.0 RPM
 PUMP EFFICIENCY =  .840
 WR2=  16.85 KG-M2

 POINTS ON HEAD CHARACT. CURVE
   -.530  -.476  -.392  -.291  -.150  -.037   .075   .200   .345
.500
    .655   .777   .900  1.007  1.115  1.188  1.245  1.278  1.290
1.287
   1.269  1.240  1.201  1.162  1.115  1.069  1.025   .992   .945
.908
    .875   .848   .819   .788   .755   .723   .690   .656   .619
.583
    .555   .531   .510   .502   .500   .505   .520   .539   .565
.593
    .615   .634   .640   .638   .630
```

```
      POINTS ON TORQUE CHARACT. CURVE
        -.350  -.474  -.180  -.062   .037   .135   .228   .320   .425
.500
.402     .548   .588   .612   .615   .600   .569   .530   .479   .440
.683     .373   .350   .340   .340   .350   .380   .437   .520   .605
.725     .750   .802   .845   .872   .883   .878   .860   .823   .780
.052     .660   .580   .490   .397   .310   .230   .155   .085   .018 -
        -.123  -.220  -.348  -.490  -.680

  PIPE NO      LENGTH      DIA      WAVE VEL.      FRI  C FACTOR
                 (M)        (M)       (M/S)
     1          450.0       .75       900.0              .010
     2          550.0       .75      1100.0              .012

  PIPE NO      ADJUSTED WAVE VEL
                     (M/S)
     1               900.0
     2              1100.0

  TIME  ALPHA     V     PIPE        HEAD (M)          DISCH. (M3/S)
                        NO.       (1)     (N+1)       (1)      (N+1)

    .0   1.00   1.00     1       60.0     59.6       .500      .500
                          2       59.6     59.0       .500      .500
    .5    .69    .69     1       28.3     59.6       .347      .500
                          2       59.6     59.0       .500      .500
   1.0    .52    .57     1       14.8     24.9       .283      .363
                          2       24.9     59.0       .363      .500
   1.5    .42    .56     1        7.6     10.0       .279      .305
                          2       10.0     59.0       .305      .227
   2.0    .36    .55     1        4.0     36.6       .276      .139
                          2       36.6     59.0       .139      .111
   2.5    .31    .00     1        7.4     47.5      -.002      .066
                          2       47.5     59.0       .066      .050
   3.0    .29   -.24     1        8.7     24.7      -.121     -.085
                          2       24.7     59.0      -.085      .020
   3.5    .26   -.32     1        9.4     15.2      -.159     -.152
                          2       15.2     59.0      -.152     -.221
   4.0    .21   -.36     1        9.2     38.8      -.181     -.300
                          2       38.8     59.0      -.300     -.324
   4.5    .11   -.73     1       24.6     48.0      -.367     -.367
                          2       48.0     59.0      -.367     -.379
   5.0   -.09   -.89     1       31.3     41.4      -.446     -.447
                          2       41.4     59.0      -.447     -.409
   5.5   -.34   -.96     1       34.5     39.6      -.479     -.484
                          2       39.6     59.0      -.484     -.514
   6.0   -.58   -.97     1       39.0     49.6      -.485     -.549
                          2       49.6     59.0      -.549     -.558
   6.5   -.81  -1.06     1       53.3     56.3      -.529     -.566
                          2       56.3     59.0      -.566     -.584
   7.0  -1.02  -1.05     1       64.7     62.0      -.523     -.569
                          2       62.0     59.0      -.569     -.574
   7.5  -1.19  -1.00     1       75.5     67.8      -.502     -.537
                          2       67.8     59.0      -.537     -.554
   8.0  -1.31   -.93     1       82.7     74.0      -.463     -.492
                          2       74.0     59.0      -.492     -.499
   8.5  -1.37   -.86     1       87.1     76.1      -.428     -.430
```



```
                          2       76.1     59.0      -.430     -.431
   9.0  -1.39   -.76     1       86.5     74.9      -.379     -.367
                          2       74.9     59.0      -.367     -.361
   9.5  -1.37   -.66     1       82.1     72.1      -.332     -.308
                          2       72.1     59.0      -.308     -.304
  10.0  -1.32   -.59     1       75.2     68.5      -.293     -.266
                          2       68.5     59.0      -.266     -.256
  10.5  -1.26   -.53     1       68.1     63.7      -.267     -.237
                          2       63.7     59.0      -.237     -.228
  11.0  -1.20   -.50     1       61.4     59.5      -.248     -.226
                          2       59.5     59.0      -.226     -.218
  11.5  -1.15   -.48     1       56.0     56.9      -.242     -.226
                          2       56.9     59.0      -.226     -.223
  12.0  -1.10   -.50     1       52.3     55.2      -.248     -.238
                          2       55.2     59.0      -.238     -.234
  12.5  -1.07   -.52     1       50.3     53.7      -.261     -.254
                          2       53.7     59.0      -.254     -.253
  13.0  -1.06   -.55     1       49.4     53.2      -.275     -.275
                          2       53.2     59.0      -.275     -.275
  13.5  -1.05   -.58     1       49.7     53.7      -.291     -.295
                          2       53.7     59.0      -.295     -.297
  14.0  -1.06   -.62     1       50.9     54.5      -.308     -.314
                          2       54.5     59.0      -.314     -.315
  14.5  -1.08   -.64     1       52.8     55.4      -.322     -.328
                          2       55.4     59.0      -.328     -.331
  15.0  -1.10   -.66     1       54.9     56.6      -.330     -.339
                          2       56.6     59.0      -.339     -.342

  PIPE NO.      MAX. PRESS.      MIN. PRESS.
                    (M)              (M)

     1             87.4              4.0
     2             76.1             10.0
```

View Verification Case 3 Model

Verification Case 3

M. H. Chaudhry, Applied Hydraulic Transients, 3rd ed. Springer, pp. 131, 535-543. Transients Caused by Power Failiure to Pumps.

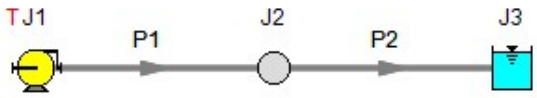

Verification Case 4

View Model Problem Statement

PRODUCT: AFT Impulse

TITLE: ImpVerify4.imp

REFERENCE: Fluid Transients in Systems, 1993, Prentice-Hall, E. Benjamin Wylie, Victor L. Streeter, Page 195, Example 8-5

FLUID: Water

ASSUMPTIONS: Valve is described as “fast closing”. Closing profile is not specified. Impulse model assumes instantaneous closure.

RESULTS:

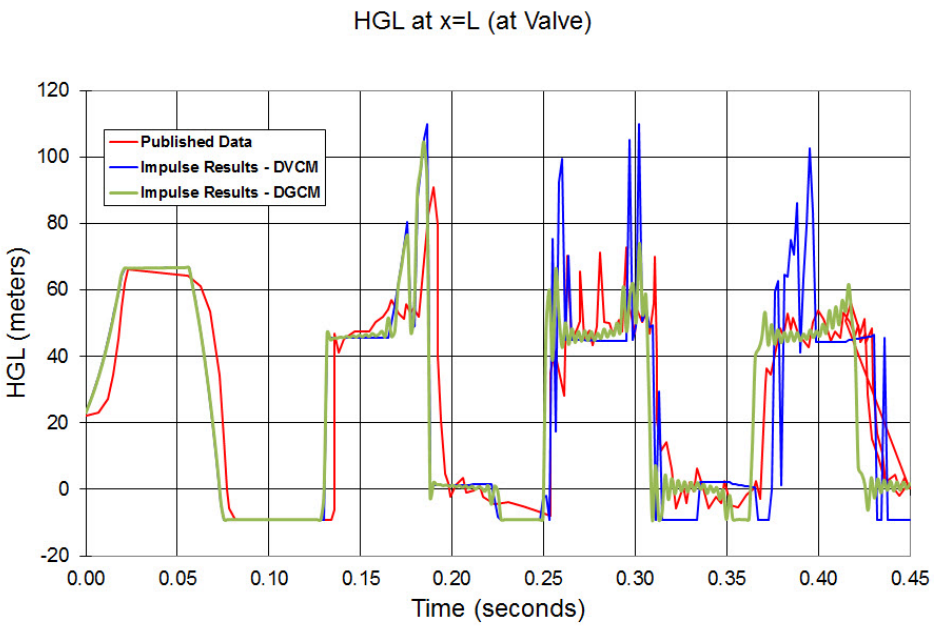

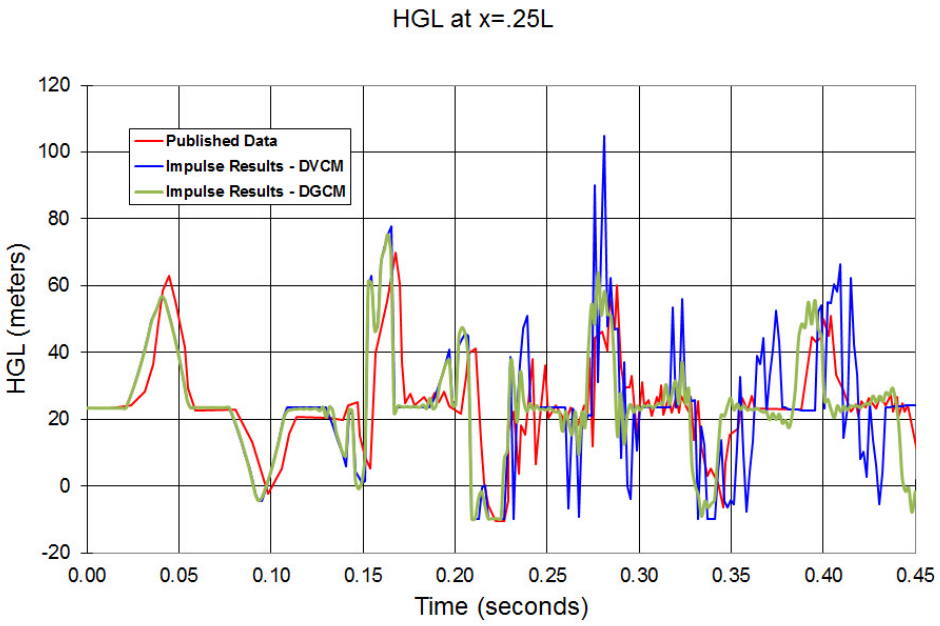

DISCUSSION:

This experiment was designed to cause transient cavitation, and the flow does cavitate. As is common with cavitation modeling the timing of pressure spikes is marginal, but the major features and magnitude of prominent spikes is represented.

List of All Verification Models

Verification Case 4 Problem Statement

Verification Case 4

Fluid Transients in Systems, 1993, Prentice-Hall, E. Benjamin Wylie, Victor L. Streeter, Page 195

Wylie Title Page

cavities at fixed locations, although there may be minor variations in computing results, depending on the number of reaches, upon the manner in which the void space volume is calculated, and so on.[20]

Although the early time transient in this example shows a void space only at the endpoint, it is possible to produce vapor at other positions in the system as a result of intersecting low-pressure waves. This may be illustrated by following case (b) for a few more wave reflections after the first pressure rise. The literature[3,12,13,18,21,22] contains evidence of the physical existence of such intermediate cavities as well as distributed vaporous zones as discussed in the next section.

The main strength of the discrete vapor cavity model in Sec. 3-8 lies in its simplicity. The discrete gas cavity model presented in Sec. 8-2 has also been utilized with some degree of success in analyzing vaporous cavitation problems of this nature, as well as with distributed vaporization, as discussed in the next section.[16,31] By reducing the free-gas content in the discrete gas cavity model, the presence of the free gas is inconsequential until the local pressure drops to a level near vapor pressure. Typically, a void fraction of 10^{-7} at standard atmospheric conditions is used. At this level the wavespeed remains at 99, 96, and 88 percent of the pure liquid wave speed until the pressure drops below 0.2, 0.1, and 0.05 of atmospheric pressure, respectively. In inertially dominated transient events, with forces that would yield large negative pressures if physically permitted, the discrete gas cavity model yields a pressure that converges asymptotically to the actual liquid vapor pressure as the discrete volumes expand. This is in keeping with true physical behavior, where the discrete volumes would be occupied by air and vapor. The next example illustrates the dynamics of an isolated vapor cavity in a single line, by examining results from a physical experiment[19] and by providing a comparison to numerical results from the discrete gas cavity model.

Example 8-5

These data are obtained from an experiment[19] on a 36-m-long 19.05-mm-ID copper tubing. The pipeline had an upward slope of 1 m, with a fast-closing, $\frac{1}{2}$-in. one-quarter-turn ball valve at the downstream end and a constant-pressure tank at the upstream end. Steady-state friction-drop experiments were taken, and for this initial velocity of 0.332 m/s the friction factor was 0.0315. The upstream pressure head was 23.41 m and the vapor pressure is −9.82 m. The measured wavespeed in the liquid-filled pipeline was 1280 m/s.

With the active valve at the downstream end, vaporization occurs at the valve upon return of the rarefaction wave from the reservoir. In this low-velocity (low-friction) case the wave propagates to a higher-pressure region, so vaporization is limited to the valve location, at least until collapse of the first vapor cavity. Figure 8-10 shows experimental results at the valve and at 9 m from the upstream end, and numerical results utilizing the discrete gas cavity model with $\alpha = 10^{-7}$ at standard conditions, $N = 16$, as described in Sec. 8-2.

The experimental results show the peak pressure change following collapse of the vapor cavity to be clearly in excess of aV_0/g. Also, numerical results compare favorably with experimental data.

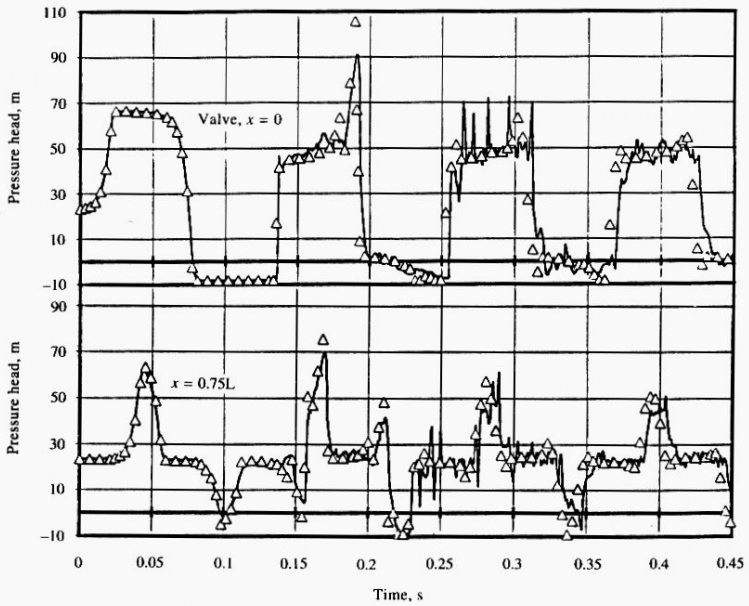

Figure 8-10 Comparison of experimental results (solid line), Simpson,[19] with discrete gas cavity model.

8-5 Mechanics of Distributed Vaporization

A distributed vaporous cavitation region in a liquid-filled pipeline occurs when a rarefaction wave drops the pressure in an extended region of the pipeline to vapor pressure. Inasmuch as the void fraction, α, remains near zero, this regime is distinctly different from isolated column separation, which normally occurs at well-defined sections in a system such as high points, at valves or dead ends, and may also occur at locations in the pipeline where two low-pressure waves traveling in opposite directions intersect. Distributed vaporization is best visualized by examining a numerical example.

Figure 8-11 illustrates a physical system in which the pipeline is sloping upward, 4 m, in the direction of flow. When the initial inflow of 0.4 m/s is stopped at the upstream end, the pressure drops to vapor pressure, but with the upward-sloping pipe, the full-magnitude 25-m wave cannot propagate into the pipeline since the lower limit

View Verification Case 4 Model

Verification Case 4

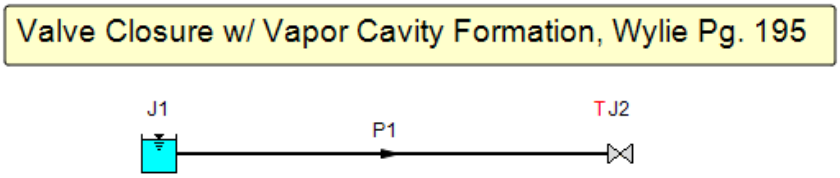

Verification Case 5

View Model Problem Statement

PRODUCT: AFT Impulse

TITLE: ImpVerify5.imp

REFERENCE: Fluid Transients in Systems, 1993, Prentice-Hall, E. Benjamin Wylie, Victor L. Streeter, Page 202, Example 8-6

FLUID: Water

ASSUMPTIONS: N/A

RESULTS:

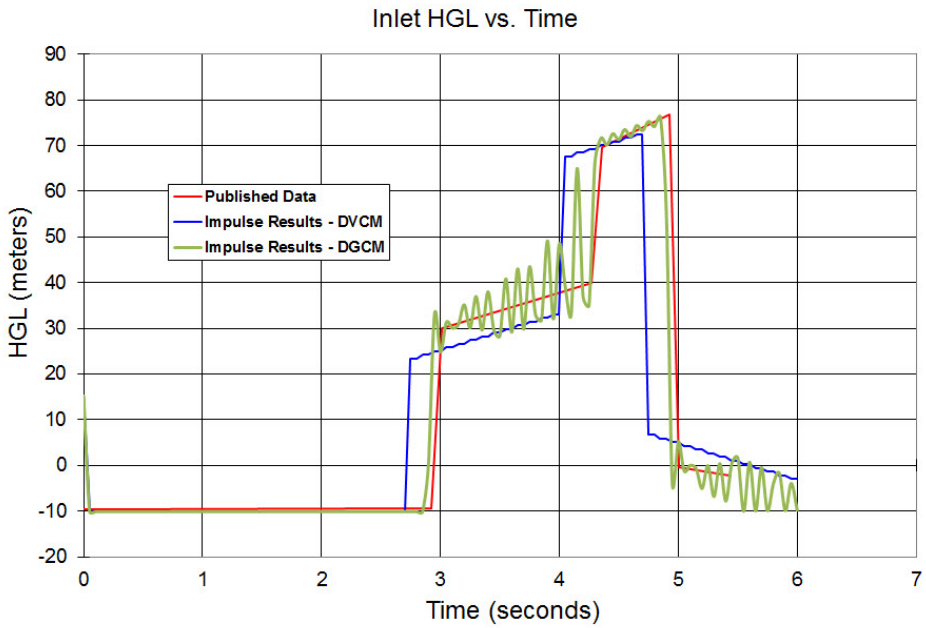

DISCUSSION:

This example was designed to cause transient cavitation, and the flow does cavitate. As is common with cavitation modeling the timing of pressure spikes is marginal, but the major features and magnitude of prominent spikes is represented.

List of All Verification Models

Verification Case 5 Problem Statement

Verification Case 5

Fluid Transients in Systems, 1993, Prentice-Hall, E. Benjamin Wylie, Victor L. Streeter, Page 202, Example 8-6

Wylie Title Page

at 15.0 m, the upstream pipe elevation at zero, and L = 980 m, a = 980 m/s, D = 1.1284 m, f = 0.03, and H_v = −10.0 m. In the discrete gas cavity model $\psi = 1$ and $\alpha = 10^{-7}$ at atmospheric pressure.

Example 8-6

In this case the change in elevation Δz = 4.0 m, and V_0 = 0.4 m/s. Figure 8-14 provides a comparison of the two computational procedures with N = 20. Reasonable agreement exists between the two methods. The vaporous zone is sustained only slightly longer than $2L/a$ seconds (to 2.22 s) in the upstream region of the pipe and the void fraction grows to only about 0.0002 before collapsing. The isolated cavity exists for approximately 2.9 s. It may be noted that the pressure exceeds a maximum of 55 m ($aV_0/g + H_0$).

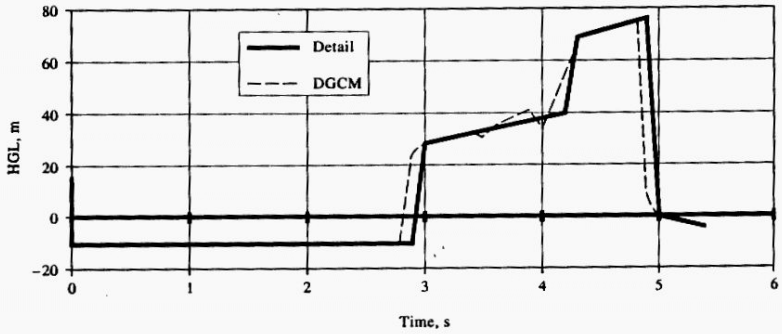

Figure 8-14 Example 8-6, distributed vaporization, V_0 = 0.4 m/s, ΔZ = 4.0 m.

Example 8-7

In this case Δz = 4.0 m and V_0 = 1.56 m/s. Figure 8-15 shows general agreement in results. The vaporous zone is sustained for 2.33 s and the isolated cavity exists until 12.2 s. The pressure rise is approximately what might be expected from stopping the original flow abruptly.

Example 8-8

The rising slope is increased to Δz = 12.0 m, and V_0 = 1.48 m/s. The void fraction reaches 0.001 in the distributed vaporization zone, which lasts until approximately 3.71 s. The isolated cavity lasts until approximately 11.8 s. The pressure trace at the upstream end is shown in Fig. 8-16 for both analyses. Again the agreement in timing is reasonable and the pressure magnitudes are similar.

The detailed modeling, provided in the distributed vapor model, is superior in these examples since it provides a reasonable description of the physical behavior.

View Verification Case 5 Model

Verification Case 5

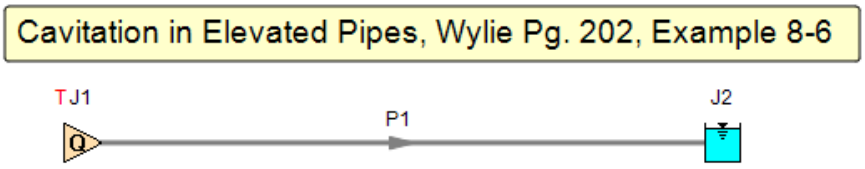

Verification Case 6

View Model Problem Statement

PRODUCT: AFT Impulse

TITLE: ImpVerify6.imp

REFERENCE: Fluid Transients in Systems, 1993, Prentice-Hall, E. Benjamin Wylie, Victor L. Streeter, Page 202, Example 8-7

FLUID: Water

ASSUMPTIONS: N/A

RESULTS:

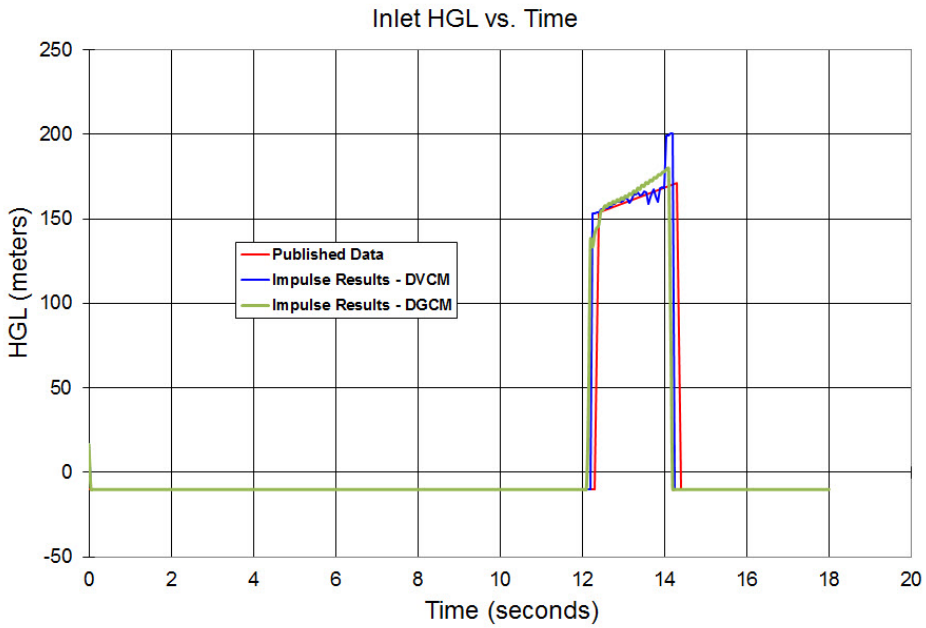

DISCUSSION:

This example was designed to cause transient cavitation, and the flow does cavitate. As is common with cavitation modeling the timing of pressure spikes is marginal, but the major features and magnitude of prominent spikes is represented.

List of All Verification Models

Verification Case 6 Problem Statement

Verification Case 6

Fluid Transients in Systems, 1993, Prentice-Hall, E. Benjamin Wylie, Victor L. Streeter, Page 202, Example 8-7

Wylie Title Page

at 15.0 m, the upstream pipe elevation at zero, and L = 980 m, a = 980 m/s, D = 1.1284 m, f = 0.03, and H_v = −10.0 m. In the discrete gas cavity model $\psi = 1$ and $\alpha = 10^{-7}$ at atmospheric pressure.

Example 8-6

In this case the change in elevation Δz = 4.0 m, and V_0 = 0.4 m/s. Figure 8-14 provides a comparison of the two computational procedures with N = 20. Reasonable agreement exists between the two methods. The vaporous zone is sustained only slightly longer than $2L/a$ seconds (to 2.22 s) in the upstream region of the pipe and the void fraction grows to only about 0.0002 before collapsing. The isolated cavity exists for approximately 2.9 s. It may be noted that the pressure exceeds a maximum of 55 m ($aV_0/g + H_0$).

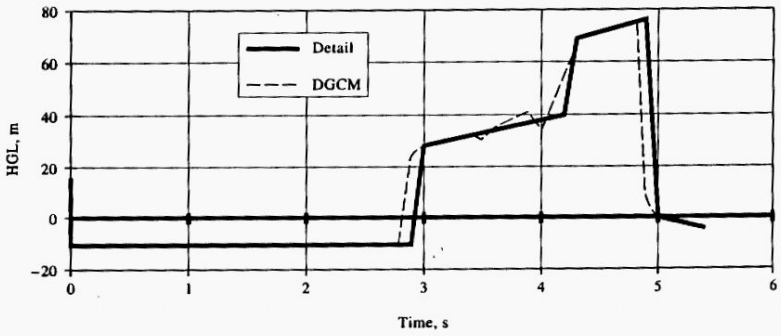

Figure 8-14 Example 8-6, distributed vaporization, V_0 = 0.4 m/s, ΔZ = 4.0 m.

Example 8-7

In this case Δz = 4.0 m and V_0 = 1.56 m/s. Figure 8-15 shows general agreement in results. The vaporous zone is sustained for 2.33 s and the isolated cavity exists until 12.2 s. The pressure rise is approximately what might be expected from stopping the original flow abruptly.

Example 8-8

The rising slope is increased to Δz = 12.0 m, and V_0 = 1.48 m/s. The void fraction reaches 0.001 in the distributed vaporization zone, which lasts until approximately 3.71 s. The isolated cavity lasts until approximately 11.8 s. The pressure trace at the upstream end is shown in Fig. 8-16 for both analyses. Again the agreement in timing is reasonable and the pressure magnitudes are similar.

The detailed modeling, provided in the distributed vapor model, is superior in these examples since it provides a reasonable description of the physical behavior.

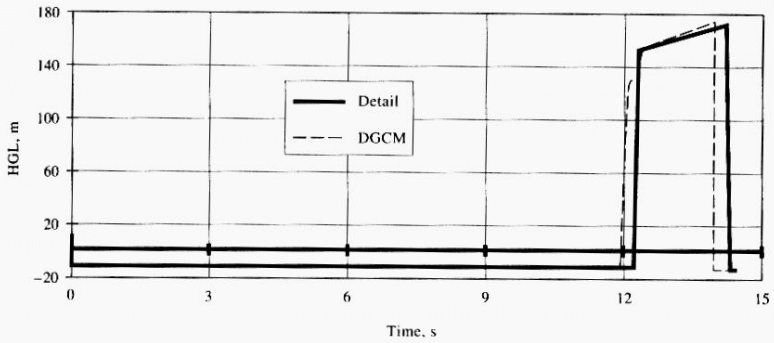

Figure 8-15 Example 8-7, distributed vaporization, V_0 = 1.56 m/s, ΔZ = 4.0 m.

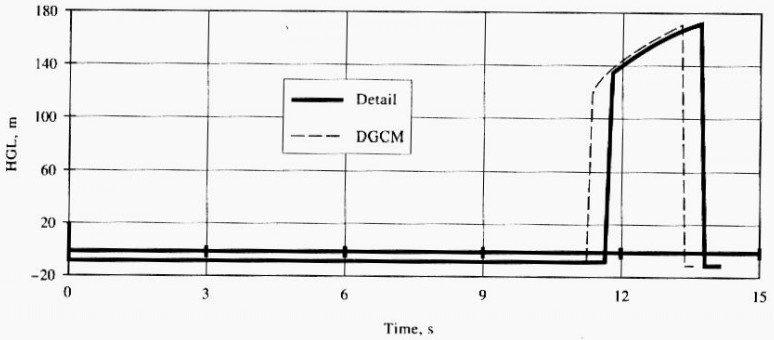

Figure 8-16 Example 8-8, distributed vaporization, V_0 = 1.48 m/s, ΔZ = 12.0 m.

However, it is fraught with numerical coding difficulties when modeling more general cases. Thus the discrete gas cavity model, with a low mass of free gas, offers a convenient alternative, and it is simple to implement. It is seen that it simulates these cases reasonably well, and the model is fairly robust. It should be used with caution and with understanding, as it, too, may yield excessive numerical oscillations in cases with distributed vaporization at large void fractions.

View Verification Case 6 Model

Verification Case 6

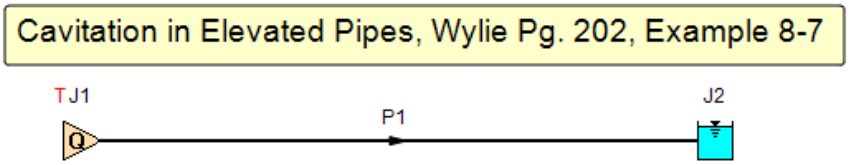

Verification Case 7

View Model Problem Statement

PRODUCT: AFT Impulse

TITLE: ImpVerify7.imp

REFERENCE: Fluid Transients in Systems, 1993, Prentice-Hall, E. Benjamin Wylie, Victor L. Streeter, Page 202, Example 8-8

FLUID: Water

ASSUMPTIONS: N/A

RESULTS:

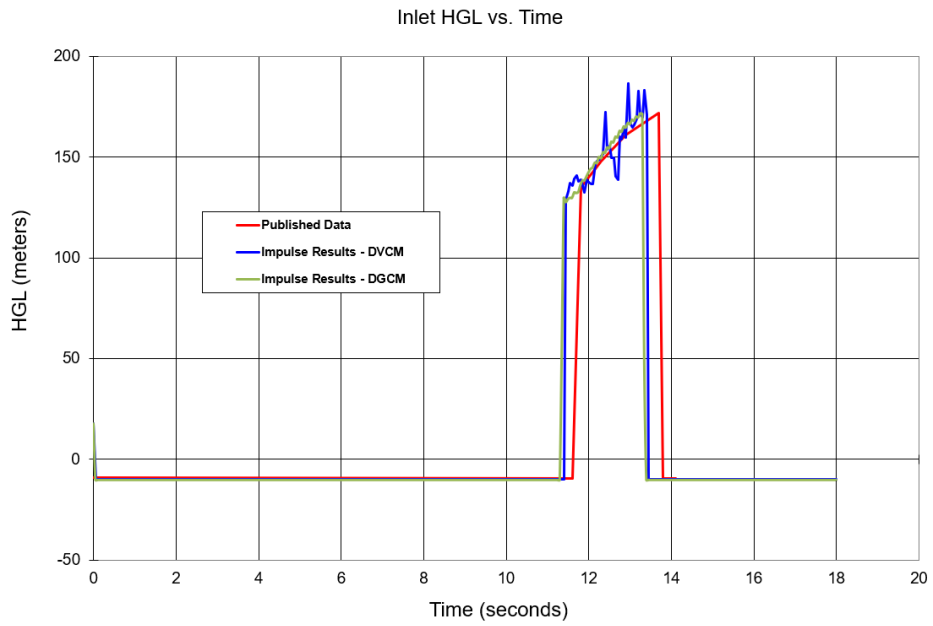

DISCUSSION:

This example was designed to cause transient cavitation, and the flow does cavitate. As is common with cavitation modeling the timing of pressure spikes is marginal, but the major features and magnitude of prominent spikes is represented.

List of All Verification Models

Verification Case 7 Problem Statement

Verification Case 7

Fluid Transients in Systems, 1993, Prentice-Hall, E. Benjamin Wylie, Victor L. Streeter, Page 202, Example 8-8

Wylie Title Page

at 15.0 m, the upstream pipe elevation at zero, and L = 980 m, a = 980 m/s, D = 1.1284 m, f = 0.03, and H_v = −10.0 m. In the discrete gas cavity model $\psi = 1$ and $\alpha = 10^{-7}$ at atmospheric pressure.

Example 8-6

In this case the change in elevation Δz = 4.0 m, and V_0 = 0.4 m/s. Figure 8-14 provides a comparison of the two computational procedures with N = 20. Reasonable agreement exists between the two methods. The vaporous zone is sustained only slightly longer than $2L/a$ seconds (to 2.22 s) in the upstream region of the pipe and the void fraction grows to only about 0.0002 before collapsing. The isolated cavity exists for approximately 2.9 s. It may be noted that the pressure exceeds a maximum of 55 m ($aV_0/g + H_0$).

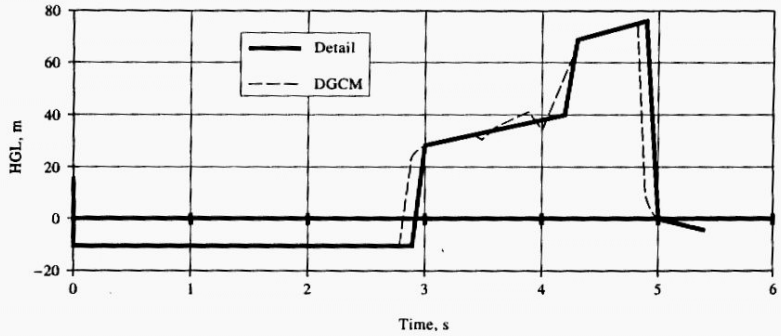

Figure 8-14 Example 8-6, distributed vaporization, V_0 = 0.4 m/s, ΔZ = 4.0 m.

Example 8-7

In this case Δz = 4.0 m and V_0 = 1.56 m/s. Figure 8-15 shows general agreement in results. The vaporous zone is sustained for 2.33 s and the isolated cavity exists until 12.2 s. The pressure rise is approximately what might be expected from stopping the original flow abruptly.

Example 8-8

The rising slope is increased to Δz = 12.0 m, and V_0 = 1.48 m/s. The void fraction reaches 0.001 in the distributed vaporization zone, which lasts until approximately 3.71 s. The isolated cavity lasts until approximately 11.8 s. The pressure trace at the upstream end is shown in Fig. 8-16 for both analyses. Again the agreement in timing is reasonable and the pressure magnitudes are similar.

The detailed modeling, provided in the distributed vapor model, is superior in these examples since it provides a reasonable description of the physical behavior.

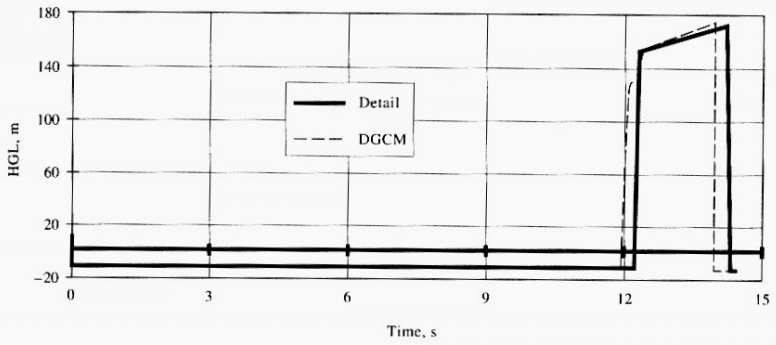

Figure 8-15 Example 8-7, distributed vaporization, V_0 = 1.56 m/s, ΔZ = 4.0 m.

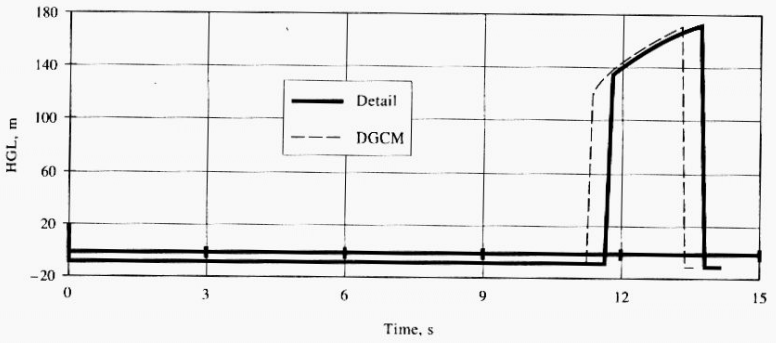

Figure 8-16 Example 8-8, distributed vaporization, V_0 = 1.48 m/s, ΔZ = 12.0 m.

However, it is fraught with numerical coding difficulties when modeling more general cases. Thus the discrete gas cavity model, with a low mass of free gas, offers a convenient alternative, and it is simple to implement. It is seen that it simulates these cases reasonably well, and the model is fairly robust. It should be used with caution and with understanding, as it, too, may yield excessive numerical oscillations in cases with distributed vaporization at large void fractions.

View Verification Case 7 Model

Verification Case 7

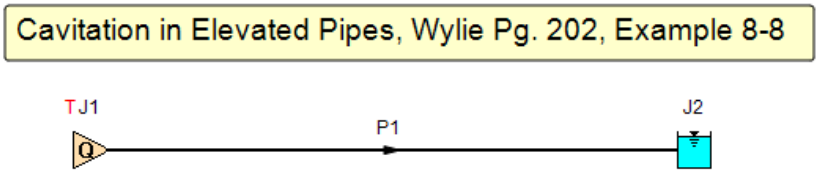

Verification Case 8

View Model Problem Statement

PRODUCT: AFT Impulse

TITLE: ImpVerify8.imp

REFERENCE: Fluid Transients in Systems, 1993, Prentice-Hall, E. Benjamin Wylie, Victor L. Streeter, Page 204

FLUID: Water

ASSUMPTIONS: The problem statement from Wylie does not specify the valve closing transient. It says merely that “most” of the flow reduction occurs in the first 16 ms, and that the valve fully closes after 39 ms. It was therefore estimated that “most” means that the valve closes linearly to 3% open over 16 ms, and then linearly to fully closed at 39 ms.

RESULTS:

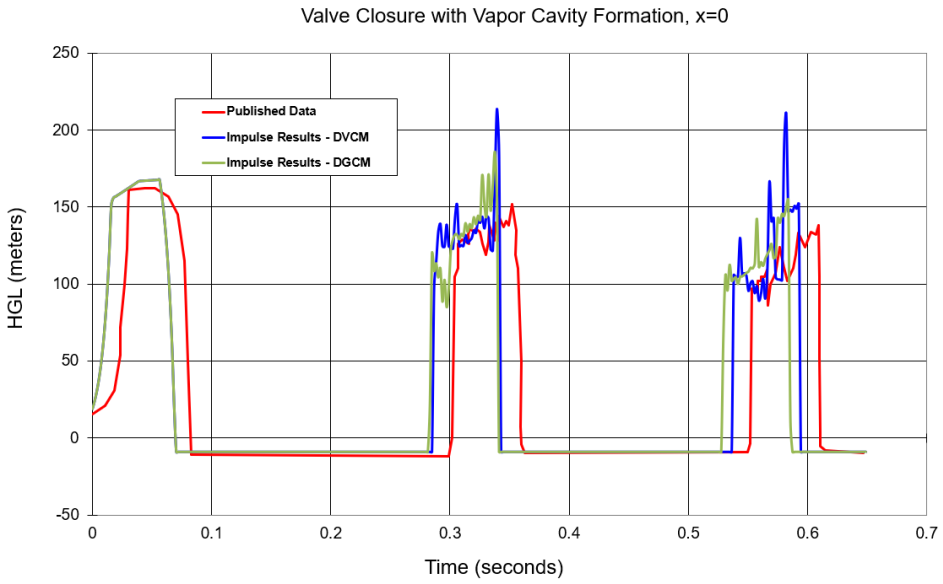

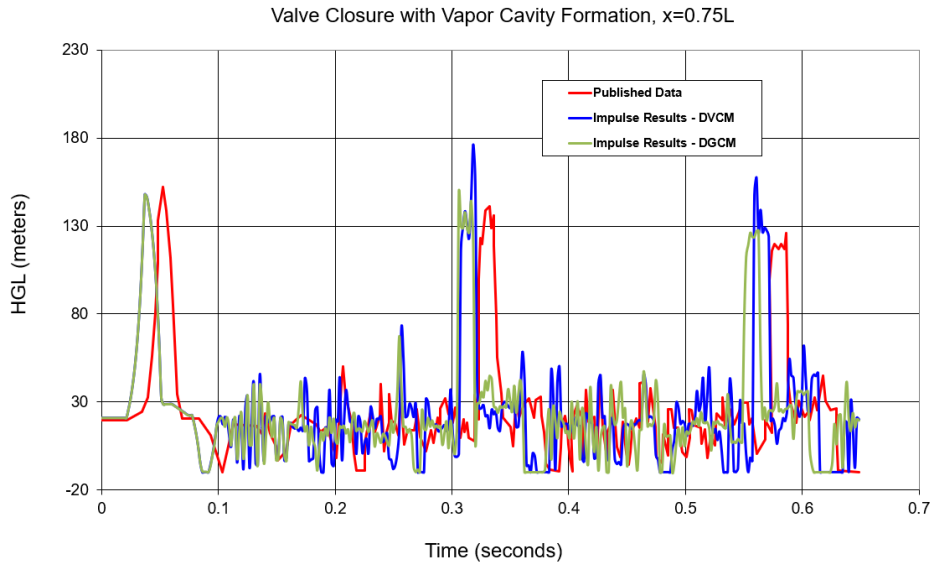

DISCUSSION:

This experiment was designed to cause transient cavitation, and the flow does cavitate. As is common with cavitation modeling the timing of pressure spikes is marginal, but the major features and magnitude of prominent spikes is represented.

List of All Verification Models

Verification Case 8 Problem Statement

Verification Case 8

Fluid Transients in Systems, 1993, Prentice-Hall, E. Benjamin Wylie, Victor L. Streeter, Page 204

Wylie Title Page

8-6 Additional Vaporization Examples

Experimental results are presented for two cases, with comparisons to the discrete free-gas cavity model. Simpson[19] provided several examples of experimental results using the apparatus described in Example 8-5, with initial velocities larger than in that case. With sufficiently high velocities the pressure gradient in this particular system at the time of vaporization, $2L/a$ seconds, is such that the hydraulic gradient and the pipeline converge in the direction of vaporization, the upstream direction. A combination of a distributed vaporization zone and a discrete downstream cavity develop and subsequently collapse. Simpson's original material[19] may be referred to for additional comparisons with experimental results in this apparatus. The second example involves an experiment in the Delft Hydraulics Laboratory, simulating pump failure and restarting of a pump at the upstream end of a horizontal test pipeline. In this case the upstream pressure reduction pulse, which simulates the pump failure, rides down the steady pressure gradient. An interior distributed vaporous zone develops when the low-pressure wave reaches vapor pressure. An isolated cavity does not develop.

Example 8-9

For this case, in the test apparatus as described in Example 8-5, $V_0 = 1.125$ m/s, $f = 0.023$, upstream pressure head 21.74 m, and vapor pressure -9.83 m. Velocity variation at the valve during valve closure was determined numerically by Simpson[19] with the downstream measured pressure head specified. In this case, flow is reduced to zero in about 39 ms, with most of flow reduction occurring in about 16 ms. The wave reflection time is approximately 56 ms in the system.

Figure 8-17 shows the experimental results at the valve and at 9 m from the upstream end, and numerical results utilizing the discrete gas cavity model with $N = 16$ and $\alpha = 10^{-7}$ at standard conditions. Although the agreement is reasonable, the timing is slightly off for each of the pressure peaks following cavity collapse, and the numerical results produce a short-duration pressure peak at the valve at about 0.35 s that does not appear in the experimental record.

In the pressure history at the valve during the first high-pressure pulse following valve closure it is noted that there is a divergence between the experimental and calculated results. In fact, the pressure reduction displayed in the experimental trace is unrealistic for a nondeforming pipeline system during the first $2L/a$ seconds. To be more confident that the discrete gas cavity model was simulating the same problem as the physical experiment, it was decided to calculate the velocity variation at the valve necessary to produce the measured pressure history until the instant of return of the first major rarefaction wave. This resulted in a positive flow at the valve even after the valve was closed. A volume of approximately 0.5 cc of liquid was removed from the system, which corresponds to an elongation of the pipeline during this period. Since this volume represented an additional temporary storage capacity at the valve end, it had to be returned to the system during the low-pressure part of the cycle, when the short-term longitudinal strain is relaxed. Since a vapor space exists at the valve during this time the manner in which the volume is reintroduced is arbitrary. This velocity pattern was used at the valve for the simulation shown in Fig. 8-18; that is, the flow was stopped in 39 ms, then the additional volume of 0.5 cc was removed over the next 46 ms in a manner that provided agreement between the two pressure traces. From that point on, the valve was considered a dead end. Clearly,

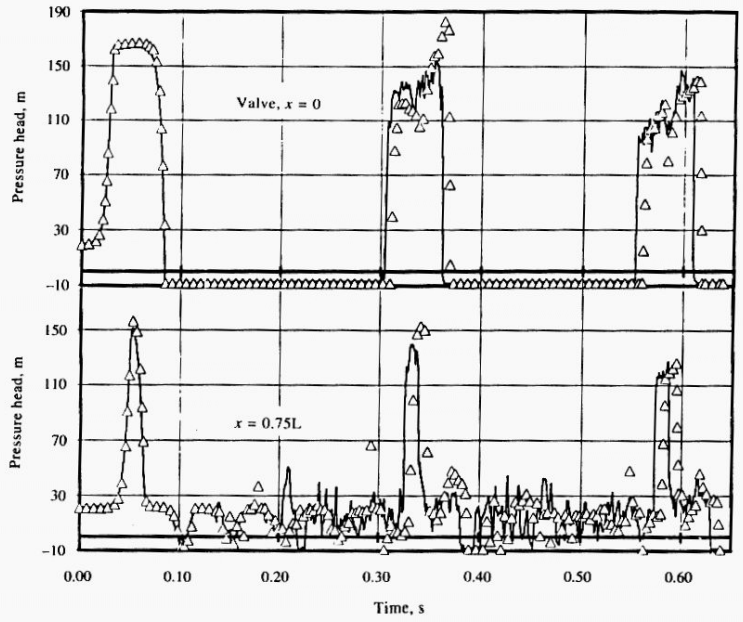

Figure 8-17 Example 8-9, comparison of experimental results (solid line), Simpson,[19] with discrete gas cavity model, V_0 = 1.125 m/s.

there must be similar deformation at the valve during each of the high-pressure pulses, but short of a complete fluid-structure interaction calculation, there is no reliable way to calculate the actual velocity history during these deformations. This second simulation (Fig. 8-18) provides closer pressure magnitude agreement with the measured experimental values, but the timing is advanced.

These comparisons demonstrate once again that there are many features present in experimental results that represent the combined response of the system. It is asking too much of a vaporization model, even if 100 percent accurate, to reproduce, religiously, experimental results that include the combined influences of other important phenomena.

Example 8-10

From the literature[9,15] experimental results are available in a horizontal test pipe in the Delft Hydraulics Laboratory for a simulated pump failure and pump restart. At the upstream end a pressure–time pattern was specified to simulate the pump behavior. A

View Verification Case 8 Model

Verification Case 8

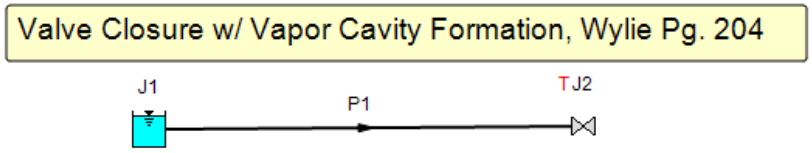

Verification Case 9

View Model Problem Statement

PRODUCT: AFT Impulse

TITLE: ImpVerify9.imp

REFERENCE: Fluid Transients in Systems, 1993, Prentice-Hall, E. Benjamin Wylie, Victor L. Streeter, Page 205, Example 8-10

FLUID: Water

ASSUMPTIONS: Downstream pressure constant at 64 kPa. Problem statement is merely that the downstream pressure is fixed, but the actual value is not given. To achieve the given flowrate of 0.0158 m3/sec, a pressure of 64 kPa is required. Unfortunately, the initial HGL at the specified locations of 30 and 10 meters was not able to be matched. Thus the Impulse results shown below are likely off in the vertical direction to some degree. Nevertheless, Impulse predictions follow the major trends quite well.

RESULTS:

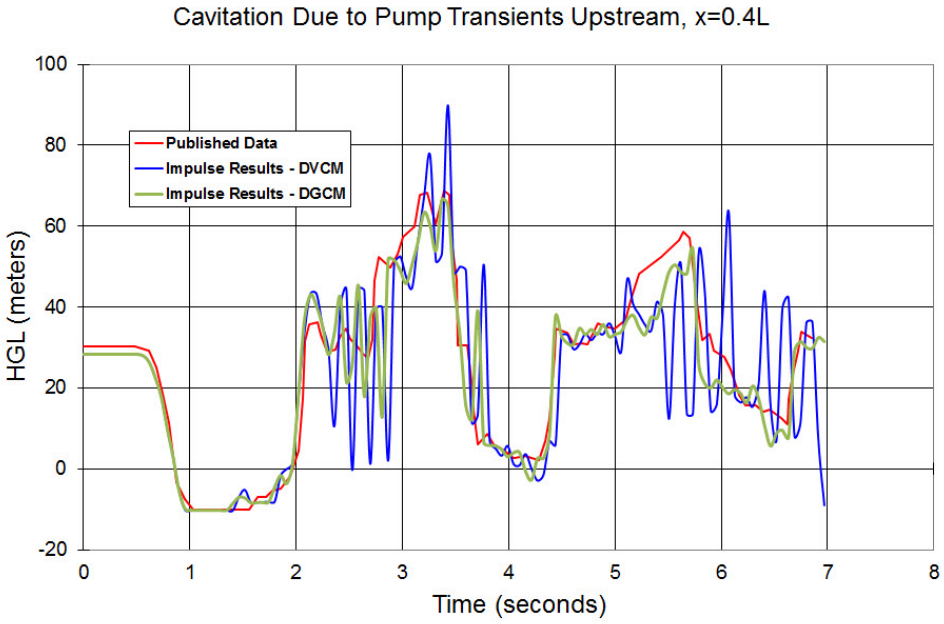

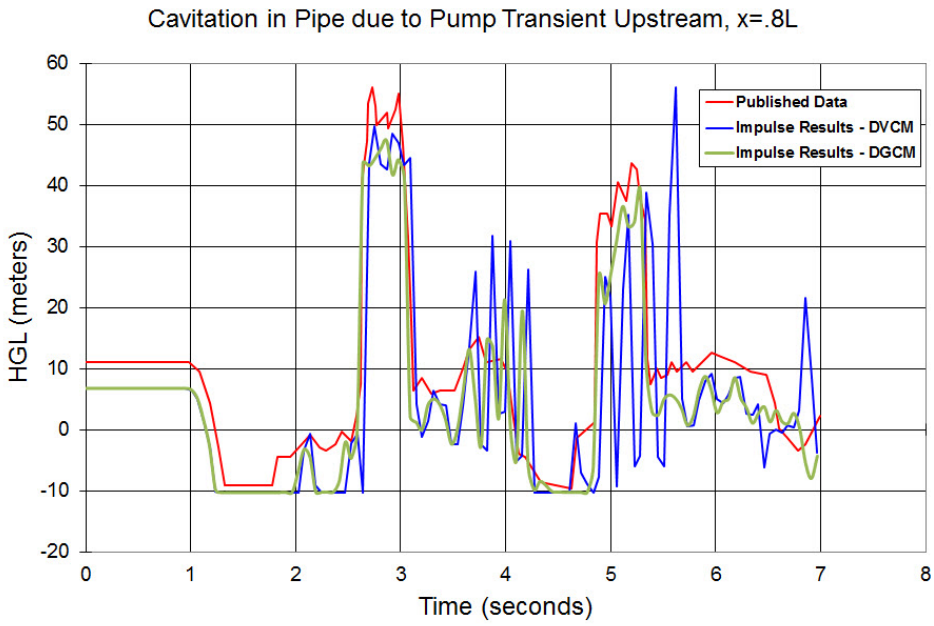

DISCUSSION:

This experiment was designed to cause transient cavitation, and the flow does cavitate. As is common with cavitation modeling the timing of pressure spikes is marginal, but the major features and magnitude of prominent spikes is represented.

List of All Verification Models

Verification Case 9 Problem Statement

Verification Case 9

Fluid Transients in Systems, 1993, Prentice-Hall, E. Benjamin Wylie, Victor L. Streeter, Page 205, Example 8-10

Wylie Title Page

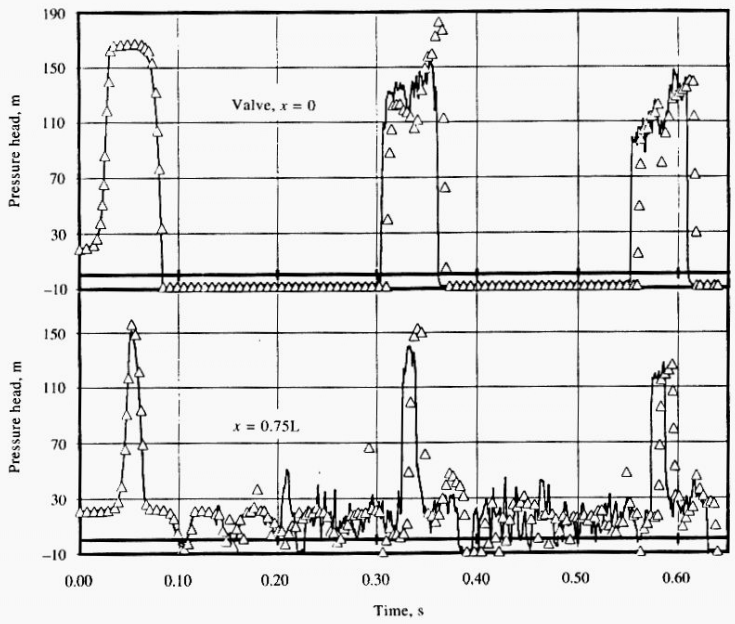

Figure 8-17 Example 8-9, comparison of experimental results (solid line), Simpson,[19] with discrete gas cavity model, V_0 = 1.125 m/s.

there must be similar deformation at the valve during each of the high-pressure pulses, but short of a complete fluid-structure interaction calculation, there is no reliable way to calculate the actual velocity history during these deformations. This second simulation (Fig. 8-18) provides closer pressure magnitude agreement with the measured experimental values, but the timing is advanced.

These comparisons demonstrate once again that there are many features present in experimental results that represent the combined response of the system. It is asking too much of a vaporization model, even if 100 percent accurate, to reproduce, religiously, experimental results that include the combined influences of other important phenomena.

Example 8-10

From the literature[9,15] experimental results are available in a horizontal test pipe in the Delft Hydraulics Laboratory for a simulated pump failure and pump restart. At the upstream end a pressure–time pattern was specified to simulate the pump behavior. A

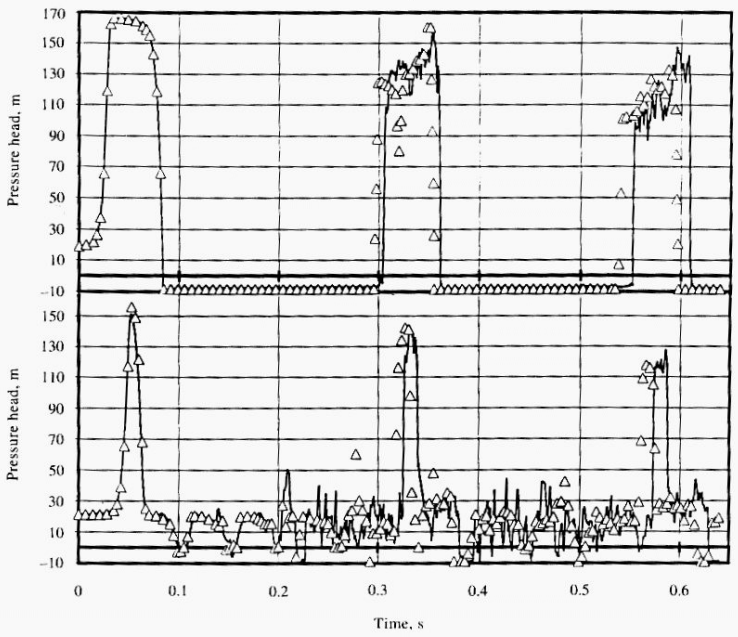

Figure 8-18 Example 8-9, comparison of experimental results (solid line), Simpson,[19] with discrete gas cavity model, $V_0 = 1.125$ m/s. Flow specified for approximately 0.1 s.

large pressure tank provided constant downstream pressure. The system data include $D = 0.10$ m, $L = 1450$ m, $f = 0.018$, $Q_0 = 0.0158$ m^3/s, $a = 1290$ m/s, $\rho = 1000$ kg/m^3, $H_R^* = 60.2$ m, $z = 0.0$ m, $H_v = -10.10$ m, $\alpha_0 = 10^{-7}$ at standard conditions, and $N = 20$.

Figure 8-19 shows the experimental record at $x = 0.4L$ and at $x = 0.8L$, as well as the upstream controlled pressure. In addition, the numerical results from the discrete gas cavity model are presented with $\psi = 1.0$.[31] Agreement is observed to be quite acceptable. The same experimental results have been compared with numerical results from a vapor column separation model (no free gas other than vapor).[32]

Experimental data on column separation are presented by many others for both pure liquid transients and for cases with free and evolving gases. Some of the physical measurements indicate considerably more dissipation than in analytical studies. The example by Li[10] presented in Fig. 3-24 lacks agreement after the first cavity collapse.

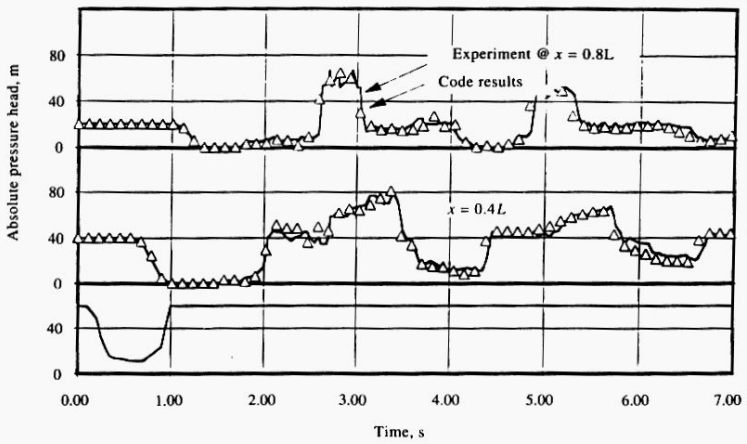

Figure 8-19 Example 8-10, distributed vaporization in a horizontal pipeline.

Baltzer[2] and Weyler[27] provide similar results. Swaffield[25] and Driels[5] have reported experimental comparisons with kerosene as the liquid. Kranenburg[9] indicates the need for gas release to bring about better correlation between theory and experiment, as do Wiggert and Sundquist.[28] A note of caution may be in order when attempting to match numerical results with experimental records. The collapse of vapor pockets in pipelines represent one of the few examples of truly instantaneous transients. With such a rapid transient event several dissipative mechanisms, normally unimportant, may be significant. Some of these include frequency-dependent viscous losses, frequency-dependent elastic wall properties, viscoelastic wall properties, and fluid–structure interaction, among others.

The situation shown in Fig. 8-20 may arise with rapid valve closure at the upstream end of a short pipe. Most of the liquid escapes, but a portion is trapped in the

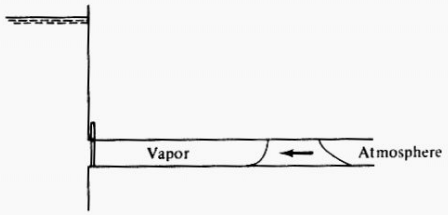

Figure 8-20 Trapped column of liquid in short line.

View Verification Case 9 Model

Verification Case 9

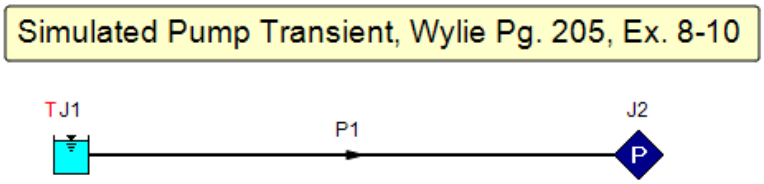

Verification Case 10

View Model Problem Statement

PRODUCT: AFT Impulse

TITLE: ImpVerify10.imp

REFERENCE: Fluid Transients in Systems, 1993, Prentice-Hall, E. Benjamin Wylie, Victor L. Streeter, Page 69, DVC Model Case

FLUID: Water

ASSUMPTIONS: N/A

RESULTS:

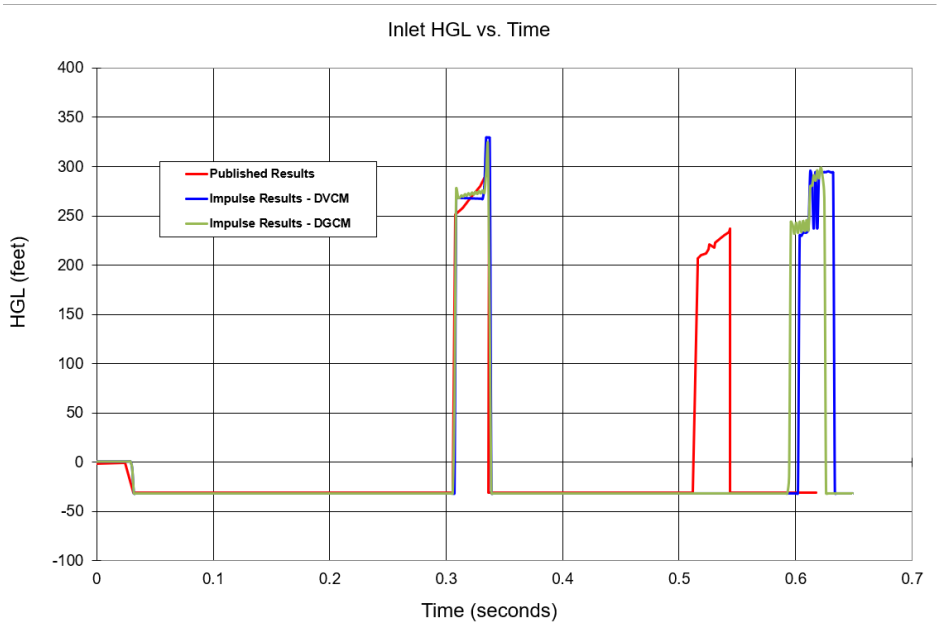

DISCUSSION:

This experiment was designed to cause transient cavitation, and the flow does cavitate. As is common with cavitation modeling the timing of pressure spikes is marginal, but the major features and magnitude of prominent spikes is represented.

List of All Verification Models

Verification Case 10 Problem Statement

Verification Case 10

Fluid Transients in Systems, 1993, Prentice-Hall, E. Benjamin Wylie, Victor L. Streeter, Page 69, DVC Model Case

Wylie Title Page

lists the FORTRAN code for an internal section calculation. End conditions are handled similarly.

An experimental record[17] of an isolated cavity formation at the downstream side of a valve is shown in Fig. 3-22. These data were taken in a 2-in. plastic pipe with 31.3 ft of length downstream of the valve. The wavespeed was measured to be 2070 ft/s, and the initial fluid velocity in this case was 4.58 ft/s. The duration of existence

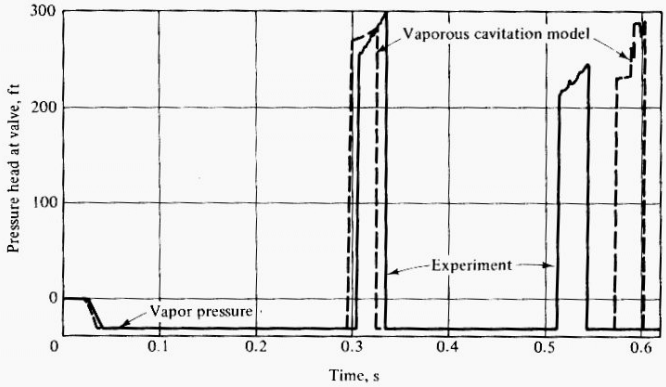

Figure 3-22 Column separation downstream from valve.

of the first cavity at the valve may be seen to be about $17L/a$ seconds. The vaporous cavitation model described above was used to model this experiment, and the results are presented in Fig. 3-22. It may be seen that the timing and magnitude of the pressure rise upon collapse of the first cavity are in reasonable agreement. The calculated maximum size of the cavity was about 0.0058 ft^3. However, the growth and collapse of the second cavity in experiment and numerical model are clearly not in agreement. The physical measurements indicate considerably more dissipation than the analytical study, and a short-duration pulse appears in the numerical results that is not present in the experimental record.

3-9 Algebraic Method

In many low-friction systems, and in systems with sensitive dynamic boundary conditions that require extremely small time steps, an algebraic representation of the compatibility equations offers appeal. In this procedure the characteristic lines extend more than one reach, generally the full pipe length, but time steps are utilized that are related by integers to L/a seconds. The algebraic equations are also an integral part of the valve stroking developments in Chapter 9.

View Verification Case 10 Model

Verification Case 10

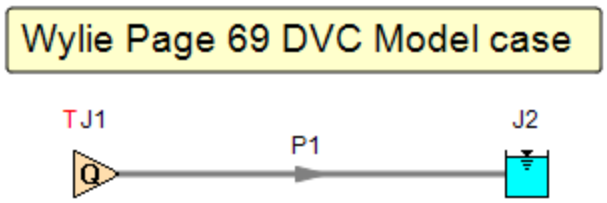

Verification Case 11

View Model Problem Statement

PRODUCT: AFT Impulse

TITLE: ImpVerify11.imp

REFERENCE: Efficient Calculation of Transient flow in Simple Pipe Networks, 1992, Journal of Hydraulic Engineering, Vol. 118, No. 7, No. 26648, July, Karney, Bryan W. and McInnis, Duncan, pp. 1022-1030

FLUID: Water

ASSUMPTIONS: Karney uses a relief valve connected to 3 pipes which discharges to atmosphere. AFT Impulse does not support a relief valve with this configuration. Thus an additional pipe (called P8) is used and made as short as possible without increasing pipe sectioning. The valve at J6 is then located at the end of pipe P8, and is modeled with an event transient to simulate Karney's relief valve.

RESULTS:

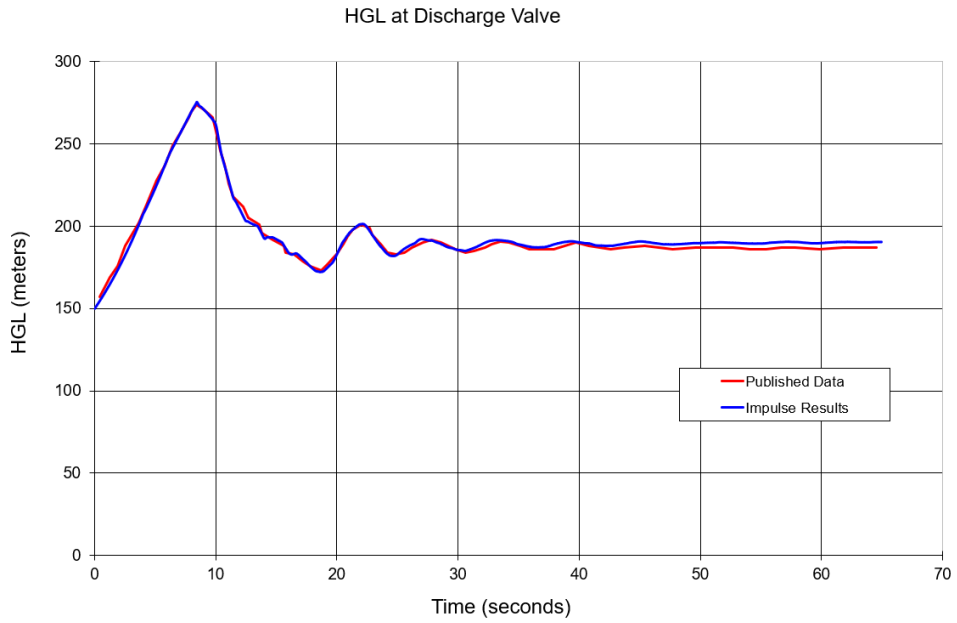

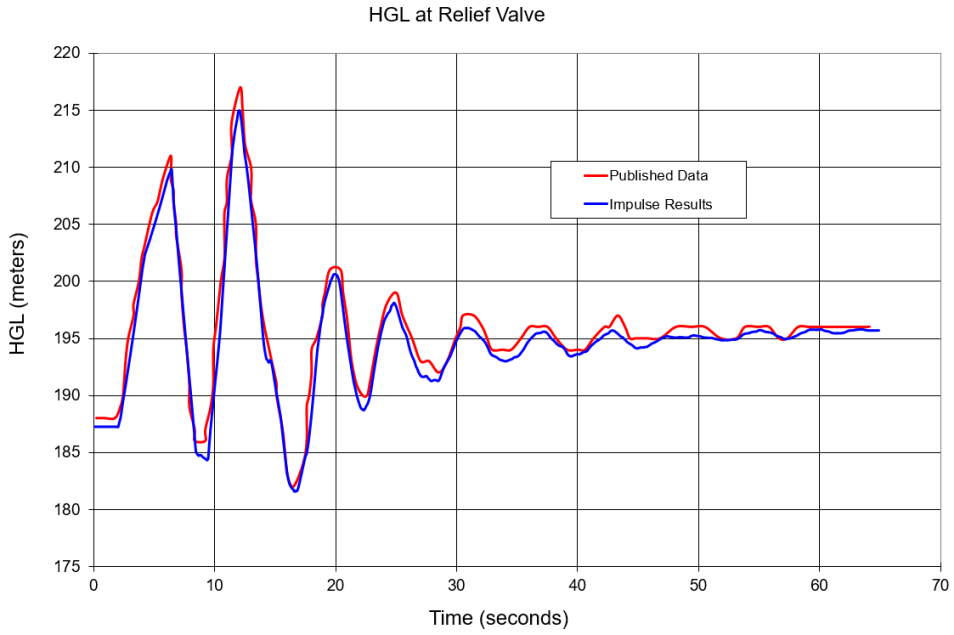

DISCUSSION:

This model represents the solution for how a network responds to changes in a control valve. Differences between the published results and results from AFT Impulse may be attributed to the differences in how the relief valve is modeled in AFT Impulse, as is discussed in the assumptions above.

List of All Verification Models

Verification Case 11 Problem Statement

Verification Case 11

Efficient Calculation of Transient flow in Simple Pipe Networks, 1992, Journal of Hydraulic Engineering, Vol. 118, No. 7, No. 26648, July, Karney, Bryan W. and McInnis, Duncan, pp. 1022-1030

Karney Title Page

TABLE 4. Summary of Maximum and Minimum Hydraulic Grade-Line (HGL) Elevations

Node number (1)	Case 1		Case 2	
	Maximum HGL (m) (2)	Minimum HGL (m) (3)	Maximum HGL (m) (4)	Minimum HGL (m) (5)
1	200.4	200.0	200.3	199.9
2	208.7	186.3	208.7	181.8
3	192.1	186.6	192.1	186.6
4	175.1	175.0	175.1	175.0
5	199.6	177.5	199.6	164.6
6	215.6	181.8	215.6	155.6
7	275.6	151.9	275.6	80.2

negative pressure wave. By allowing fluid storage, the reservoirs and surge tank limit the pressure changes at their respective nodes.

More detailed information about the system transient response is provided in Figs. 6 and 7. Note the expected correspondence in case 1 and case 2 head and flow traces during the initial period of valve closure. The high-pressure waves initiated at node 7 by the closing valve are propagated throughout the system. As the head builds at node 6, the relief valve set point is exceeded at 6 s. When the valve opens, the release of fluid at that location reduces the pressure. The work done in forcing water through the valves at nodes 6 and 7 attenuates the transient and allows the system to reach state quickly.

The behavior of the system changes dramatically as the control valve at node 7 reopens (between 25 and 30 s). The increased demand at node 7 causes a severe drop in the pressure, thus increasing the flow at the node 1 reservoir. In addition, the surge-tank flow reverses and begins to discharge water into the network. Note how slowly the water level in the surge tank changes compared to the rapid pressure fluctuations at node 3. The role of orifice and connector losses, as well the importance of inertial effects, is strongly indicated by these differences (bottom left graphs of Figs. 6 and 7).

The preceding remarks are merely intended to convey a sense of how the system reacts to the control-valve operations. This is not, however, the intent of the example. More important are the following points.

1. Five of the seven boundary conditions are explicitly solved by (32) (which also permits connector, tank inertia, and friction terms) in a way tha automatically accounts for flow reversal. Thus, only a single pass through the solution is required. No known reference capitalizes on the explicit nature of the general solution to this entire class of devices. In one reference, nine separately formulation boundary conditions are presented to deal with storage-like boundary conditions. Despite this, not all boundary conditions present in this example network can be solved. Nor do standard references determine the sign of the flow in advance of the solution, except in the simplest of cases.
2. Although the maximum number of pipes at any junction in the example is only three, no restriction on this number is required. Wylie and Streeter (1982) clearly state this fact. Watter's (1984) approach, by contrast, separately

1026

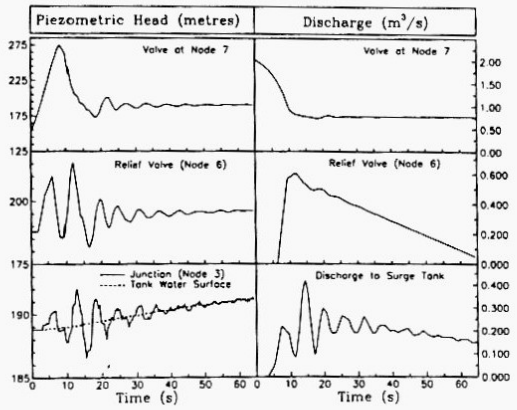

FIG. 6. Hydraulic Grade-Line Elevations and External Flows at Selected Locations: Case 1

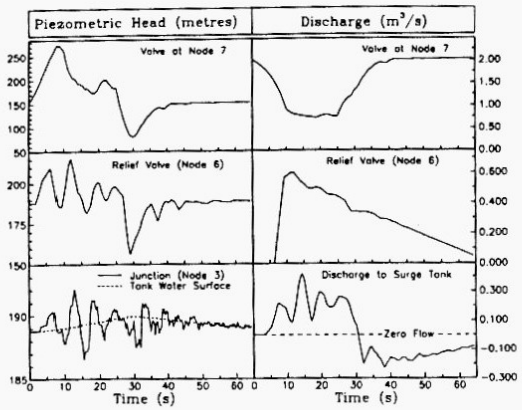

FIG. 7. Hydraulic Grade-Line Elevations and External Flows at Selected Locations: Case 2

1027

View Verification Case 11 Model

Verification Case 11

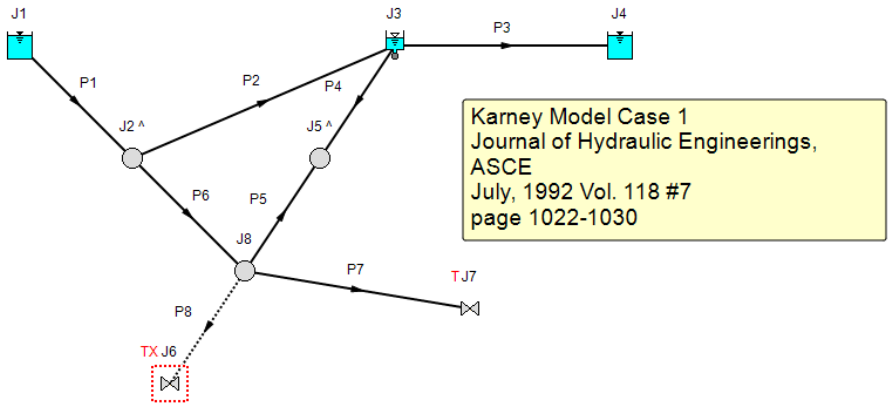

Verification Case 12

View Model Problem Statement

PRODUCT: AFT Impulse

TITLE: ImpVerify12.imp

REFERENCE: Efficient Calculation of Transient flow in Simple Pipe Networks, 1992, Journal of Hydraulic Engineering, Vol. 118, No. 7, No. 26648, July, Karney, Bryan W. and McInnis, Duncan, pp. 1022-1030

FLUID: Water

ASSUMPTIONS: Karney uses a relief valve connected to 3 pipes which discharges to atmosphere. AFT Impulse does not support a relief valve with this configuration. Thus an additional pipe (called P8) is used and made as short as possible without increasing pipe sectioning. The relief valve at J6 is then located at the end of pipe P8.

RESULTS:

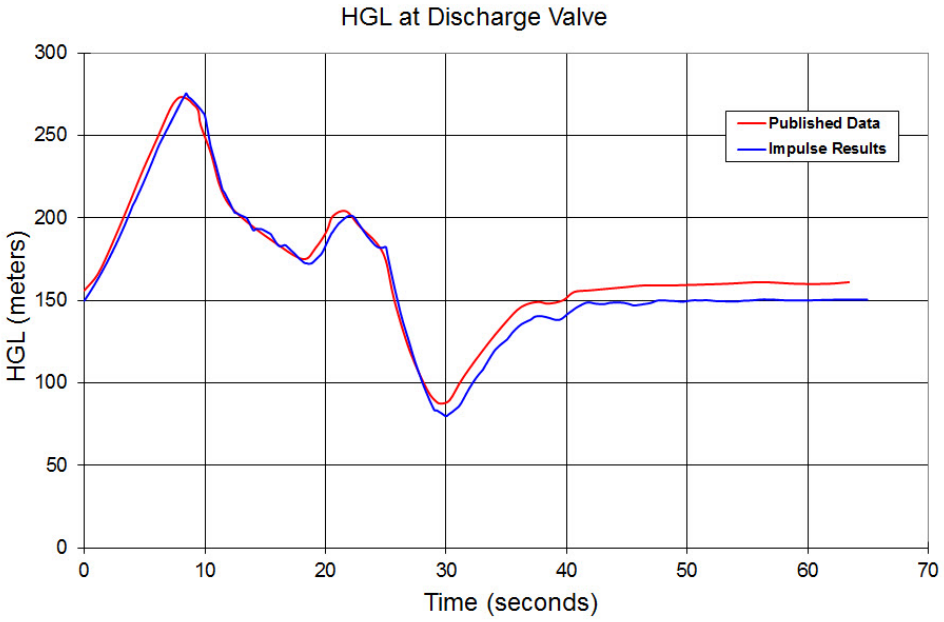

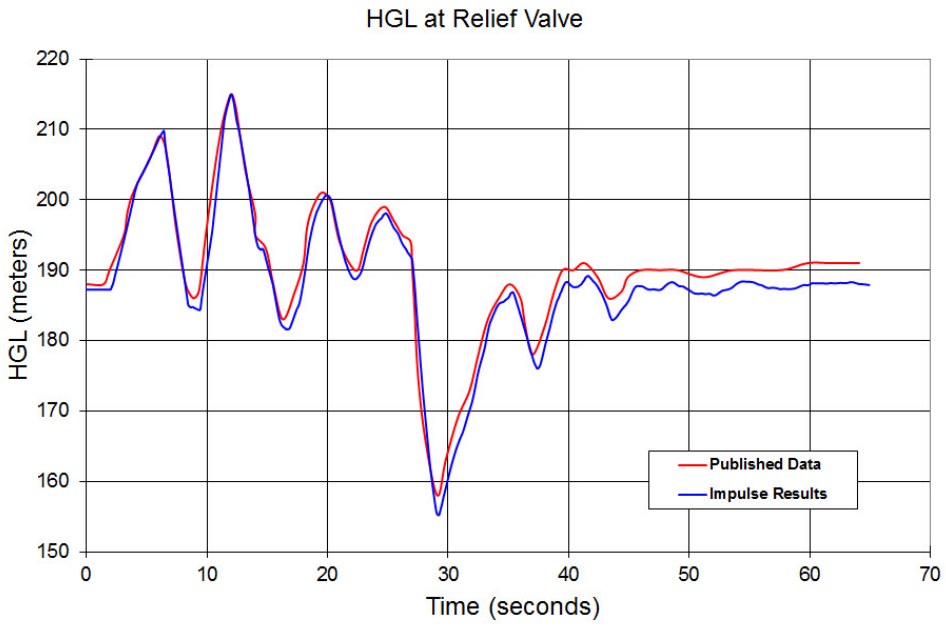

DISCUSSION:

This model represents the solution for how a network responds to changes in a control valve. Differences between the published results and results from AFT Impulse may be attributed to the differences in how the relief valve is modeled in AFT Impulse, as is discussed in the assumptions above.

List of All Verification Models

Verification Case 12 Problem Statement

Verification Case 12

Efficient Calculation of Transient flow in Simple Pipe Networks, 1992, Journal of Hydraulic Engineering, Vol. 118, No. 7, No. 26648, July, Karney, Bryan W. and McInnis, Duncan, pp. 1022-1030

Karney Title Page

TABLE 4. Summary of Maximum and Minimum Hydraulic Grade-Line (HGL) Elevations

Node number (1)	Case 1		Case 2	
	Maximum HGL (m) (2)	Minimum HGL (m) (3)	Maximum HGL (m) (4)	Minimum HGL (m) (5)
1	200.4	200.0	200.3	199.9
2	208.7	186.3	208.7	181.8
3	192.1	186.6	192.1	186.6
4	175.1	175.0	175.1	175.0
5	199.6	177.5	199.6	164.6
6	215.6	181.8	215.6	155.6
7	275.6	151.9	275.6	80.2

negative pressure wave. By allowing fluid storage, the reservoirs and surge tank limit the pressure changes at their respective nodes.

More detailed information about the system transient response is provided in Figs. 6 and 7. Note the expected correspondence in case 1 and case 2 head and flow traces during the initial period of valve closure. The high-pressure waves initiated at node 7 by the closing valve are propagated throughout the system. As the head builds at node 6, the relief valve set point is exceeded at 6 s. When the valve opens, the release of fluid at that location reduces the pressure. The work done in forcing water through the valves at nodes 6 and 7 attenuates the transient and allows the system to reach state quickly.

The behavior of the system changes dramatically as the control valve at node 7 reopens (between 25 and 30 s). The increased demand at node 7 causes a severe drop in the pressure, thus increasing the flow at the node 1 reservoir. In addition, the surge-tank flow reverses and begins to discharge water into the network. Note how slowly the water level in the surge tank changes compared to the rapid pressure fluctuations at node 3. The role of orifice and connector losses, as well the importance of inertial effects, is strongly indicated by these differences (bottom left graphs of Figs. 6 and 7).

The preceding remarks are merely intended to convey a sense of how the system reacts to the control-valve operations. This is not, however, the intent of the example. More important are the following points.

1. Five of the seven boundary conditions are explicitly solved by (32) (which also permits connector, tank inertia, and friction terms) in a way tha automatically accounts for flow reversal. Thus, only a single pass through the solution is required. No known reference capitalizes on the explicit nature of the general solution to this entire class of devices. In one reference, nine separately formulation boundary conditions are presented to deal with storage-like boundary conditions. Despite this, not all boundary conditions present in this example network can be solved. Nor do standard references determine the sign of the flow in advance of the solution, except in the simplest of cases.
2. Although the maximum number of pipes at any junction in the example is only three, no restriction on this number is required. Wylie and Streeter (1982) clearly state this fact. Watter's (1984) approach, by contrast, separately

1026

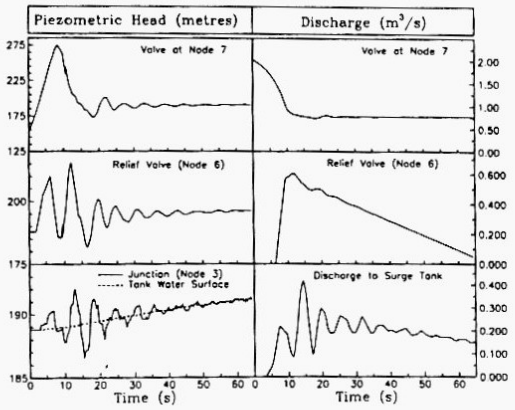

FIG. 6. Hydraulic Grade-Line Elevations and External Flows at Selected Locations: Case 1

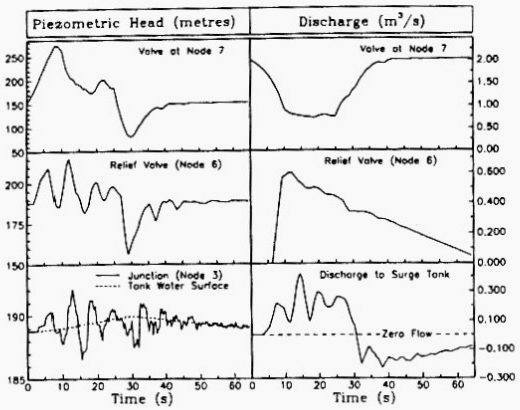

FIG. 7. Hydraulic Grade-Line Elevations and External Flows at Selected Locations: Case 2

1027

View Verification Case 12 Model

Verification Case 12

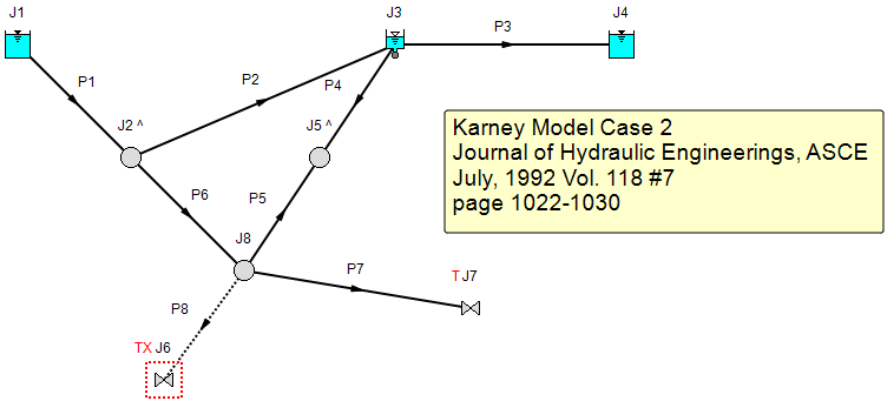

Verification Case 13

View Model Problem Statement

PRODUCT: AFT Impulse

TITLE: ImpVerify13.imp

REFERENCE: *Modern Analysis and Control of Unsteady Flow in Pipelines*, 1979, Ann Arbor Science, Watters, Gary Z., PE, Page 181, Ex. 7-2

FLUID: Water

ASSUMPTIONS: N/A

RESULTS:

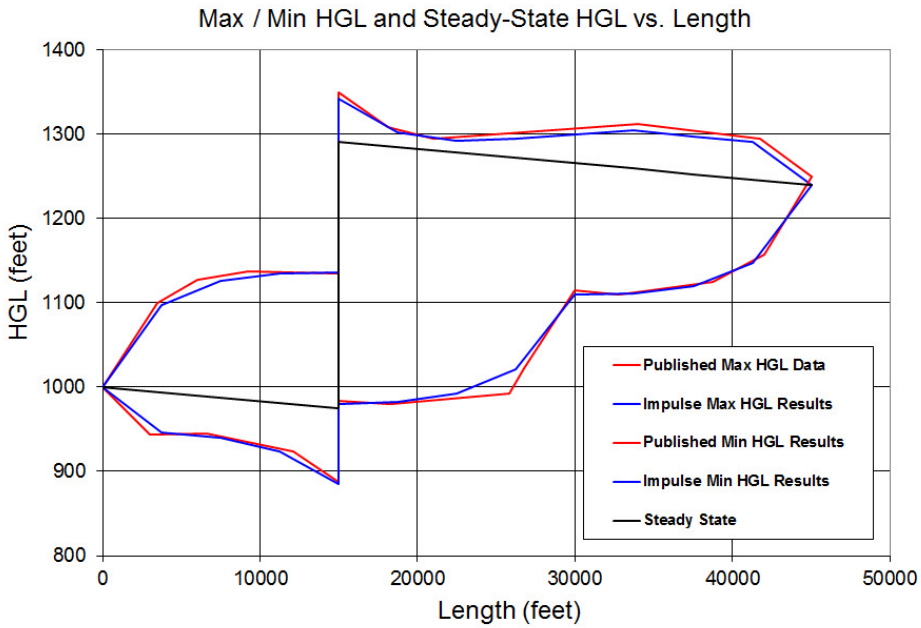

DISCUSSION:

The AFT Impulse model is built with one pump junction that represents four identical pumps operating in parallel which are simultaneously tripped in order to replicate the problem statement in Watters.

List of All Verification Models

Verification Case 13 Problem Statement

Verification Case 13

Modern Analysis and Control of Unsteady Flow in Pipelines, 1979, Ann Arbor Science, Watters, Gary Z., PE, Page 181, Ex. 7-2

Watters Title Page

Example 7-2

To illustrate the effects of booster pumps under a power failure situation, the same four pumps of example 7-1 are placed in the interior of a pipeline. The pipeline is 30 inches in diameter, 45,000 feet long and constructed of welded steel. The f-value is 0.0128 and the wave speed is 3590 fps. A profile of the pipeline and the steady state EL-HGL is shown on Figure 7-8.

The booster pump power failure program no. 9 is used to analyze the resulting water hammer. Check valves are installed to prevent backflow and a frictionless forward-flow bypass is activated when the pump head drops to zero with forward flow occurring. The data necessary to run the analysis is shown below and the program listing is given in Figure 7-9.

Minimum and maximum head envelope curves graphically show the range of head fluctuation for a 60 second simulation. Note that high heads on the suction side of the pumps occur as well as low head on the discharge side. No column separation occurs in this case.

DATA

```
$SPECS NPIPES=2,IOUT=2,NPARTS=5,TMAX=60.,HATM=30.,IEND=1100.,QACC=.50,
     IPUMP=1,HRESUP=1000.,HRESDN=1240.  $END
        1 30.        15000.     .0120      3590.      000.
        2 30.        30000.     .0120      3590.      000.
$PUMPS NPUMPS=4,RPN=1760.,WRSQ=675.,NSTAGE=3,
  QN=0.,1000.,2000.,3000.,4000.,5000.,
  HNSQ=136.,120.,117.,96.,61.,24.,
  TNSQ=55.,61.,75.,87.,93.,95.,
$END
```

182 UNSTEADY FLOW IN PIPELINES

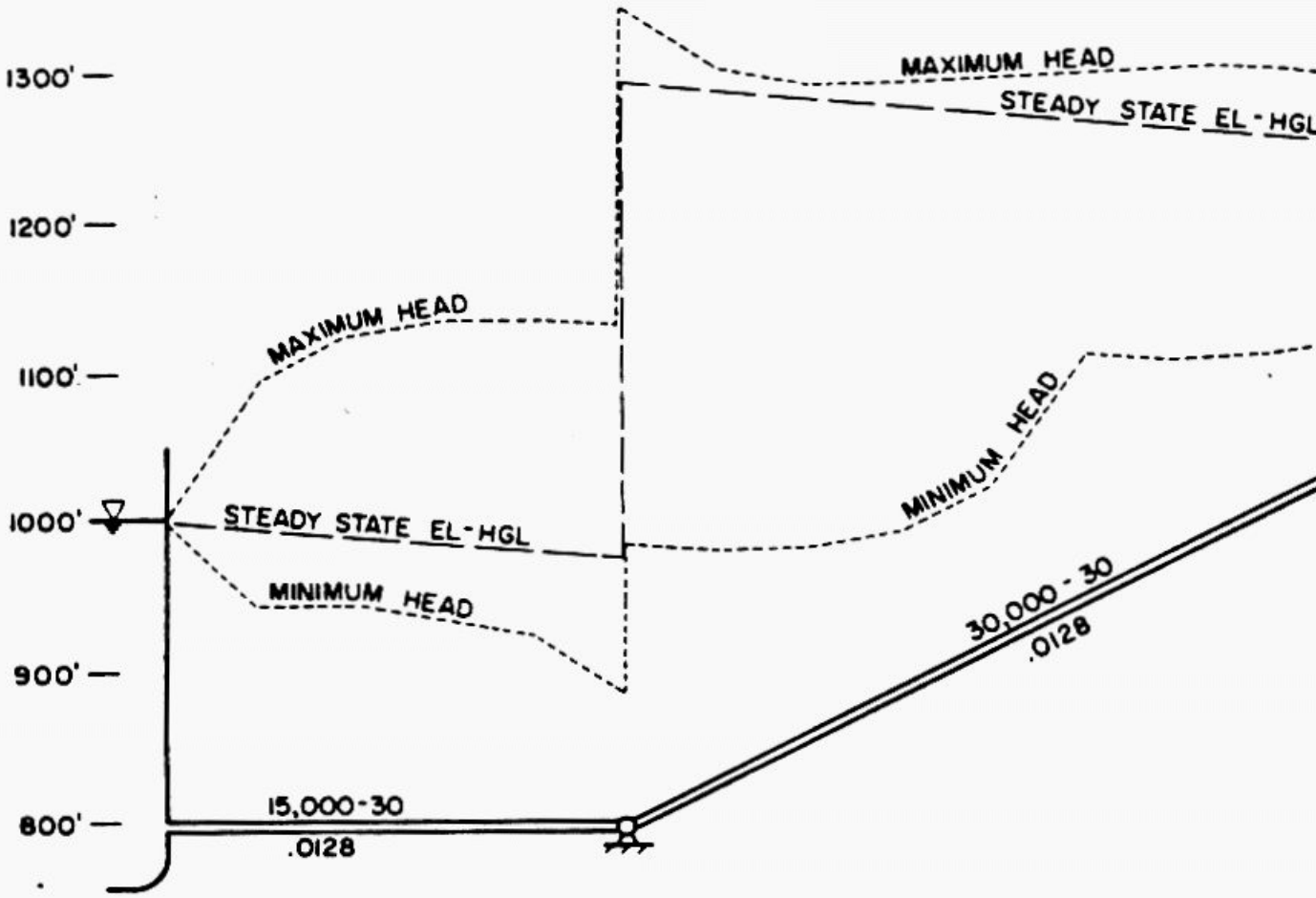

Figure 7-8. Pressure extremes resulting from power failure in a booster pump config

View Verification Case 13 Model

Verification Case 13

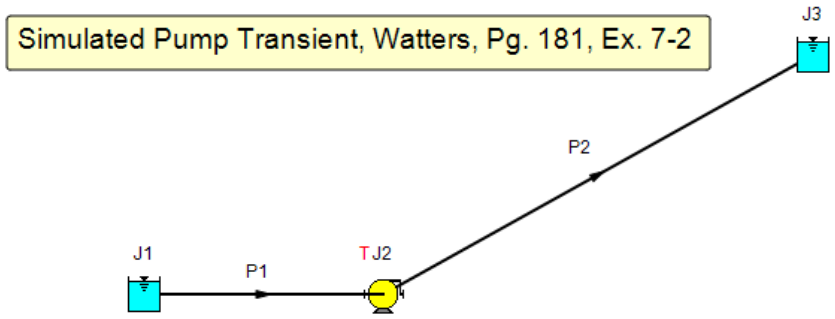

Verification Case 14

View Model Problem Statement

PRODUCT: AFT Impulse

TITLE: ImpVerify14.imp

REFERENCE: *Fluid Transients in Systems*, 1993, Prentice-Hall, E. Benjamin Wylie, Victor L. Streeter, Page 153, Ex. 7-1

FLUID: Water

ASSUMPTIONS: Wylie's method includes a combined discharge valve and pump four quadrant element. AFT Impulse does not support this combined element – the pump and valve must be modeled as separate elements. Thus the AFT Impulse model places the valve at the equivalent of one computing station downstream of the pump which is 72 feet. The total pipe length between pipes 1 and 2 is 1440 feet, the same as Wylie.

Because of this, the appropriate location to compare transient head and flow is the inlet of pipe 2, which represents the valve discharge. This data is shown below.

RESULTS:

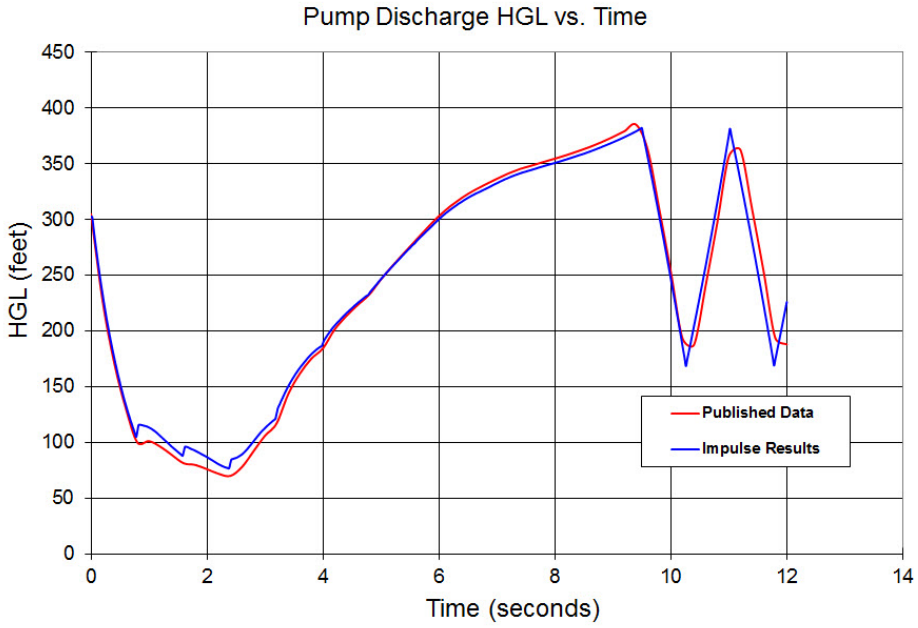

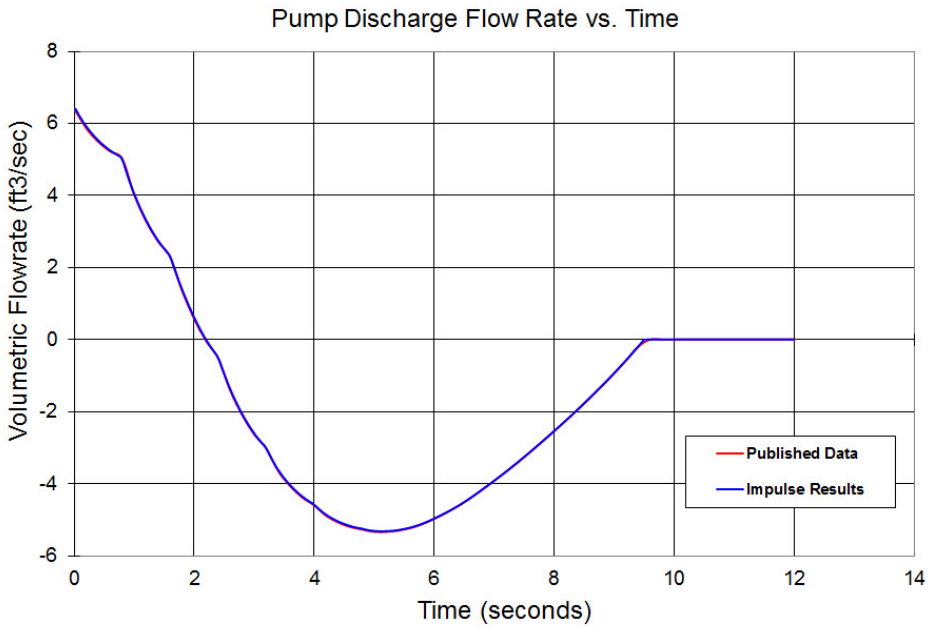

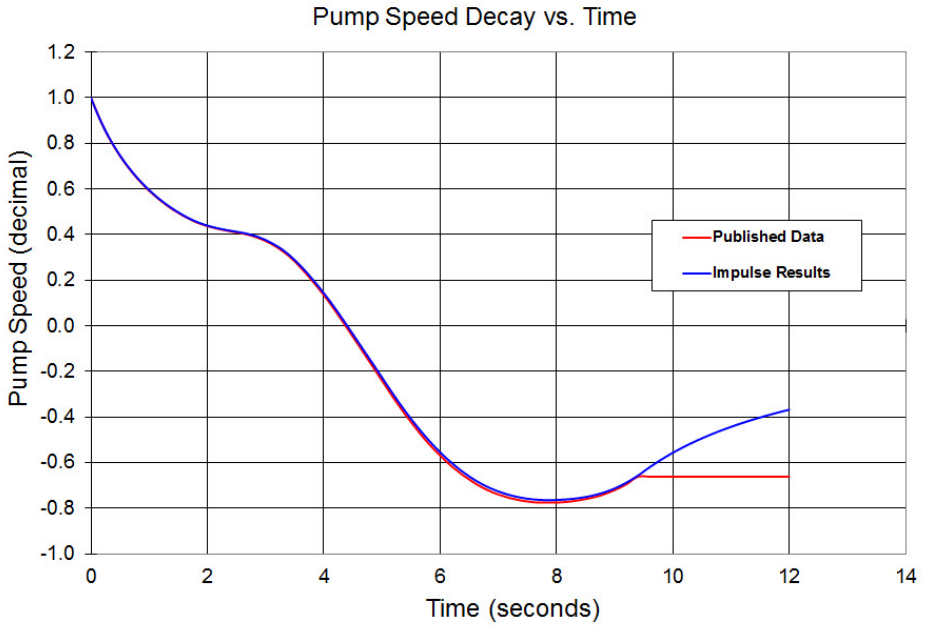

DISCUSSION:

The results in Wylie are based on a computer program in Appendix D which assumes that once the flow goes to zero at the pump discharge (this occurs when the valve closes at about 9.5 seconds) then the pump speed stays constant at whatever value it has at that time. This is not a completely valid assumption, and AFT Impulse does not assume this. Thus the pump speeds do not agree as well after this time. The HGL prediction is not impacted because it is downstream of the valve which, once closed, the pump speed can no longer impact.

List of All Verification Models

Verification Case 14 Problem Statement

Verification Case 14

Fluid Transients in Systems, 1993, Prentice-Hall, E. Benjamin Wylie, Victor L. Streeter, Page 153, Ex. 7-1.

Wylie Title Page

say 0.0001, τ should be set to zero, which effectively removes the pump from the system in favor of a closed valve.

Example 7-1

The pump in the system in Fig. 7-5 is to be analyzed for a pump failure, including a prescribed valve closure. The pump characteristic curve data for N_s = 1270 in Fig. 7-2 are used with H_R = 310 ft, Q_R = 6.3 ft^3/s, N_R = 1760 rpm, T_R = 730 lb-ft, and WR_g^2 = 187 lb-ft^2. The power is removed from the pump at time zero, and there is a 1.5-s delay before the valve begins to close.

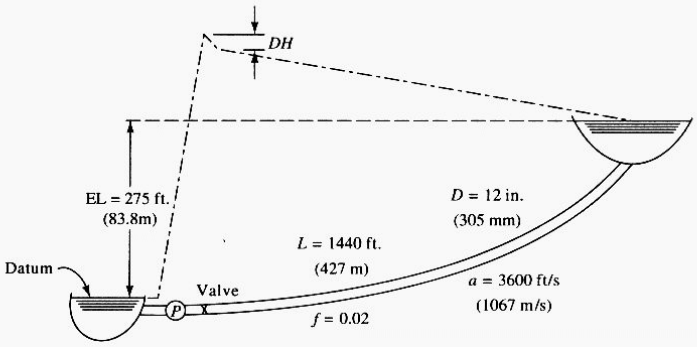

Figure 7-5 Pipeline system for pump failure.

The program to solve this problem, called PUMP, is provided in Fig. D-3a, Appendix D. Four reaches have been used in the pipeline in this example. The loss coefficient for the valve in the fully open position is identified by the variable CK. The prescribed valve motion is defined in the vector TAU with tabular values identified at equal intervals of time, DTAU. One of the first steps in the algorithm is to find the steady operating condition. This requires a simultaneous solution utilizing the pump characteristic head curve and the system characteristics, including the open valve. An estimated dimensionless velocity, VI, is provided in data to begin Newton's method search to find the initial operating point that matches the pump and system characteristics.

Output from the program for a particular specified valve operation is also presented in Fig. D-3b, Appendix D, while pressure, flow, and speed change are shown in Fig. 7-6. It is noted that this particular valve closure is not necessarily optimal in the sense of controlling the transient; it is only an illustration of system behavior. In the output it should be observed that the flow reverses at the pump before the rotational speed reverses, as would be anticipated when pumping against a gravity load. Another system response to observe in the output is the head–discharge relationship at the pump prior to the first reflection from the downstream reservoir. The results produce a straight line whose slope is the pipeline characteristic impedance.

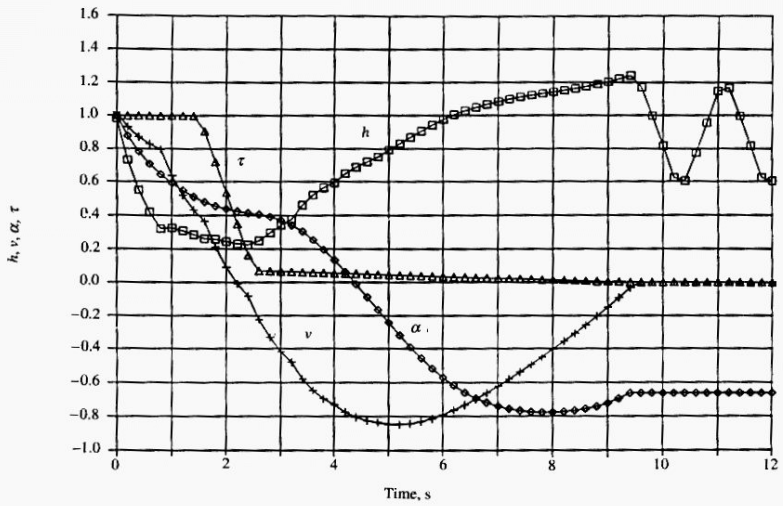

Figure 7-6 Example 7-1, dimensionless head, velocity, speed, and valve position.

```
 A, XL, EL, D, F=  3600.0  1440.0   275.0   1.000    .020
 QR,HR,TR,RN,WRR=     6.3   310.0   730.0  1760.0   187.0
   G,TM,TOL,VI,V=  32.200  12.000   .0002   .9000  1.0183
 N,KIT,JPR,IGRAF=       4       5       1       1
   CK, DTAU, TAU=   .300   .500
                   1.000  1.000  1.000  1.000   .535   .070   .065   .060
                    .055   .050   .045   .040   .035   .030   .025   .020
                    .015   .010   .005   .000

   TIME     TAU    ALPHA     BETA      V      Q(1)    Q(NS)      H(1)     H(NS)
    .000   1.000   1.000    1.001   1.018    6.415    6.415   304.836  275.000
    .200   1.000    .879     .775    .932    5.870    6.415   226.601  275.000
    .400   1.000    .784     .618    .872    5.491    6.415   171.095  275.000
    .600   1.000    .707     .504    .829    5.221    5.358   130.346  275.000
    .800   1.000    .645     .418    .798    5.024    4.620    99.721  275.000
   1.000   1.000    .592     .352    .638    4.022    4.090   101.025  275.000
   1.200   1.000    .548     .295    .520    3.279    3.701    95.899  275.000
   1.400   1.000    .511     .247    .431    2.718    2.740    88.364  275.000
   1.600    .907    .480     .210    .364    2.296    1.982    81.152  275.000
   1.800    .721    .455     .156    .213    1.345    1.384    79.647  275.000
   2.000    .535    .437     .109    .091     .574     .922    75.857  275.000
   2.200    .349    .424     .079   -.008    -.047    -.030    71.713  275.000
   2.400    .163    .414     .064   -.082    -.519    -.825    69.823  275.000
   2.600    .069    .405     .074   -.224   -1.414   -1.472    77.619  275.000
   2.800    .067    .392     .119   -.333   -2.100   -1.951    91.965  275.000
   3.000    .065    .371     .179   -.418   -2.636   -2.777   106.075  275.000
   3.200    .063    .343     .231   -.480   -3.026   -3.347   117.067  275.000
   3.400    .061    .305     .329   -.579   -3.649   -3.769   143.227  275.000
   3.600    .059    .255     .400   -.646   -4.073   -4.067   161.630  275.000
   3.800    .057    .197     .451   -.696   -4.384   -4.489   175.214  275.000
   4.000    .055    .133     .487   -.731   -4.605   -4.769   184.447  275.000
   4.200    .053    .064     .537   -.777   -4.894   -4.973   201.218  275.000
   4.400    .051   -.011     .559   -.806   -5.079   -5.118   213.173  275.000
   4.600    .049   -.088     .564   -.826   -5.202   -5.279   223.362  275.000
   4.800    .047   -.164     .563   -.837   -5.276   -5.373   232.712  275.000
********
   7.600    .019   -.775     .034   -.495   -3.117   -3.138   348.172  275.000
   7.800    .017   -.777     .005   -.449   -2.832   -2.853   351.345  275.000
   8.000    .015   -.777    -.018   -.403   -2.540   -2.562   354.321  275.000
   8.200    .013   -.773    -.037   -.356   -2.240   -2.262   357.490  275.000
   8.400    .011   -.766    -.060   -.307   -1.932   -1.956   361.036  275.000
   8.600    .009   -.756    -.089   -.256   -1.612   -1.641   364.757  275.000
   8.800    .007   -.741    -.126   -.203   -1.282   -1.314   369.045  275.000
   9.000    .005   -.721    -.168   -.149    -.938    -.973   373.769  275.000
   9.200    .003   -.695    -.214   -.092    -.578    -.617   378.987  275.000
   9.400    .001   -.663    -.261   -.032    -.199    -.243   384.955  275.000
   9.600    .000   -.663    -.261    .000     .000     .153   362.697  275.000
   9.800    .000   -.663    -.261    .000     .000     .574   309.532  275.000
  10.000    .000   -.663    -.261    .000     .000     .615   253.317  275.000
  10.200    .000   -.663    -.261    .000     .000     .242   193.473  275.000
  10.400    .000   -.663    -.261    .000     .000    -.152   187.491  275.000
  10.600    .000   -.663    -.261    .000     .000    -.572   240.528  275.000
  10.800    .000   -.663    -.261    .000     .000    -.614   296.644  275.000
*******
 HMAX,HMIN =   384.955      .000
```

Figure D-3(b) PUMP.FOR (Chapter 7) Output, Example 7-1

View Verification Case 14 Model

Verification Case 14

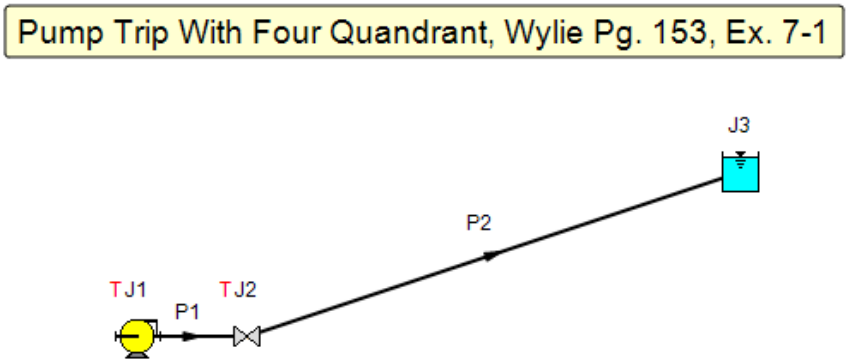

Verification Case 15

View Model Problem Statement

PRODUCT: AFT Impulse

TITLE: ImpVerify15.imp

REFERENCE:*Fluid Transients in Pipeline*, 1988, Nippon Kokan Technical Report, Overseas No. 52, Toshihiko Kamemura, et. al., Page 48, Case B.

FLUID: Water

ASSUMPTIONS: N/A

RESULTS:

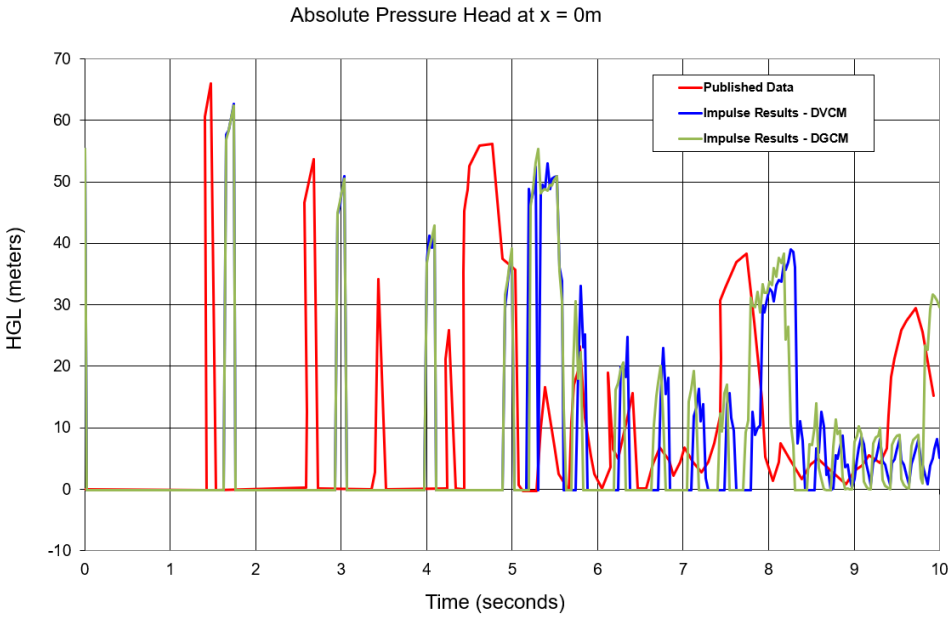

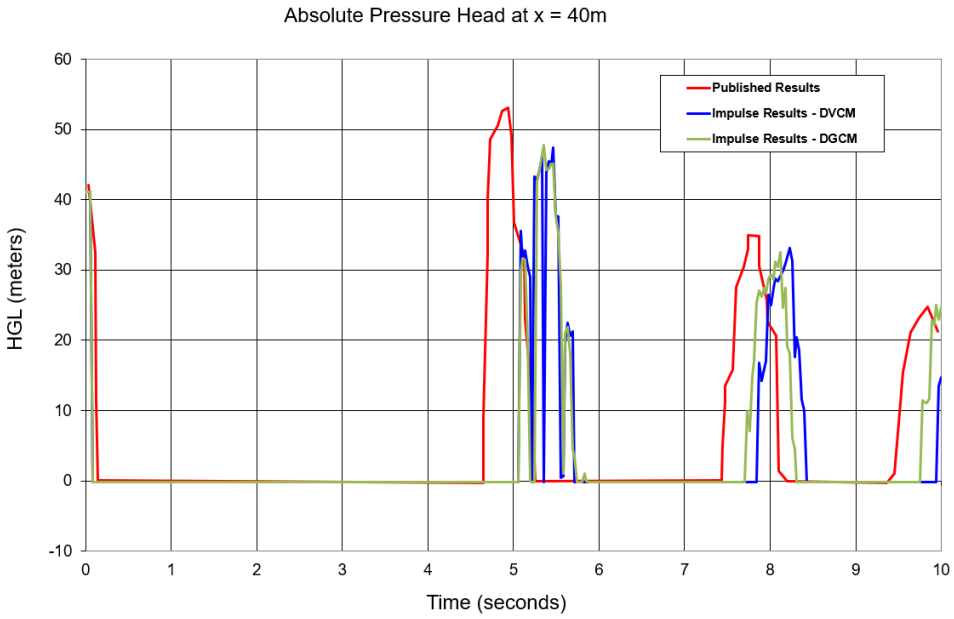
Absolute Pressure Head at x = 40m
Published Results
Impulse Results - DVCM
Impulse Results - DGCM
HGL (meters)
Time (seconds)
60
50
40
30
20
10
0
-10
0
1
2
3
4
5
6
7
8
9
10

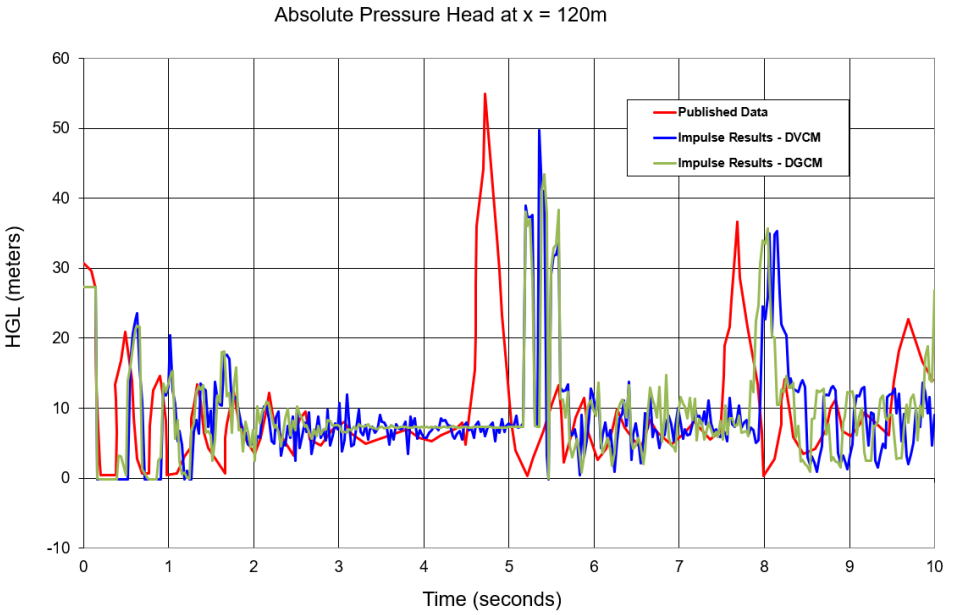
Absolute Pressure Head at x = 120m
Published Data
Impulse Results - DVCM
Impulse Results - DGCM
HGL (meters)
Time (seconds)
60
50
40
30
20
10
0
-10
0
1
2
3
4
5
6
7
8
9
10

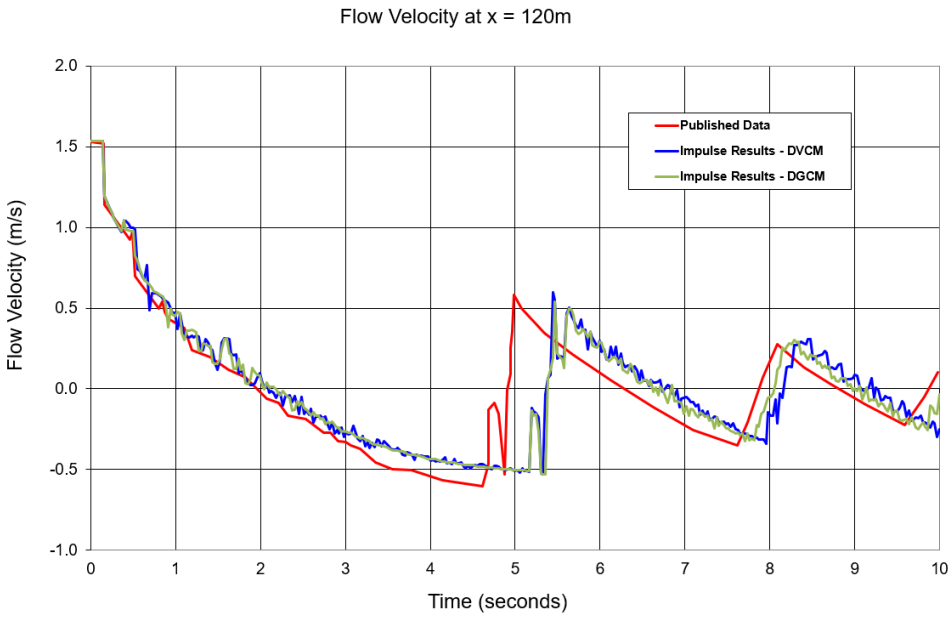

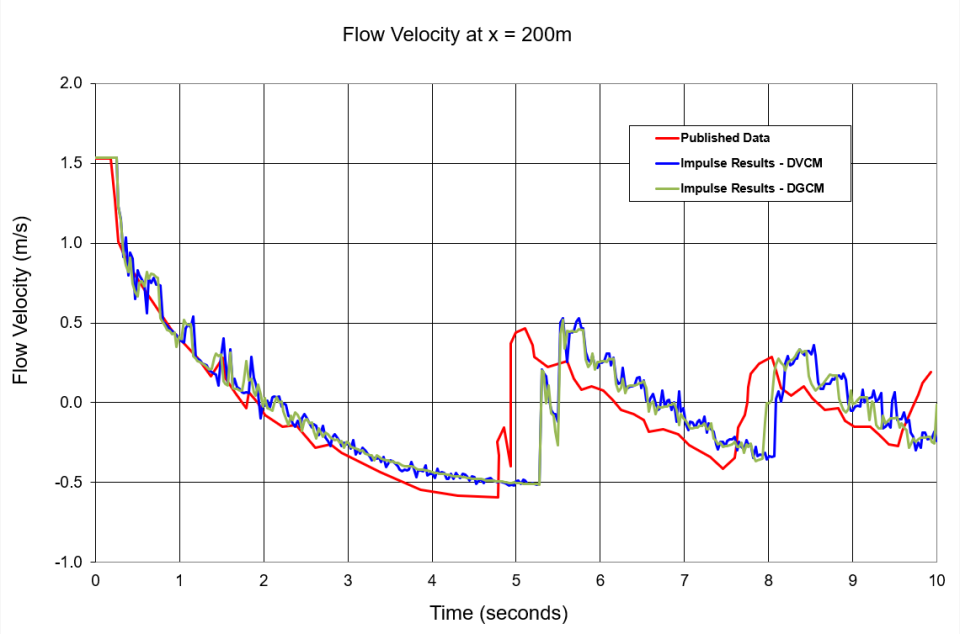

DISCUSSION:

All of the results from Impulse were compared to the measured results plotted in figures 13-17 found in the reference. This was accomplished by scanning the figures, and using digitization software to obtain values for the plotted results.

Figures 13-15 in the reference plot the results as Absolute Pressure Head, whereas Impulse plots pressure head as the Hydraulic Gradeline, which is a relative pressure. In the case of Figure 14, the results

for Hydraulic Gradeline plotted from Impulse had to be adjusted by 4.56 m to match the absolute pressure head due to the change in pipe elevation at x = 40m.

List of All Verification Models

Verification Case 15 Problem Statement

Verification Case 15

Fluid Transients in Pipeline, 1988, Nippon Kokan Technical Report, Overseas No. 52, Toshihiko Kamemura, et. al., Page 48, Case B.

Kamemura Title Page

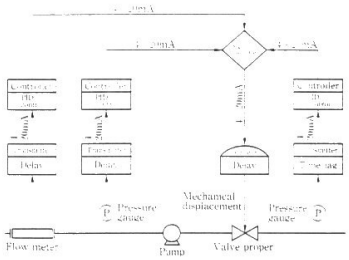

Fig. 5 Schematic of typical control valve

3.4 Application of SURGE 2

As described in Par. 3.1, the calculation results of SURGE 2 are output graphically, and hence evaluation of analyzed results can be done easily. Also, as the program contains almost all equipment used in the actual pipeline, it can calculate not only maximum or minimum pressure but also analyze sequence and control systems.

The following are examples of subjects that can be analyzed:

(1) Computation of adequate pump capacity and pipe diameter, by obtaining flow rate and pressure balance at each part of the piping system, based on specified boundary condition, piping layout, and kinds of equipment connected to the piping.

(2) In the case a pipeline is operated according to a certain sequence, the calculation of maximum pressure and judgement of negative pressure produced in the pipeline, by following the changes in the pressure and flow rate in the pipeline with the passage of time.

(3) Determination of an optimum operation sequence such as line change, valve stroke, and start-up and stop of pumps.

(4) Function check of control valves.

(5) In the case a pulsation occurs in the flow, presence of resonance in fluid vibration.

(6) Determination of optimum specifications for equipments such as accumulators, surge tanks, surge relievers, and air valves.

(7) Capacity calculation of slop tanks for surge relievers.

(8) Comparison between fluctuation pattern of pressure or flow rate at occurrence of leakage and fluctuation pattern caused by other factors.

4. Experiment and analysis of liquid column separation phenomenon

4.1 Outline

Analysis method of SURGE 2 follows that of SURGE 1 which has an application record of over ten years, and its reliability can be regarded quite high, with the exception of liquid column separation. Therefore, this paper presents the results of experiments and analysis with regard to liquid column separation phenomenon and aims to verify reliability of SURGE 2.

There are not many actual pipeline data regarding liquid column separation phenomenon in the world. Accordingly, in order to obtain data for comprehension and analysis of liquid column separation phenomenon, fundamental and practicable experiments of liquid column separation were carried out in two kinds of pipelines. These experiments were carried out with the cooperations of the Takenaka and Kitagawa Laboratory, Faculty of Engineering, Tokyo Institute of Technology.

4.2 Test pipelines

The outlines of the test pipelines A and B used in the experiments are shown in *Fig. 6* and *Fig. 7*. Both pipelines are made of transparent acrylic pipe, 200m long, 15.2mm inside diameter, and 5mm wall thickness, so that the entire inside of the pipeline can be observed. The pipeline is built of ten rounds of track, each round beings 20m long, and its downstream end is connected to a reservoir with 0.5m pressure head. However, in test pipeline B, one round of 20m track is vertically raised so that the highest part of the pipeline reaches 4.56m in height.

The upstream end of the pipeline is connected to a pump and a valve. When water is pumped into the pipeline and the valve at upstream end is instantaneously closed, transients phenomenon occurs. Initial flow rate and initial pressure at the upstream end were measured by the area flow meter and the Bourdon tube pressure gauge which were inserted immediately in front of the valve at upstream end.

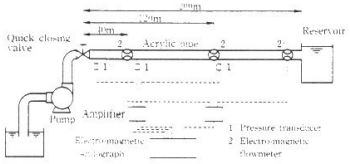

Fig. 6 Schematic of test pipeline: case A

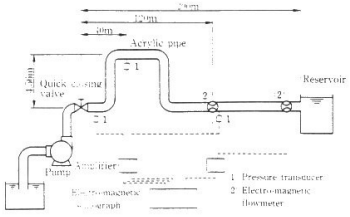

Fig. 7 Schematic of test pipeline: case B

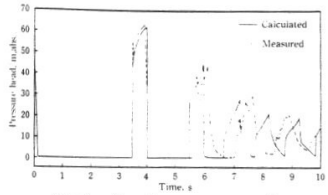

Fig. 8 Case A: pressure at x = 0m

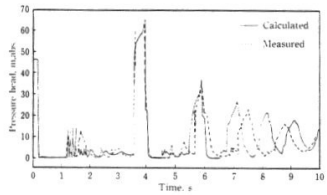

Fig. 9 Case A: pressure at x = 40m

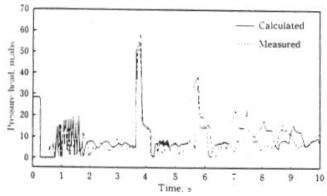

Fig. 10 Case A: pressure at x = 120m

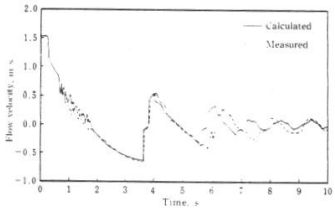

Fig. 11 Case A: flow velocity at x = 120m

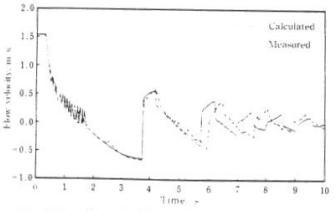

Fig. 12 Case A: flow velocity at x = 200m

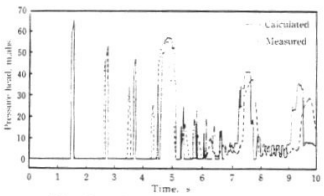

Fig. 13 Case B: pressure at x = 0m

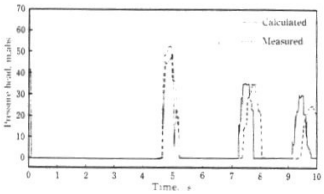

Fig. 14 Case B: pressure at x = 40m

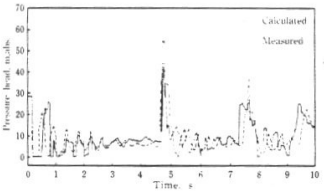

Fig. 15 Case B: pressure at x = 120m

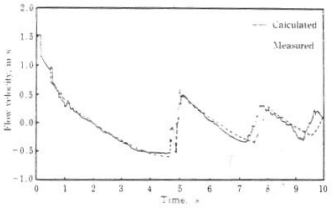

Fig. 16 Case B: flow velocity at x = 120m

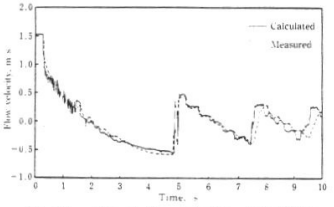

Fig. 17 Case B: flow velocity at x = 200m

Also, pressure and flow rate fluctuations at transients were measured by the semiconductor pressure transducer and the electro-magnetic flow meter and recorded by the electro-magnetic oscillograph.

4.3 Experiments

Experiments were conducted in two cases, case A and case B. Case A used test pipeline A in which the upstream end valve was instantaneously closed to produce liquid column separation immediately behind the valve. Case B used test pipeline B in which the upstream end valve is instantaneously closed to produce liquid column separations immediately behind the valve and at higher location. Experimental conditions are shown in *Table 1*.

Propagation speed of pressure wave was obtained by producing transient phenomenon without accompanying liquid column separation and by recording wave forms.

4.4 Comparison between test results and analysis results

4.4.1 Case A

The state of liquid column separation occurring immediately behind the valve is shown in *Photo 1*, and the test and analysis results in *Fig. 8* to *Fig. 12*.

Pressure at $x = 0$ m was dropped to vapor pressure by closing the valve and rarefaction wave was propagated to downstream side, thus causing pressures at other measuring points to be dropped to vapor pressure. Pressure at $x = 120$ m started to violently oscillate after it had once dropped to vapor pressure. During this period, flow velocity was reduced and the direction of flow reversed. The first re-form occurred in 3.3 seconds after the closure of the valve, and thereafter, separation and re-form were repeated several times and transients phenomenon attenuated.

As can be seen from *Fig. 8* to *Fig. 12*, calculated values and measured values well agree with each other.

4.4.2 Case B

The state of liquid column separation which occurred at high location is shown in *Photo 2*, and the results of experiment and analysis in *Fig. 13* to *Fig. 17*.

Pressure at $x = 0$ m was dropped to vapor pressure by closing the valve and rarefaction wave was propagated to downstream side, thus producing large cavities immediately behind the valve and the high location. Also, flow speed was rapidly reduced with propagation of rarefaction wave. The cavity produced immediately behind the valve collapsed quicker than the one produced at the high location. And, after separation and re-form were repeated four times immediately behind the valve, the vapor cavity at the high location collapsed and re-form pressure generated.

As shown in *Fig. 13* to *Fig. 17*, in the first re-form at the high location, there are good agreements between the calculated and measured values both in re-form pressure and time. The calculated value thereafter differs somewhat from the experimental value

Table 1 Test conditions

	Initial pressure at upstream end m. aq.	Initial flow velocity m/s	Water temperature ℃	Speed of pressure pulse m/s
Case A	38.2	1.53	17	810
Case B	48.2	1.53	20	815

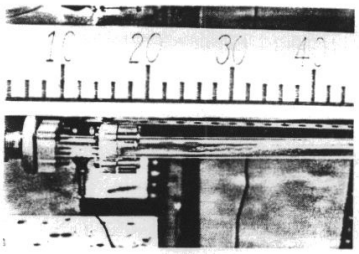

Photo 1 Liquid column separation at valve downstream

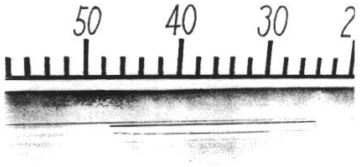

Photo 2 Liquid column separation at high location

but is sufficient accurate for engineering purpose.

5. Conclusion

The contents of this paper can be summarized as follows:

(1) The program, SURGE 2, which can analyze liquid column separation phenomenon in a pipeline, has been developed by utilizing the characteristics method which introduces released gas dispersion model.

(2) SURGE 2 is a general purpose program which can analyze not only the liquid column separation phenomenon but also any fluid transients phenomenon in a pipeline.

(3) Experiments of liquid column separation were carried out using test pipelines 15.2 mm in diameter and 200 m in length. It was found that the experimental results well agreed with the calculated

View Verification Case 15 Model

Verification Case 15

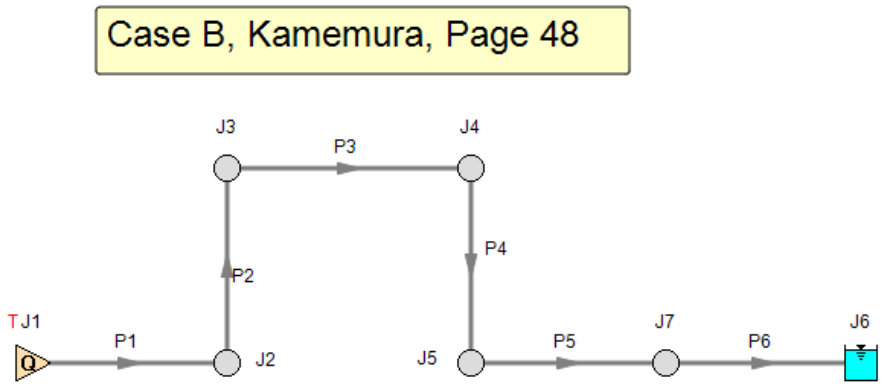

Verification Case 16

View Model Problem Statement

PRODUCT: AFT Impulse

TITLE: ImpVerify16.imp

REFERENCE: *Waterhammer Analysis*, John Parmakian, Dover Publishing, 1963, Page 75 - 86.

FLUID: Unspecifed. Specific gravity is 1.155. Viscosity is not relevant because friction factors are assumed. Liquid bulk modulus is not relevant because all wavespeeds are specified.

ASSUMPTIONS: Parmakian assumes the pipes are frictionless. The Impulse model assumes the friction factors are very small (0.001). The specific speed of the example pumps was 0.79 (2160 gpm units). The four quadrant data set from Kittredge of 0.71 (1935 gpm units) was assumed. Neglect cavitation.

From Parmakian's Figure 56 on page 86, it was estimated that the pump discharge elevation was 36 feet and that the pipe traveled horizontally for 1000 feet before rising to the discharge reservoir. It was also estimated that the pipe entered the discharge reservoir at 200 feet.

RESULTS:

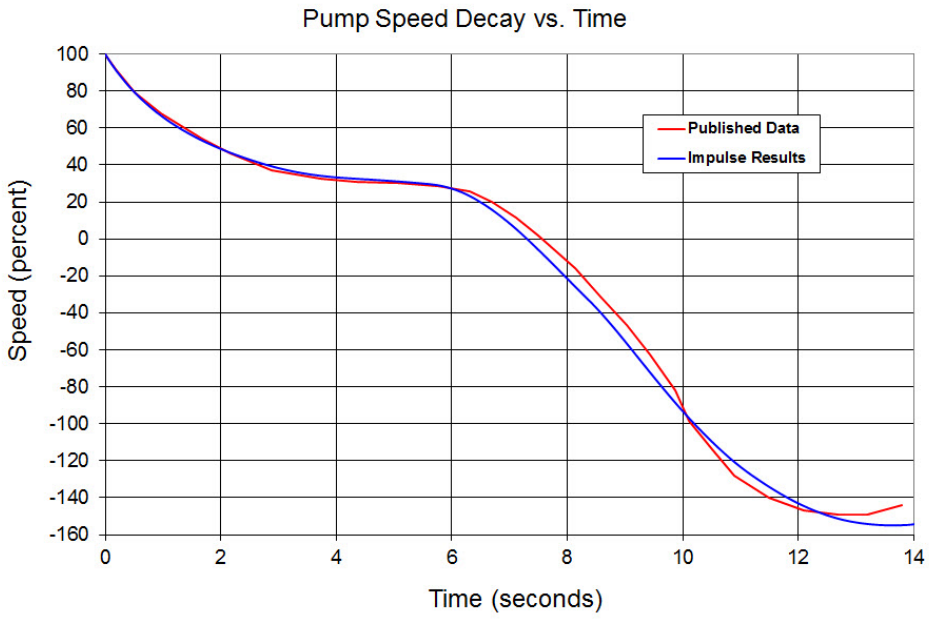

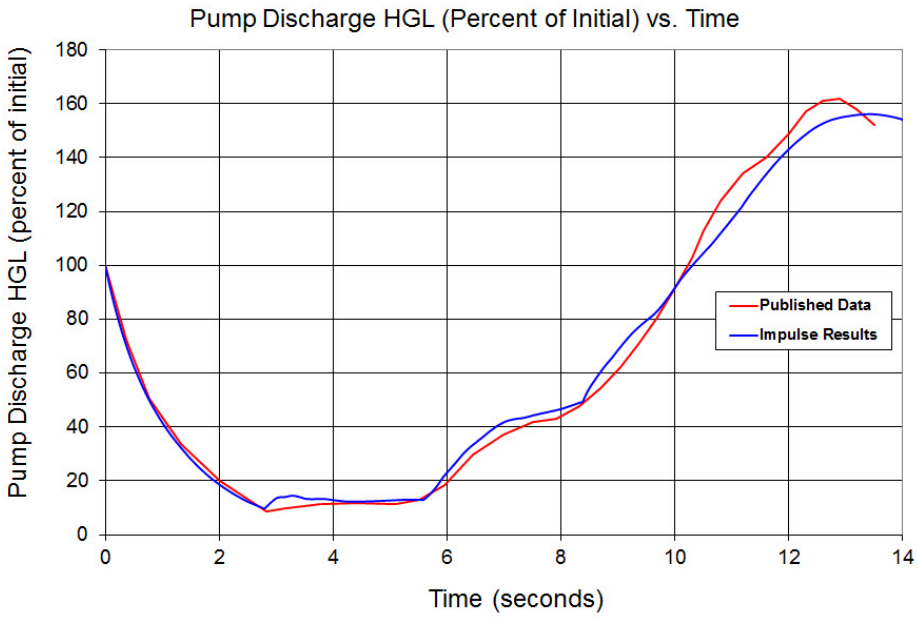
Pump Discharge HGL (Percent of Initial) vs. Time
Pump Discharge HGL (percent of initial)
180
160
140
120
100
80
60
40
20
0
0
2
4
6
8
10
12
14
Time (seconds)
Published Data
Impulse Results

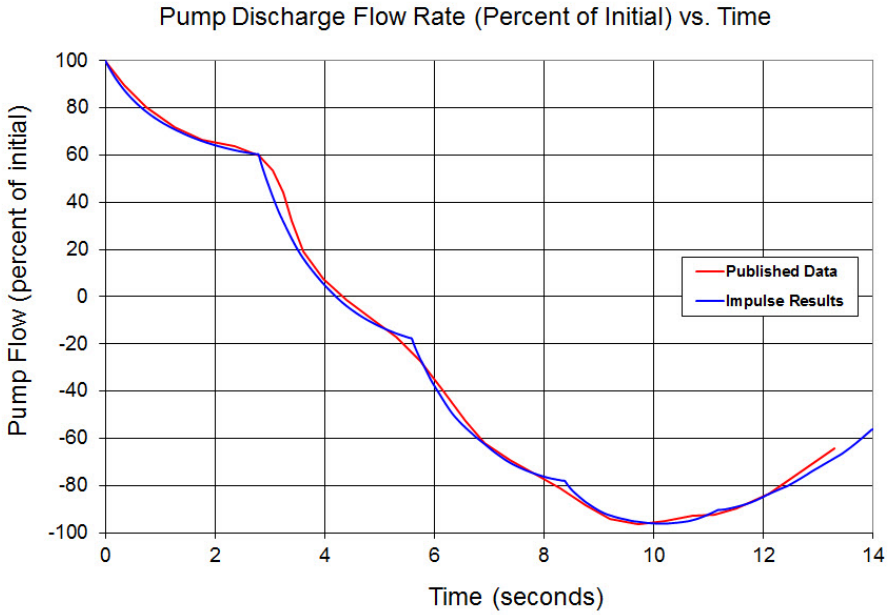
Pump Discharge Flow Rate (Percent of Initial) vs. Time
Pump Flow (percent of initial)
100
80
60
40
20
0
-20
-40
-60
-80
-100
0
2
4
6
8
10
12
14
Time (seconds)
Published Data
Impulse Results

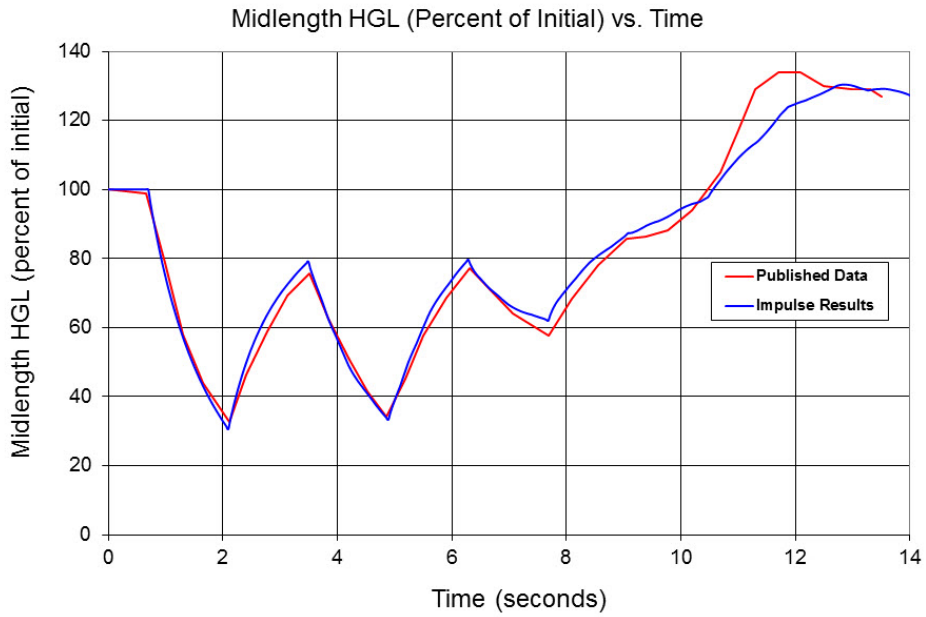

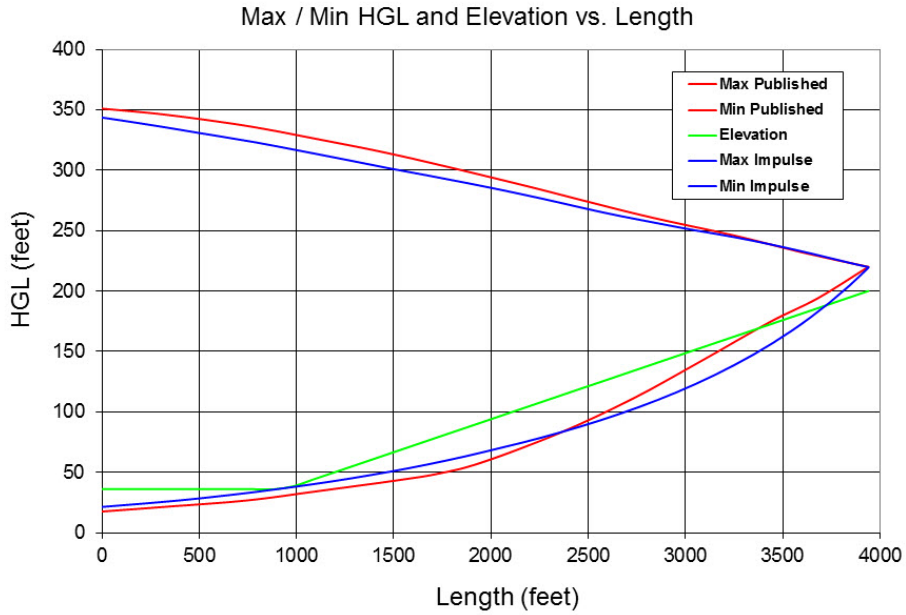

DISCUSSION:

Parmakian obtained these results using graphical waterhammer methods.

The specific speed of the example pumps was 0.79 (2160 gpm units). AFT Impulse has a data set from Thorley for exactly this specific speed. But agreement with the predictions was marginal and is not shown. The next closest specific speed of 0.71 (1935 gpm units) gave very good agreement and is shown above. The classic data from Donsky for specific speed of 0.46 (1270 gpm units) was also ran and gave good agreement (but is not shown).

List of All Verification Models

Verification Case 16 Problem Statement

Verification Case 16

Waterhammer Analysis, John Parmakian, Dover Publishing, 1963, Page 75 - 86.

turbine, reaches runaway speed in reverse. As the pump approaches runaway speed, the reverse flow through the pump reduces rapidly, and this reduction in the flow produces a pressure rise at the pump and along the length of the discharge line.

In order to determine the transient hydraulic conditions at the pump and discharge line subsequent to a power failure at the

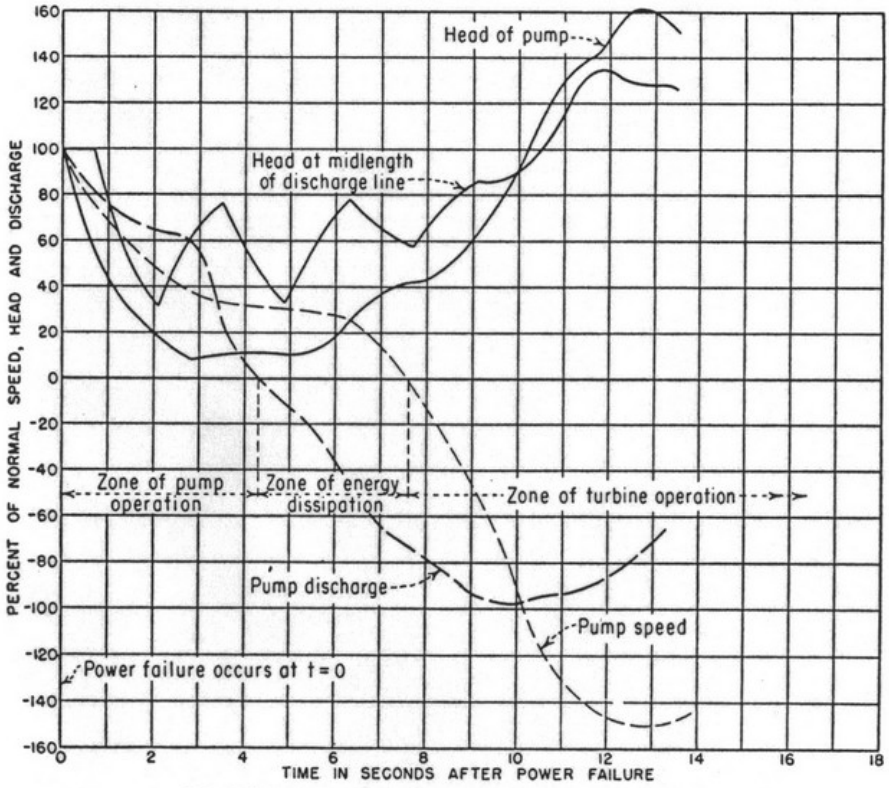

TRANSIENT CONDITIONS FOLLOWING POWER FAILURE

Figure 47

46. Graphical waterhammer analysis

Consider the pumping plant installation shown in Figure 54. If a power failure occurs at all three pump motors, $2\rho = 2.31$ and $K_1 = 0.224$. For a time interval $\Delta t = L/4a$,

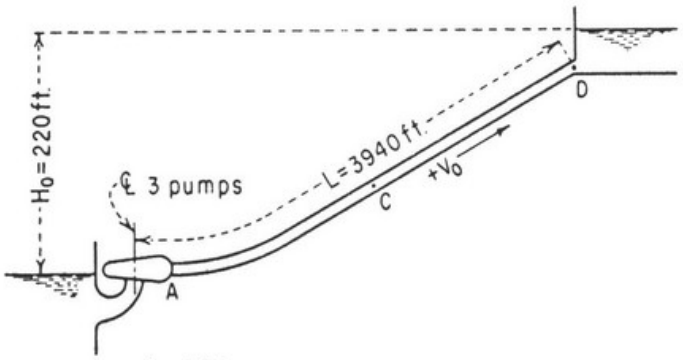

D = 32 in.
e = $\frac{3}{16}$ in.
a = 2820 ft. per sec.
V_0 = 5.81 ft. per sec. (for 3 pumps)
Q_0 = 33.7 cu. ft. per sec. (for 3 pumps)
A = 5.81 sq. ft.
$H_0 = H_R$ = 220 ft.
Pump motor rating = 400 horsepower for each pump and motor.
WR^2 of rotating parts = 384.9 lb. $ft.^2$ for each pump and motor.
Pump speed = 1760 rpm.
Pump efficiency = 84.7 percent
ρ = 1.155
$\frac{L}{a}$ = 1.397 sec.

Figure 54

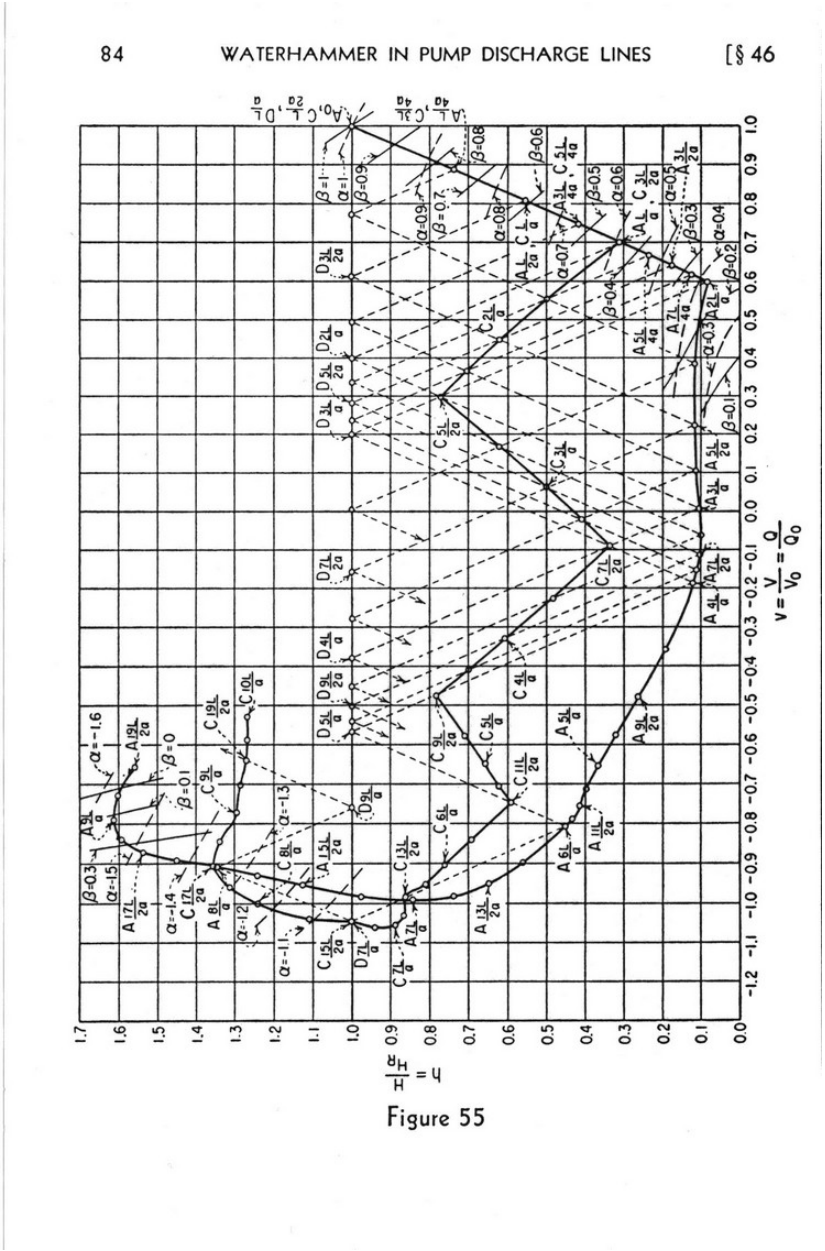
84 WATERHAMMER IN PUMP DISCHARGE LINES [§ 46
$v = \frac{V}{V_0} = \frac{Q}{Q_0}$
$\frac{\alpha}{H} = h$

Figure 55

points are shown in Table 5 and the graphical waterhammer solution is completed as shown in Figure 55, from which the following limiting values are read:

Maximum drop in head at pump

$$= 0.92H_0 = 202 \text{ feet.}$$

Maximum drop in head at mid-length of discharge line

$$= 0.69H_0 = 152 \text{ feet.}$$

Maximum head rise at pump

$$= 0.61H_0 = 134 \text{ feet.}$$

Maximum head rise at mid-length of discharge line

$$= 0.35H_0 = 77 \text{ feet.}$$

A time history of the head, flow, and speed changes as obtained from the graphical solution is shown in Figure 47.

points are shown in Table 5 and the graphical waterhammer solution is completed as shown in Figure 55, from which the following limiting values are read:

Maximum drop in head at pump

$$= 0.92H_0 = 202 \text{ feet.}$$

Maximum drop in head at mid-length of discharge line

$$= 0.69H_0 = 152 \text{ feet.}$$

Maximum head rise at pump

$$= 0.61H_0 = 134 \text{ feet.}$$

Maximum head rise at mid-length of discharge line

$$= 0.35H_0 = 77 \text{ feet.}$$

A time history of the head, flow, and speed changes as obtained from the graphical solution is shown in Figure 47.

47. Water column separation

The maximum positive and negative pressure changes obtained from the waterhammer solution are plotted on the discharge line profile in Figure 56 to show the limiting pressures for

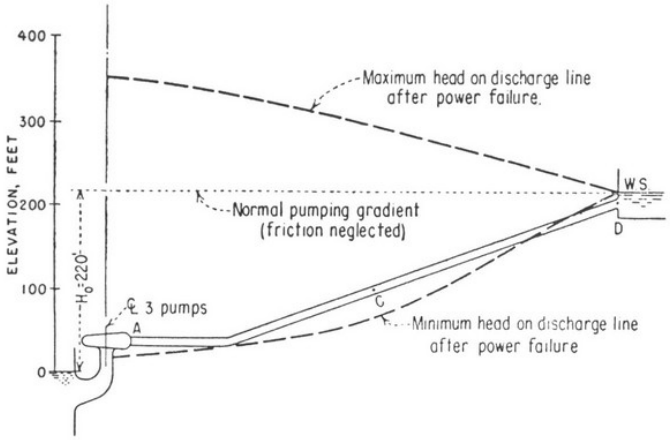

Figure 56

which the discharge line should be designed. When the minimum pressure at any point along the pump discharge line reaches the vapor pressure of water, the waterhammer solution is no longer valid. If this subatmospheric pressure condition inside the pipe persists for a sufficient period, the liquid water column parts and is separated by a section of vapor. Water column separation sometimes occurs during the initial negative surge waves on long pump discharge lines at high points which are near the hydraulic gradient. Wherever possible, this condition should be avoided by using either a surge tank, air chamber, or larger motor WR^2 because of the high pressure created when the two liquid water columns rejoin. When water column separation cannot be avoided, special means must be taken to minimize the violence of impact due to the rejoining of the water columns. This can be accomplished by positioning special control valves or other protective devices which will either reduce the reverse velocity of the upper column or increase the reverse velocity of the lower water column.

View Verification Case 16 Model

Verification Case 16

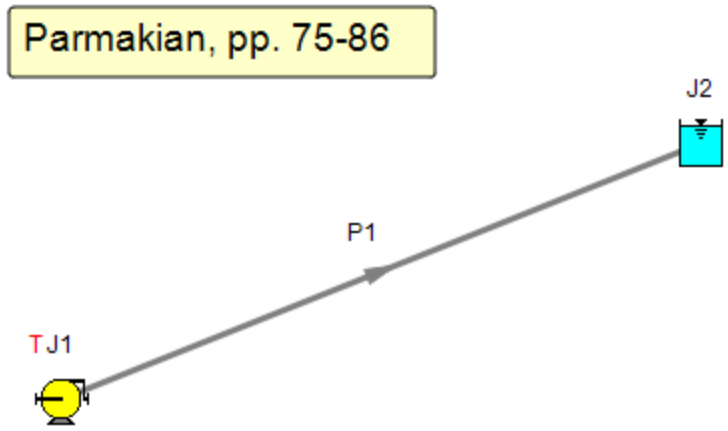

Verification Case 17

View Model Problem Statement

PRODUCT: AFT Impulse

TITLE: ImpVerify17.imp

REFERENCE: Watters, G.Z., Modern Analysis and Control of Unsteady Flow in Pipelines, Ann Arbor Science Publishers Inc. pp. 170-173, Example 7-1

FLUID: Water

ASSUMPTIONS: Transient cavitation turned off

RESULTS:

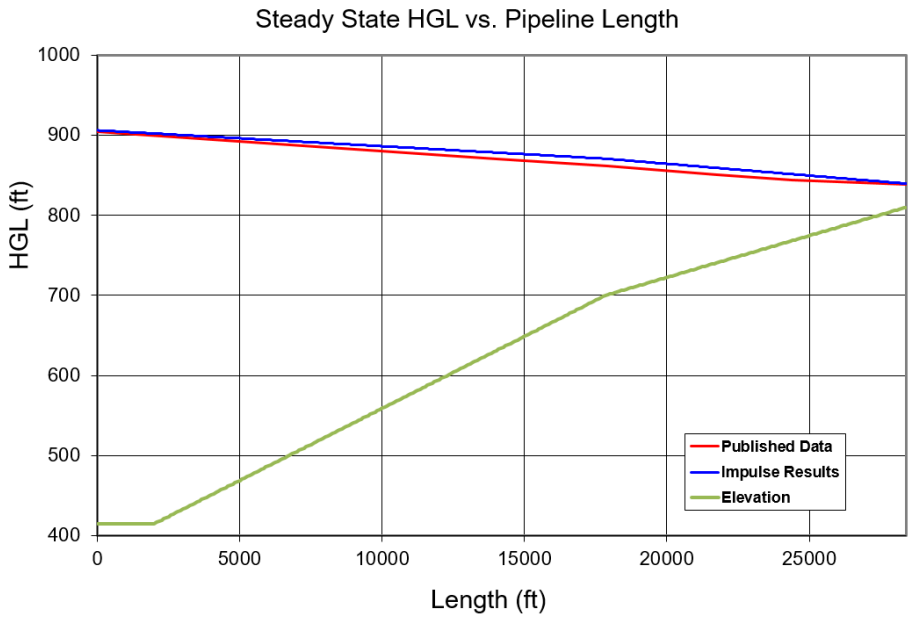

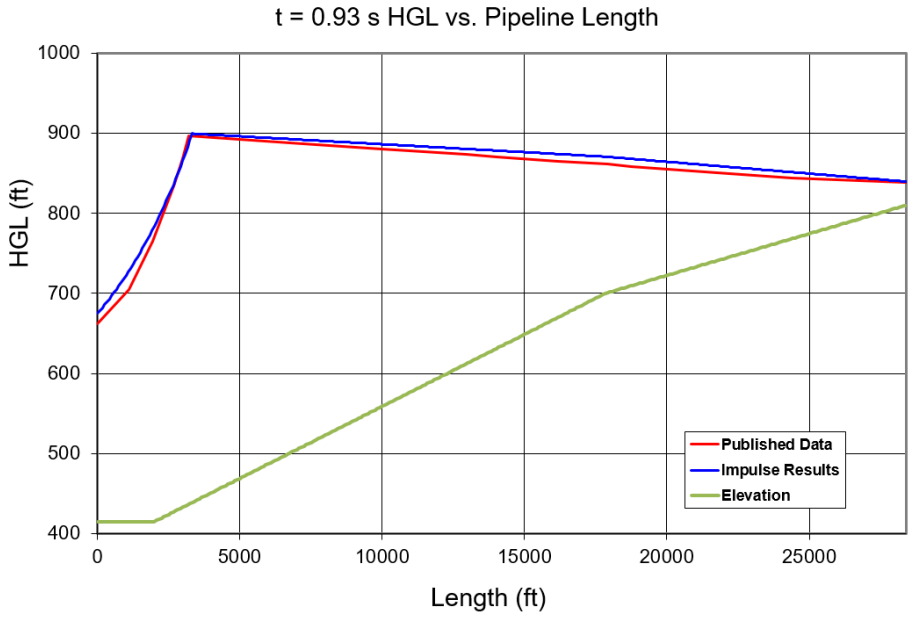
t = 0.93 s HGL vs. Pipeline Length
HGL (ft)
1000
900
800
700
600
500
400
0
5000
10000
15000
20000
25000
Length (ft)
Published Data
Impulse Results
Elevation

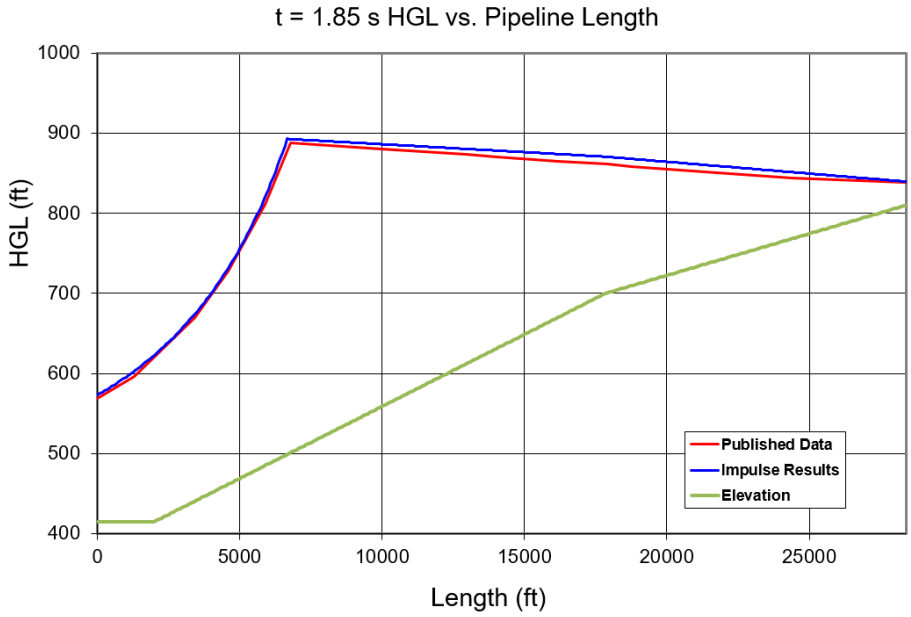
t = 1.85 s HGL vs. Pipeline Length
HGL (ft)
1000
900
800
700
600
500
400
0
5000
10000
15000
20000
25000
Length (ft)
Published Data
Impulse Results
Elevation

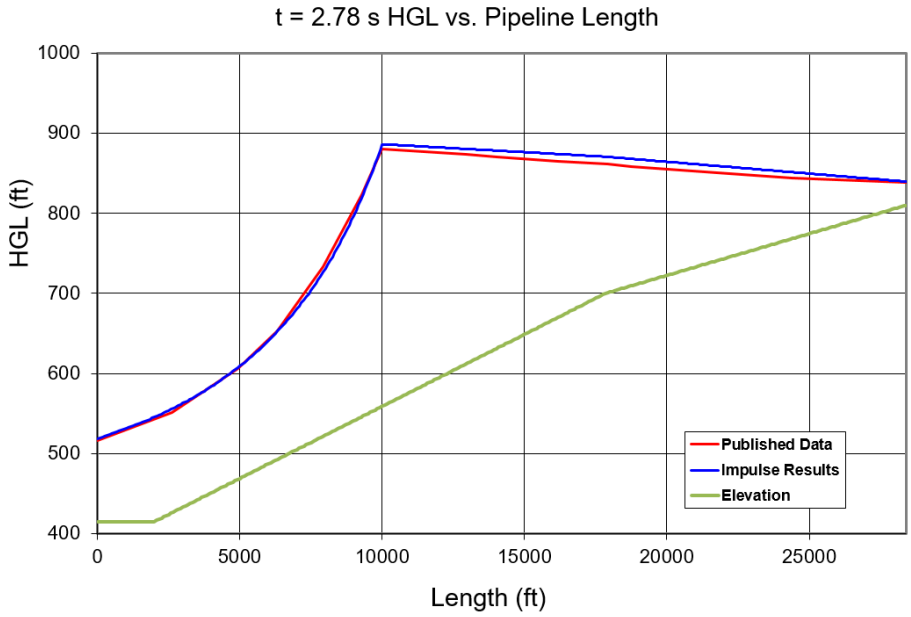
t = 2.78 s HGL vs. Pipeline Length
HGL (ft)
1000
900
800
700
600
500
400
0
5000
10000
15000
20000
25000
Length (ft)
Published Data
Impulse Results
Elevation

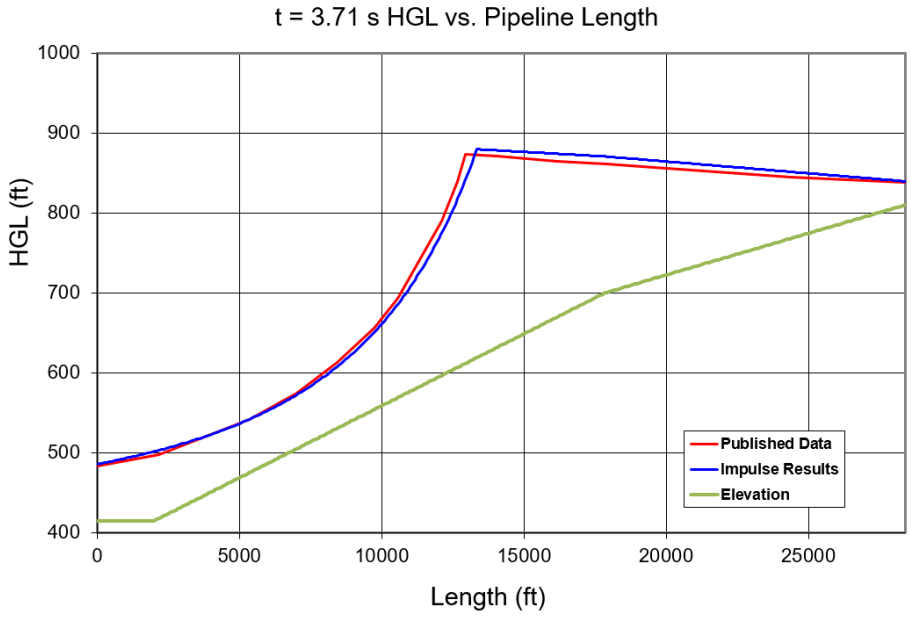
t = 3.71 s HGL vs. Pipeline Length
HGL (ft)
1000
900
800
700
600
500
400
0
5000
10000
15000
20000
25000
Length (ft)
Published Data
Impulse Results
Elevation

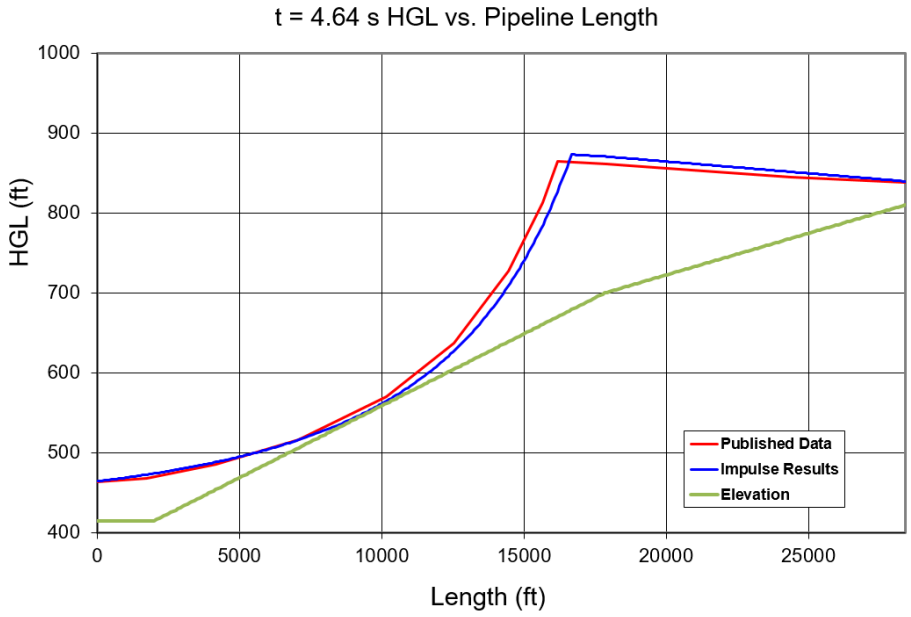

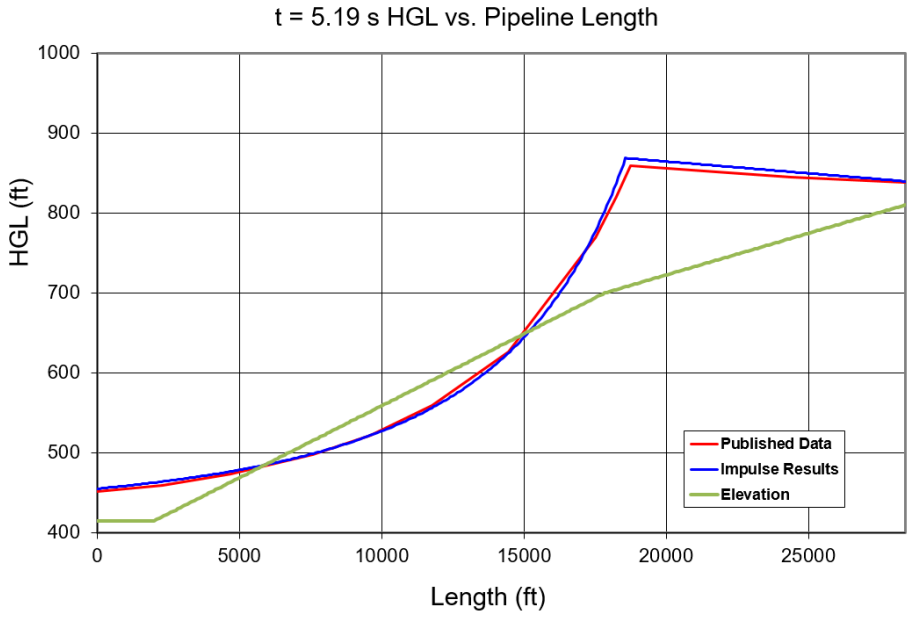

DISCUSSION:

Column separation would occur after 5.19 seconds and Watter's model did not account for this so he stopped his model at this point. AFT Impulse can model column separation, but for the purposes of this verification the cavitation capabilities are turned off in the AFT Impulse model. This will result in the warning saying system pressure has gone below vapor pressure.

List of All Verification Models

Verification Case 17 Problem Statement

Verification Case 17

Watters, G.Z., Modern Analysis and Control of Unsteady Flow in Pipelines, Ann Arbor Science Publishers Inc. pp. 170-173, Example 7-1

Watters Title Page

H_p/N^2 vs. Q/N will be a sequence of straight line segments (see Figure 7-5). The equation of the straight line over the anticipated range of Q/N is

$$\frac{H_p}{N^2} = \left[\frac{H_A - H_B}{Q_A - Q_B}\frac{Q}{N} + H_B - Q_B\frac{H_A - H_B}{Q_A - Q_B}\right] N_{st} \quad \text{.....(7-28)}$$

where N_{st} is the number of stages for each of the pumps. Condensing this equation to the form

$$\frac{H_p}{N^2} = \left[C_7\frac{Q}{N} + C_8\right] N_{st} \quad \text{.....(7-29)}$$

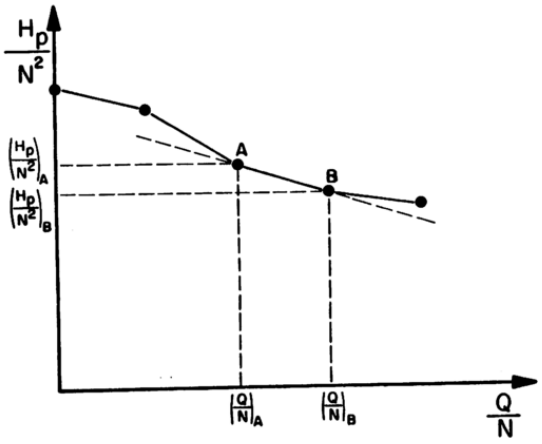

Figure 7-5. Piecewise linear representation of H_p/N^2 vs. Q/N values.

we can now combine Equation 7-29 easily with the other appropriate equations. The result of such a combination gives

$$V_{P_d} = \frac{\frac{C_1}{C_2} + N_{st}N^2C_8 + \frac{C_3}{C_4}}{\frac{1}{C_4} + \frac{A_d}{C_2A_s} - \frac{N\,C_7A_dN_{st}}{N_{pu}}} \quad \text{.....(7-30)}$$

where N_{pu} is the number of pumps in parallel. If $V_{P_s} > 0$, then Equations 7-21 through 7-5 can be used to find the remaining unknowns.

In addition, we must check H_p. If $H_p < 0$, then we set $H_p = 0$ and $H_{P_s} = H_{P_d}$ and compute the unknown velocity values from the following equations:

$$V_{P_d} = \frac{C_1C_4 + C_2C_3}{C_2 + C_4\frac{A_d}{A_s}} \quad \text{.....(7-31)}$$

$$V_{P_s} = \frac{A_d}{A_s}V_{P_d} \quad \text{.....(7-32)}$$

The Equations 7-21 and 7-22 can be used to find H_{P_s} and H_{P_d}.

If, however, V_{P_1} is negative, then $V_{P_s} = V_{P_d} = 0$ and Equations 7-21 and 7-22 are used to compute H_{P_s} and H_{P_d}. Also we must check Q/N and if we are outside the interval A-B, a new set of coefficients C_7 and C_8 must be computed and the solution process repeated.

Example 7-1

Four parallel pumps are to be used to pump approximately 11,000 gpm from a reservoir at elevation 395 feet to a storage reservoir whose surface elevation is 840 feet (see Figure 7-6).

The pump discharge lines are check-valved and manifolded into a single welded steel pipeline 30 inches in diameter. The pipe extends horizontally from the pump station at elevation 415 feet for a distance of 2000 feet. It then slopes upward for a distance of 3 miles to elevation 700 feet. The remaining two miles of pipe are reinforced concrete and it slopes upward to enter the storage reservoir at elevation 810 feet.

The f-value and wave speed in the steel pipe are 0.0128 and 3590 fps respectively. For the concrete pipe, these values are 0.0190 and 3486 fps.

The pumps are Worthington 15H-277 five-stage turbine pumps with characteristics shown on the following page (Courtesy of the Worthington Pump Corp). The 10 19/32-inch impeller is used. The moment of inertia of the rotating hardware and water is estimated to be 475 lb-ft².

The consequences of complete pump power failure to the system are to be found in the absence of any surge control devices.

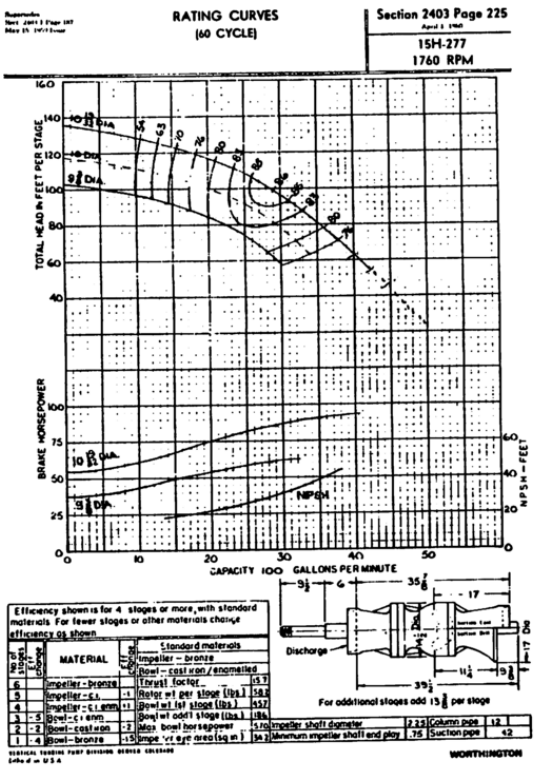

Solution

Program no. 8 for complete power failure to a source pump configuration is used. A program listing follows in Figure 7-7.

The data cards necessary to perform the computer simulation are shown below. A plot of the EL-HGL vs. time up to the point of column separation is shown on Figure 7-6.

Column separation occurs at 5 seconds after power failure. Once column separation occurs, the analysis technique is no longer valid and execution of the computer program should be terminated.

DATA

```
$SPECS NPIPES=3,IOUT=5,NPARTS=3,THAX=10.,HATM=32.,HRES=848.,ZEND=810.,
      QACC=.50  $END
        1 30.       2000.      .0120      3590.      415.
        2 30.      15040.      .0120      3590.      415.
        3 30.      10560.      .0190      3486.      700.
$PUMPS NPUMPS=4,RPM=1760.,HRSQ=675.,HSTAGE=5,HSUMP=395.,
  QH=0.,1000.,2000.,3000.,4000.,5000.,
  HHSQ=136.,128.,117.,96.,63.,24.,
  THSQ=55.,61.,75.,87.,93.,95.,
$END
```

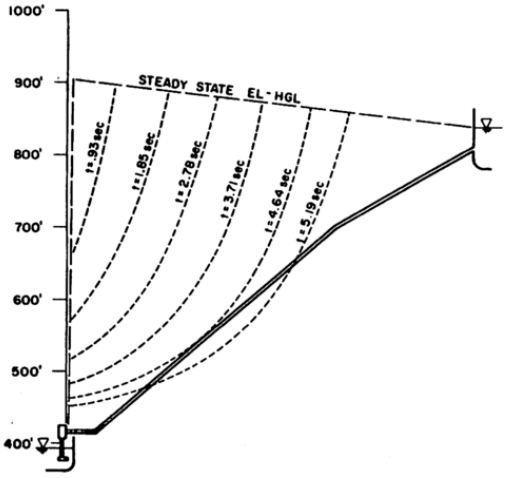

Figure 7-6. Pressure wave propagation as a result of pump power failure.

View Verification Case 17 Model

Verification Case 17

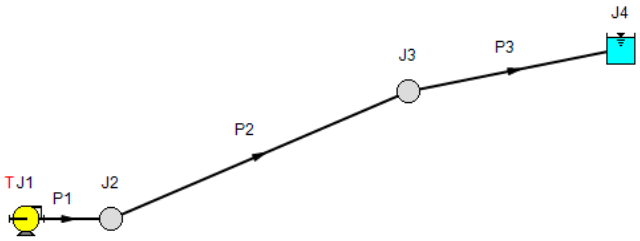

Watters, G.Z., Modern Analysis and Control of Unsteady Flow in Pipelines, Ann Arbor Science Publishers Inc. pp. 170-173, Example 7-1

Verification Case 18

View Model Problem Statement

PRODUCT: AFT Impulse

TITLE: ImpVerify18.imp

REFERENCE: M. H. Chaudhry, *Applied Hydraulic Transients*, 3rd ed. Springer, pp. 102-104, 527-533.

FLUID: Water

ASSUMPTIONS: N/A

RESULTS:

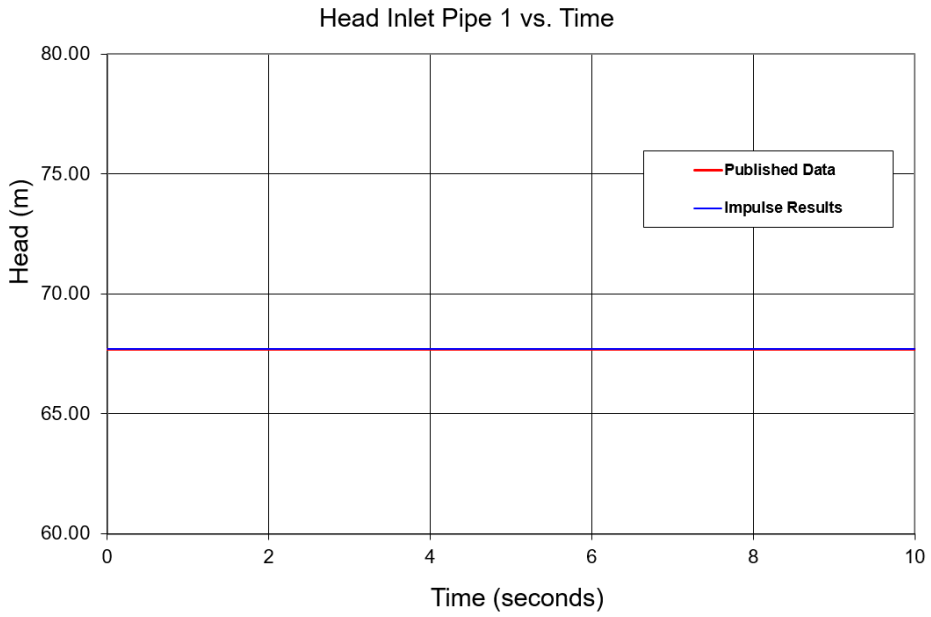

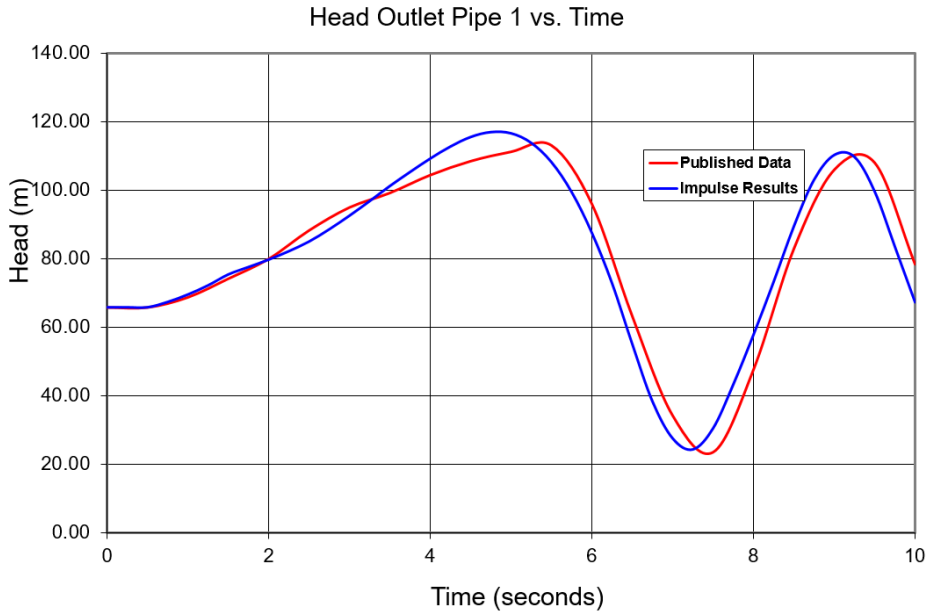
Head Outlet Pipe 1 vs. Time
140.00
120.00
100.00
80.00
60.00
40.00
20.00
0.00
Head (m)
0
2
4
6
8
10
Time (seconds)
Published Data
Impulse Results

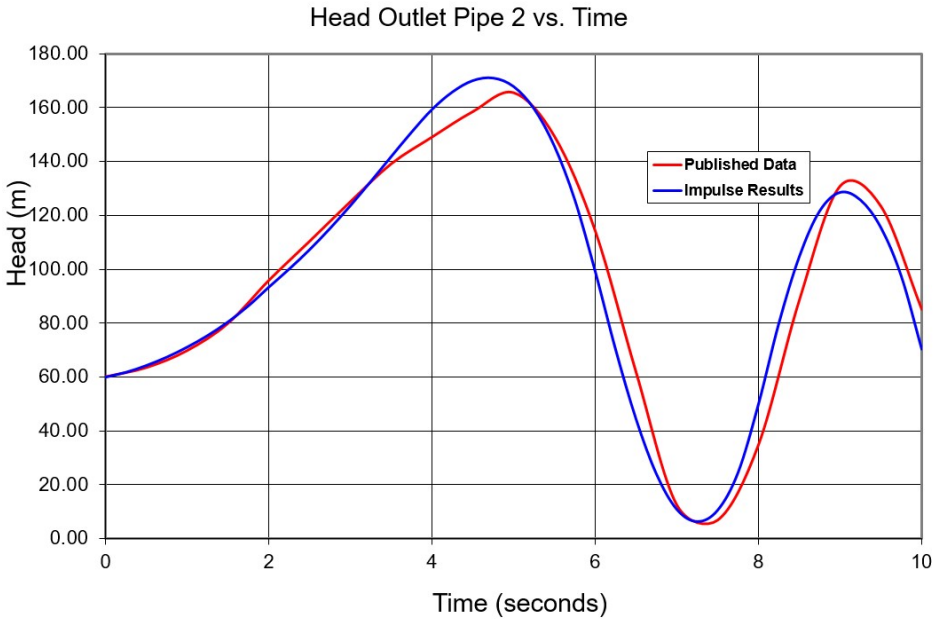
Head Outlet Pipe 2 vs. Time
180.00
160.00
140.00
120.00
100.00
80.00
60.00
40.00
20.00
0.00
Head (m)
0
2
4
6
8
10
Time (seconds)
Published Data
Impulse Results

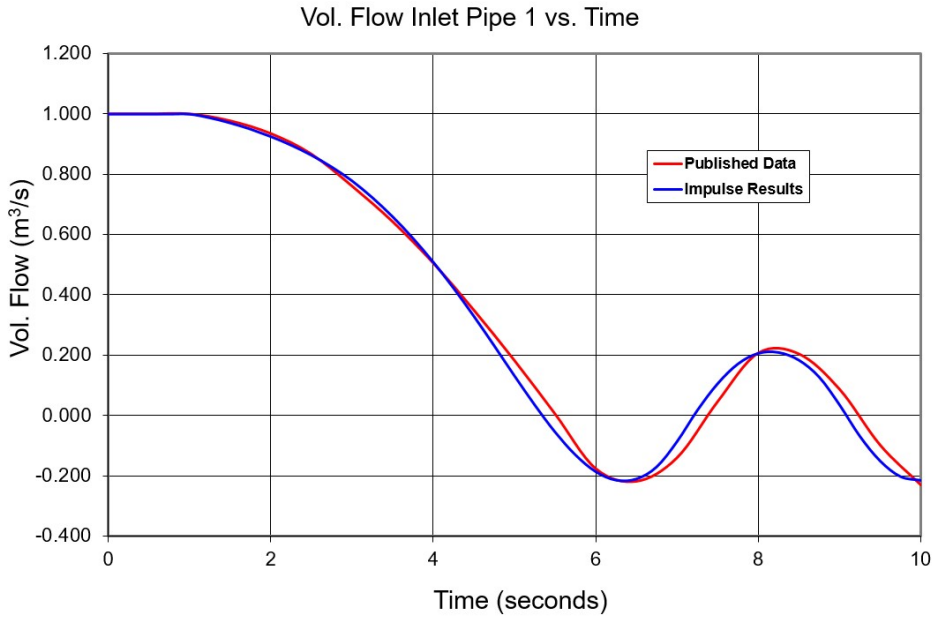
Vol. Flow Inlet Pipe 1 vs. Time
Vol. Flow (m3/s)
1.200
1.000
0.800
0.600
0.400
0.200
0.000
-0.200
-0.400
0
2
4
6
8
10
Time (seconds)
Published Data
Impulse Results

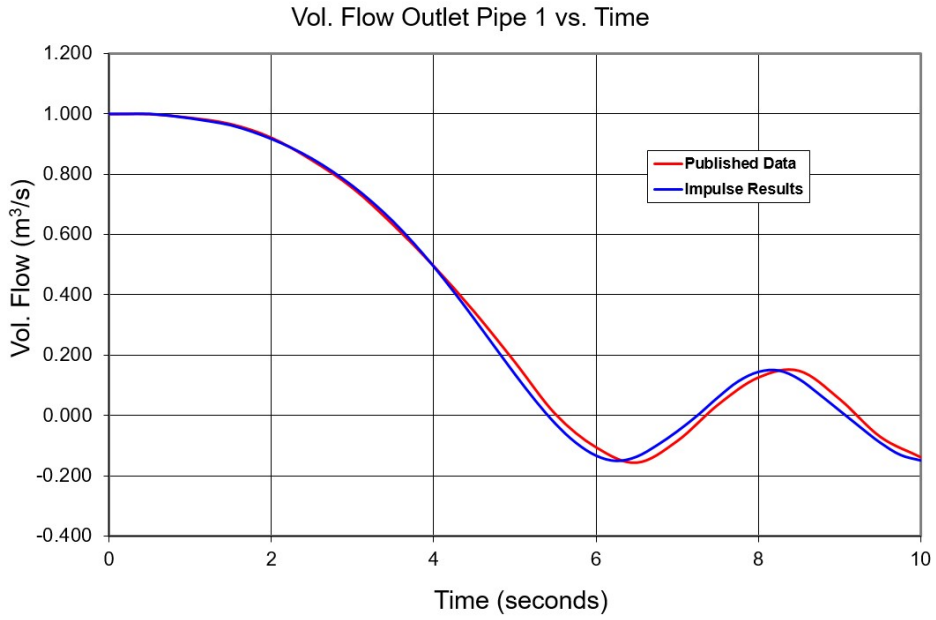
Vol. Flow Outlet Pipe 1 vs. Time
Vol. Flow (m3/s)
1.200
1.000
0.800
0.600
0.400
0.200
0.000
-0.200
-0.400
0
2
4
6
8
10
Time (seconds)
Published Data
Impulse Results

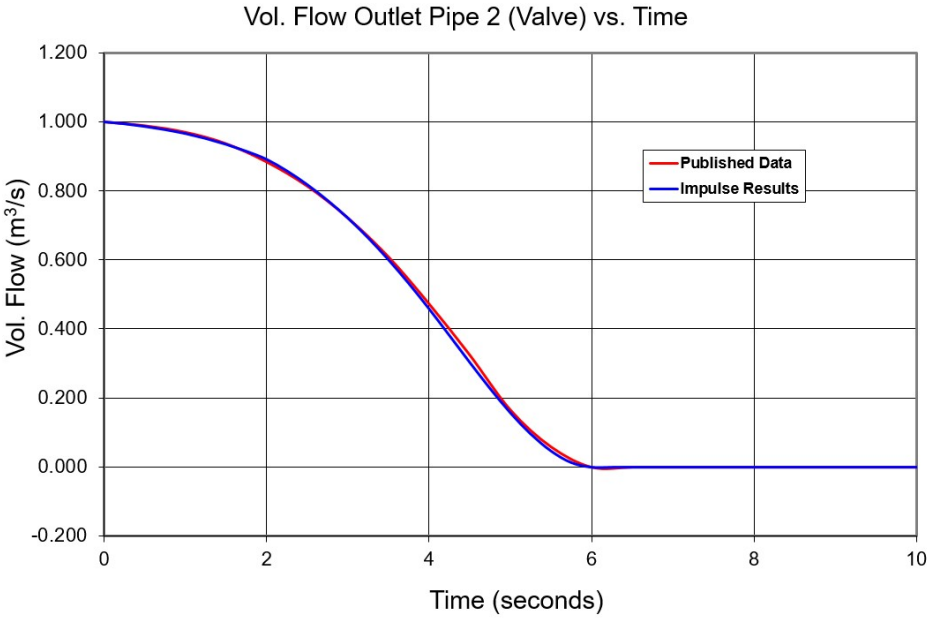

DISCUSSION:

No explicit Cv value is given for the valve, but a head loss at a given flow was provided and a full open Cv of 1716 was calculated. The given valve closure curve was then curve fit to the 4th order and then the max Cv of 1716 was applied to this curve to generate the closing profile used by Impulse.

List of All Verification Models

Verification Case 18 Problem Statement

Verification Case 18

M. H. Chaudhry, *Applied Hydraulic Transients*, 3rd ed. Springer, pp. 102-104, 527-533.

Chaudhry Title Page

3-12 Analysis Procedure

In this section, we outline steps for the analysis of transient conditions in a piping system.

The shortest conduit in the system is divided into a number of reaches so that a desired computational time interval, Δt, is obtained. According to Evangelisti [1969], a time interval equal to 1/16 to 1/24 of the transit time, i.e., wave-travel time from one end of the system to the other, should give sufficiently accurate results. We recommend, however, to use this criterion as a rough guide only, and increase or decrease Δt depending upon the rate at which transients are produced.

For the selected-value of Δt, the remaining conduits in the system are divided into equal-length reaches by using the procedure outlined in Section 3-6. If necessary, the wave velocities are adjusted to satisfy Eq. 3-69 so that characteristics pass through the grid points (i.e., $C_N = 1$).

The steady-state discharge and pressure head at all the sections are then computed. The time is now incremented by Δt. The transient conditions at all the interior nodes are computed from Eqs. 3-22 and 3-18, and at the boundaries from the appropriate boundary conditions. The steps for increasing the time by Δt and computing the transient condition are repeated until transient conditions for the required time are computed. The flowchart of Fig. 3-22 shows the computational steps for determining the transient conditions in a series piping system.

To illustrate the above procedure, transient conditions produced by closing the downstream valve in the piping system shown in Fig. 3-23a are determined by using the computer program of Appendix B. The variation of effective valve opening, τ, with time are as shown by the τ-t curve in Fig. 3-23b. Since the valve-closure time is long compared to the wave-transit time in the system, pipe no. 2 is divided into two reaches, thus giving $\Delta t = 0.25$ s. Pipe no. 1 is also divided into two reaches to satisfy Eq. 3-69. The initial steady-state conditions are computed at all sections of pipes 1 and 2. Time is incremented by Δt, and the conditions at the interior sections are determined from Eqs. 3-22 and 3-18.

The boundary conditions for the upstream reservoir (Eqs. 3-28 and 3-29) are used to determine the conditions at the upstream end, and Eqs. 3-47, 3-43, 3-44, and 3-46 are used to determine conditions at the junction of pipes 1 and 2. Seven points on the τ-t curve are stored in the computer, and the values at the intermediate times are interpolated parabolically. The conditions at the valve are determined from Eqs. 3-42 and 3-17.

Conditions at $t = \Delta t$ at all sections of the system are now known. These are stored as conditions at the beginning of the next time step. This procedure is repeated until transients for the desired duration are computed. The conditions are printed every second time step by specifying IPRINT = 2.

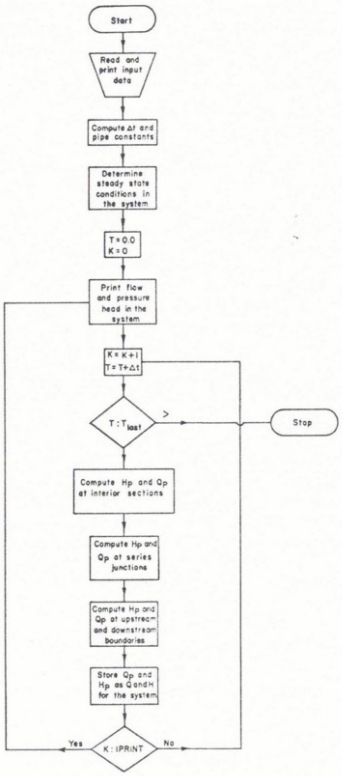

Fig. 3-22. Flowchart for a series piping system.

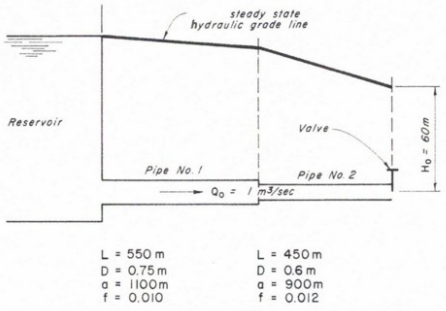

(a) Piping system

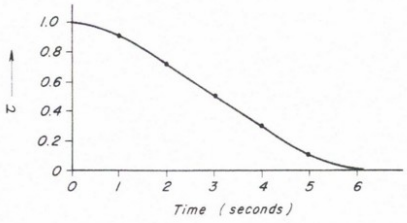

(b) Valve closure curve

Fig. 3-23. Series piping system.

3-13 Case Study

The computation of transient conditions in the upstream conduits of the Jordan River Redevelopment [Portfors and Chaudhry, 1972 and Chaudhry and Portfors, 1973] British Columbia, Canada, caused by closing the pressure regulating valve and their comparison with the prototype measurements are discussed in this section.

Figure 3-24 shows the longitudinal section of the upstream conduit, typical cross-sections and the schematic layout of the turbine and the bypass valve. The upstream conduit consists of a tunnel which has a 5.28-km-long, mainly D-shaped section; and 82-m-long, 3.96-m-diameter, and 451-m-long, 3.2-m-diameter sections; and a 1.4-km-long penstock, reducing in diameter from 3.2 to 2.7 m. The power plant, primarily used for peaking, has one Francis turbine rated at 154 MW and 265.5-m rated head. To reduce the maximum transient-state pressures, a pressure-regulating valve (PRV) is provided. The rating curve for the PRV, as determined from the prototype tests at the rated head H_r of 265.5 m, is shown in Fig. 3-25.

To compute the transient conditions caused by the opening or closing of PRV, a computer program is developed using the boundary conditions for the PRV derived in this section. (The analysis of transients caused by various turbine operations is discussed in Chapter 5 and the boundary conditions for the simultaneous operation of the PRV and wicket gates are developed in Section 10-6.) Points on the PRV rating curve (Fig. 3-25) are stored in the computer at 20 percent intervals of the valve stroke, and the discharge at the intermediate valve openings is determined by linear interpolation. Assuming the valve characteristics obtained under steady-state operation are valid during the transient state, the PRV discharge under net head H_n is given by the equation

$$Q_v = Q_r \sqrt{\frac{H_n}{H_r}} \tag{3-111}$$

in which Q_v = PRV discharge under a net head of H_n, and Q_r = discharge under rated net head H_r, both at valve opening τ. Note that both H_r and H_n are total heads, i.e., $H_n = H_P + Q_v^2/(2gA^2)$, in which A = cross-sectional area of the conduit just upstream of the PRV.

To develop the boundary condition for the PRV, Eqs. 3-17 and 3-111 are simultaneously solved. Noting that $Q_P = Q_v$ and eliminating H_n from these equations,

$$Q_P = \frac{-C_{16} + \sqrt{C_{16}^2 + 4C_{15}C_{17}}}{2C_{15}} \tag{3-112}$$

in which

$$C_{15} = 1 - \frac{{Q_r}^2}{2gH_rA^2}$$

$$C_{16} = \frac{{Q_r}^2}{C_aH_r} \tag{3-113}$$

$$C_{17} = \frac{{Q_r}^2C_p}{C_aH_r}$$

Now H_P may be determined from Eq. 3-17.

532 B TRANSIENTS CAUSED BY OPENING OR CLOSING A VALVE

VALVE OPERATION TIME = 6.00 S
TIME INTERVAL FOR STORING TAU CURVE = 1.000 S
VALVE LOSS = 60.05 M FOR QS = 1.000 M3/S
STORED TAU VALUES :
1.000 .900 .700 .500 .300 .100 .000

PIPE NO	LENGTH (M)	DIA (M)	WAVE VEL. (M/S)	FRIC FACTOR
1	550.0	.75	1100.0	.010
2	450.0	.60	900.0	.012

PIPE NO	ADJUSTED WAVE VEL (M/S)
1	1100.0
2	900.0

TIME	TAU	PIPE NO	HEAD (M) (1)	HEAD (M) (N+1)	DISCH. (M3/S) (1)	DISCH. (M3/S) (N+1)
.0	1.000	1	67.70	65.78	1.000	1.000
		2	65.78	60.05	1.000	1.000
.5	.962	1	67.70	65.78	1.000	1.000
		2	65.78	63.46	1.000	.989
1.0	.900	1	67.70	68.73	1.000	.988
		2	68.73	69.78	.988	.970
1.5	.813	1	67.70	74.16	.977	.967
		2	74.16	79.88	.967	.937
2.0	.700	1	67.70	79.93	.935	.922
		2	79.93	95.83	.922	.884
2.5	.600	1	67.70	88.25	.867	.847
		2	88.25	110.41	.847	.814
3.0	.500	1	67.70	94.96	.761	.755
		2	94.96	125.13	.755	.722
3.5	.400	1	67.70	99.19	.643	.633
		2	99.19	139.20	.633	.609
4.0	.300	1	67.70	104.41	.506	.496
		2	104.41	149.14	.496	.473
4.5	.200	1	67.70	108.47	.350	.344
		2	108.47	158.61	.344	.325
5.0	.100	1	67.70	111.20	.183	.177
		2	111.20	165.65	.177	.166
5.5	.038	1	67.70	113.07	.006	.004
		2	113.07	149.46	.004	.059
6.0	.000	1	67.70	96.01	-.175	-.106
		2	96.01	114.27	-.106	.000
6.5	.000	1	67.70	63.25	-.217	-.157
		2	63.25	61.79	-.157	.000
7.0	.000	1	67.70	34.25	-.139	-.085
		2	34.25	12.33	-.085	.000
7.5	.000	1	67.70	23.55	.047	.035
		2	23.55	6.74	.035	.000
8.0	.000	1	67.70	47.63	.208	.126
		2	47.63	34.76	.126	.000
8.5	.000	1	67.70	82.89	.205	.148
		2	82.89	88.45	.148	.000
9.0	.000	1	67.70	105.95	.088	.054
		2	105.95	130.93	.054	.000
9.5	.000	1	67.70	108.02	-.097	-.071
		2	108.02	123.44	-.071	.000
10.0	.000	1	67.70	78.39	-.229	-.139
		2	78.39	85.13	-.139	.000

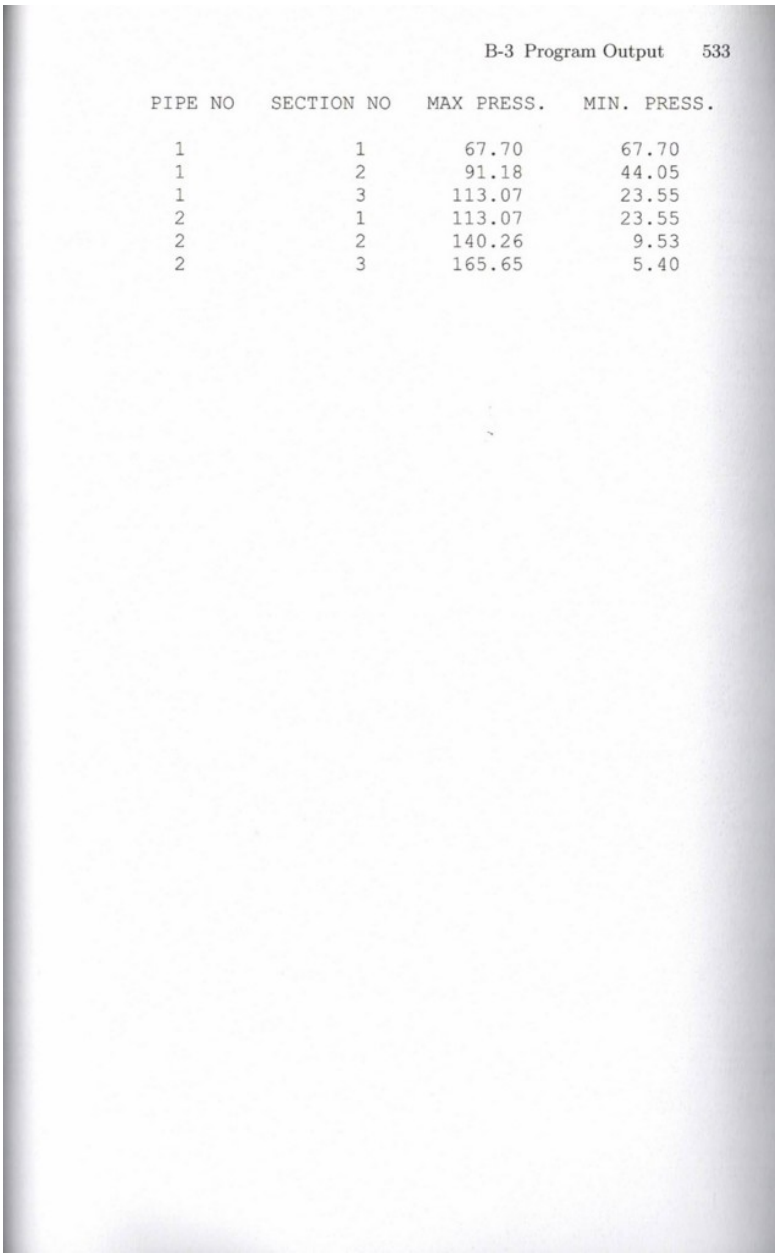

B-3 Program Output 533

PIPE NO	SECTION NO	MAX PRESS.	MIN. PRESS.
1	1	67.70	67.70
1	2	91.18	44.05
1	3	113.07	23.55
2	1	113.07	23.55
2	2	140.26	9.53
2	3	165.65	5.40

View Verification Case 18 Model

Verification Case 18

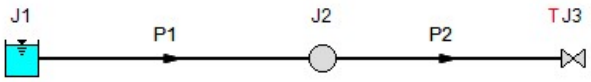

M. H. Chaudhry, Applied Hydraulic Transients, 3rd ed. New York: Springer, pp. 102-104, 527-533. Series Piping System.

Verification Case 19

View Model Problem Statement

PRODUCT: AFT Impulse

TITLE: ImpVerify19.imp

REFERENCE: Kaplan M., Streeter V., and Wylie E.B., Oil Pipeline Transients, The University of Michigan, Industry Program of the College of Engineering, August 1966, IP-743, Long Pipeline.

FLUID: Oil

ASSUMPTIONS: Fluid properties where assumed for crude oil.

RESULTS:

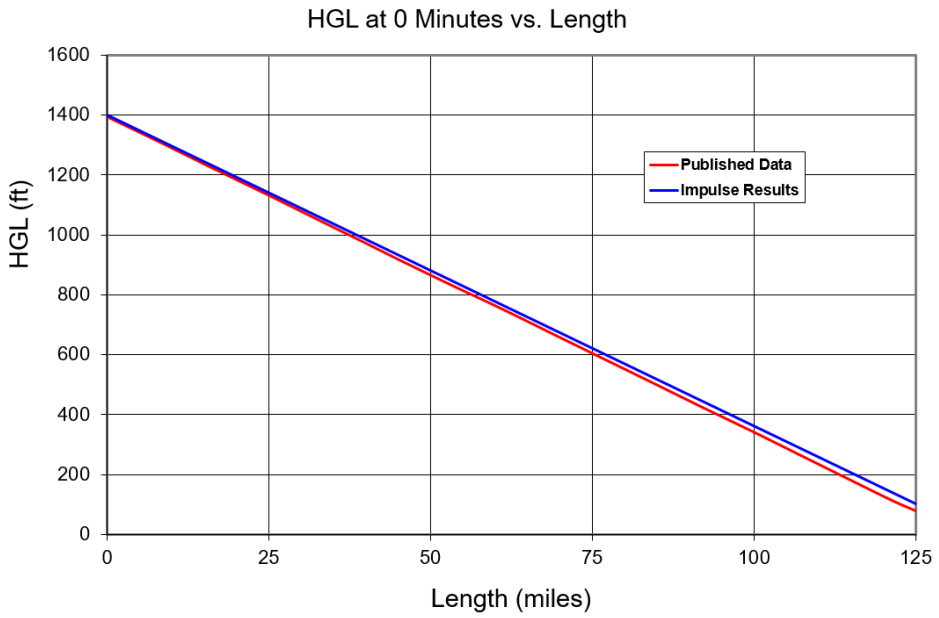

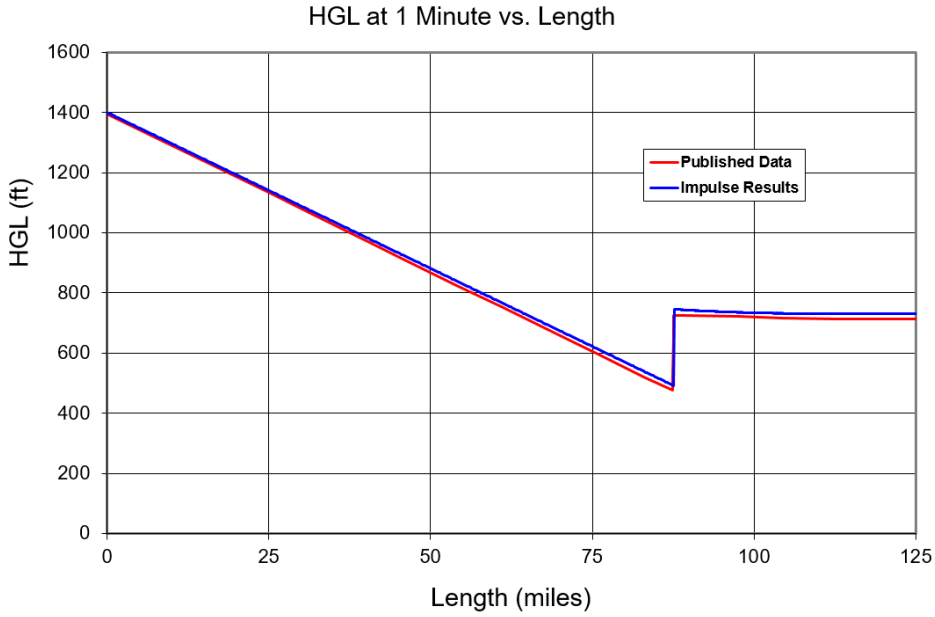
HGL at 1 Minute vs. Length
HGL (ft)
1600
1400
1200
1000
800
600
400
200
0
0
25
50
75
100
125
Length (miles)
Published Data
Impulse Results

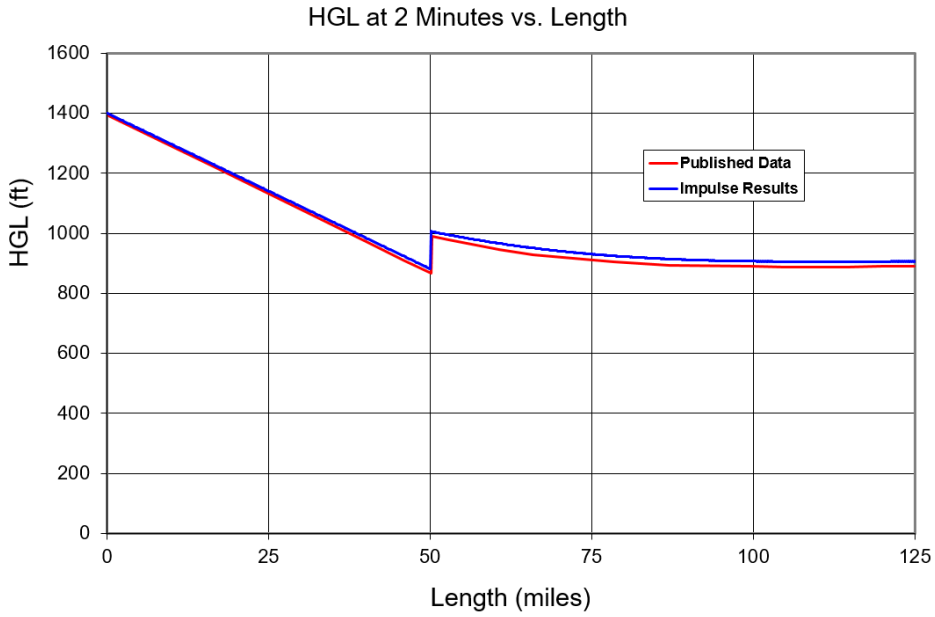
HGL at 2 Minutes vs. Length
HGL (ft)
1600
1400
1200
1000
800
600
400
200
0
0
25
50
75
100
125
Length (miles)
Published Data
Impulse Results

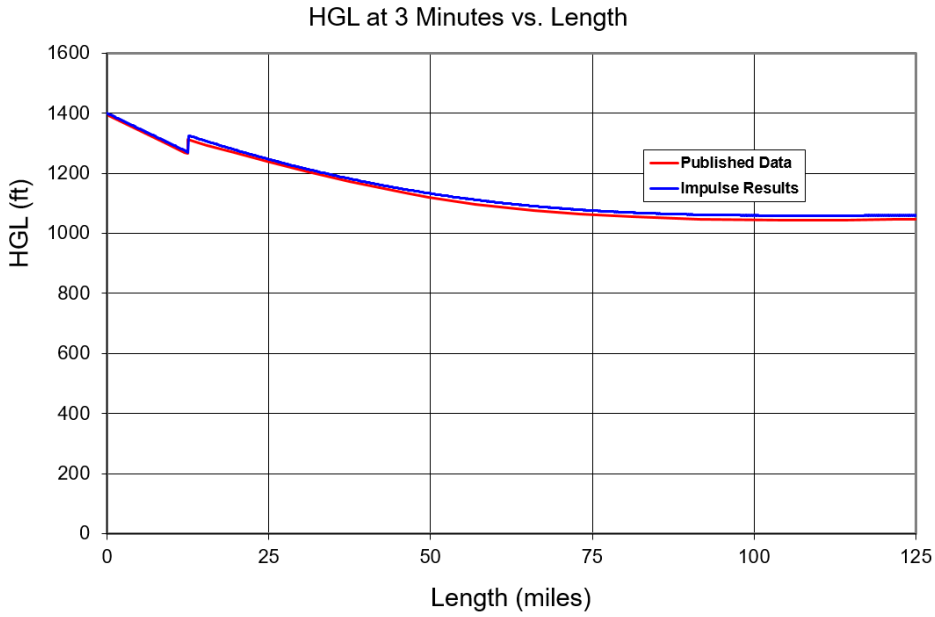
HGL at 3 Minutes vs. Length
HGL (ft)
1600
1400
1200
1000
800
600
400
200
0
0
25
50
75
100
125
Length (miles)
Published Data
Impulse Results

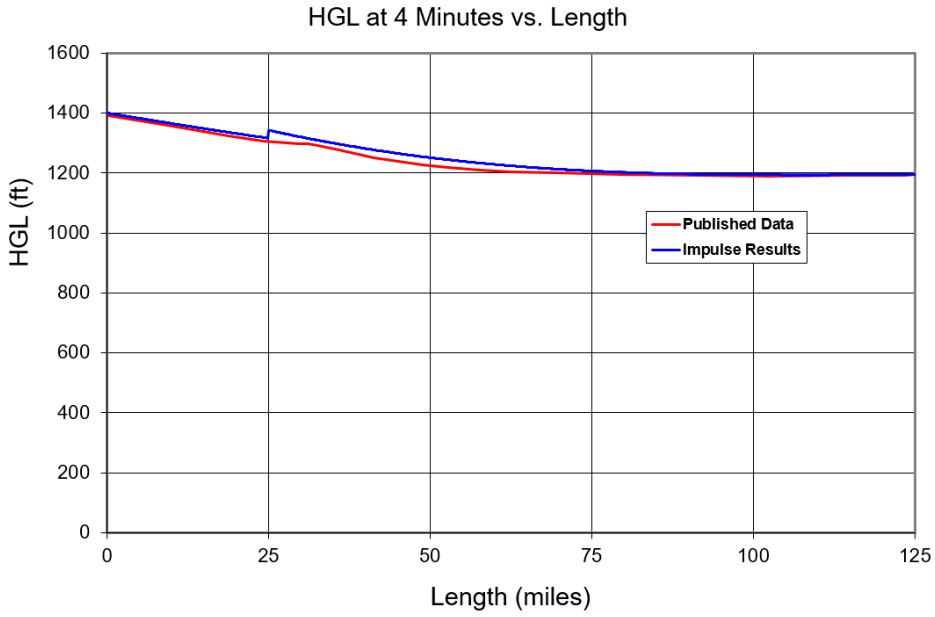
HGL at 4 Minutes vs. Length
HGL (ft)
1600
1400
1200
1000
800
600
400
200
0
0
25
50
75
100
125
Length (miles)
Published Data
Impulse Results

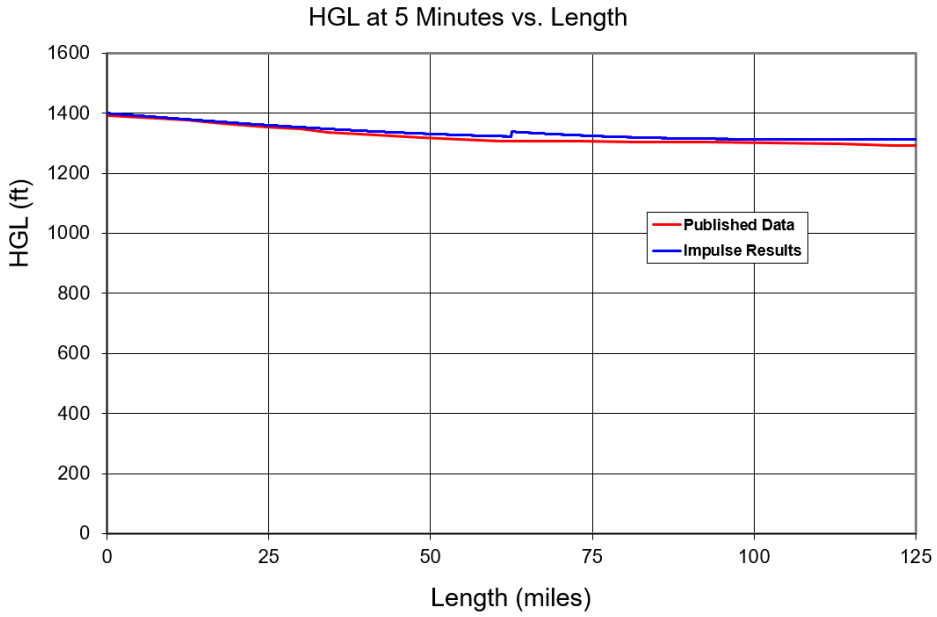
HGL at 5 Minutes vs. Length
HGL (ft)
1600
1400
1200
1000
800
600
400
200
0
0
25
50
75
100
125
Length (miles)
Published Data
Impulse Results

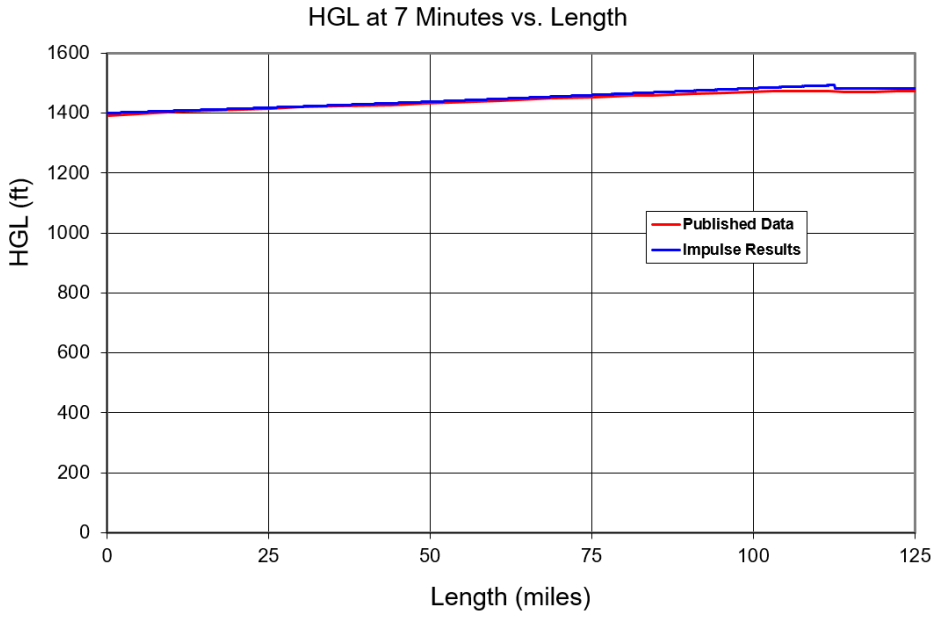
HGL at 7 Minutes vs. Length
HGL (ft)
1600
1400
1200
1000
800
600
400
200
0
0
25
50
75
100
125
Length (miles)
Published Data
Impulse Results

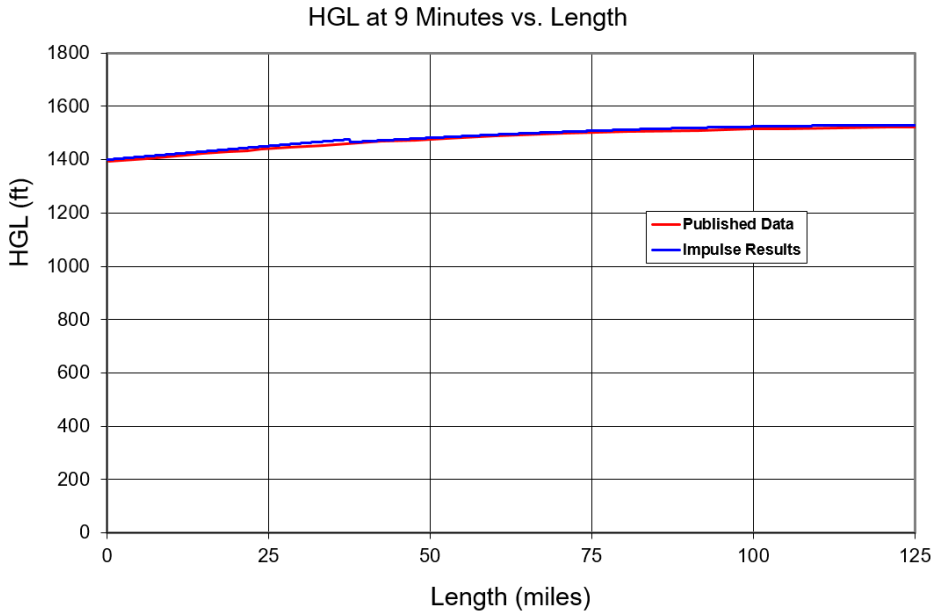

DISCUSSION:

This example demonstrates line pack as the result of closing a valve at the end of a long pipeline.

List of All Verification Models

Verification Case 19 Problem Statement

Verification Case 19

Kaplan M., Streeter V., and Wylie E.B., Oil Pipeline Transients, The University of Michigan, Industry Program of the College of Engineering, August 1966, IP-743, Long Pipeline.

Kaplan Title Page

at the wave front is shown as a dashed line in Fig. 4 and is seen to approach the original hydraulic gradeline asymptotically in the infinitely long line. In most practical situations a reflection of the attenuated wave occurs at the upstream boundary, although in the relatively long pipeline the reflected wave may be so small as to be undetected. Even after the locus of the head rise has become coincident with the orignal hydraulic gradeline the new gradeline continues to rise, gradually reducing the forward velocity to zero in the pipeline.

It is of interest to note that the attenuation described above does not directly result from frictional effects but arises out of the fact that momentum conditions must be satisfied at the wave front. Without frictional effects in the system, however, the hydraulic gradeline would be horizontal and the phenomena of line packing and attenuation would not exist.

The characteristic's method of solution of the differential equations that describe unsteady flow in a long pipeline automatically includes these newly defined effects since the complete equations are solved. Figure 5 shows the computer results of a sudden valve closure on a long pipeline, as obtained by solution of the transient flow equations for a simple pipe 125 miles long and 30 inches in diameter. The initial steady state velocity was 4.25 ft/sec and the wave speed was 3300 ft/sec. The solid lines show the original hydraulic gradeline and the gradeline at various times after valve closure. At 200 seconds after valve closure the attenuated wave reaches the upstream boundary and is reflected. The dashed lines indicate the extent of the pipeline influenced by the reflected wave as the gradeline continues to rise. At 9 minutes

after valve closure the hydraulic gradeline has reached its maximum level and the forward velocity has been reduced to zero. The adverse gradeline produces flow in the opposite direction. The surging condition continues until friction losses in the system cause the flow to come to rest. In Fig. 5 the line indicated by dots shows the magnitude of the initial wave front as it moves into the undisturbed flow. The attenuation of the wave front is evident.

The superposition of one transient pressure upon another is known as the pyramidal effect. For example, if line packing has occurred due to closure of a valve, then the head is increased upstream by starting of a pumping station, one transient is superposed on another transient.

Rarefaction control[5] is the opposite of pyramidal effect in that a negative surge wave is generated upstream by shutting down a pump or closing a valve. When this meets a surge wave being transmitted up the hydraulic gradeline they tend to partially cancel the head changes.

These latter two effects are easily demonstrated in a computer solution by proper adjustment of the boundary conditions.

Properties of Fluids. Wave-Speed Determination. Frictional Effects

Viscosity, bulk modulus of elasticity, and density are the important fluid properties needed to design for transient control of long pipelines. Viscosity is a function of temperature primarily, but the bulk modulus of elasticity of oils depends upon both temperature and pressure in some cases.

5. "Transient Pressures in Long Pipelines," by R. R. Burnett. A.P.I. Annual Pipeline Conference, Division of Transportation, April, 1960.

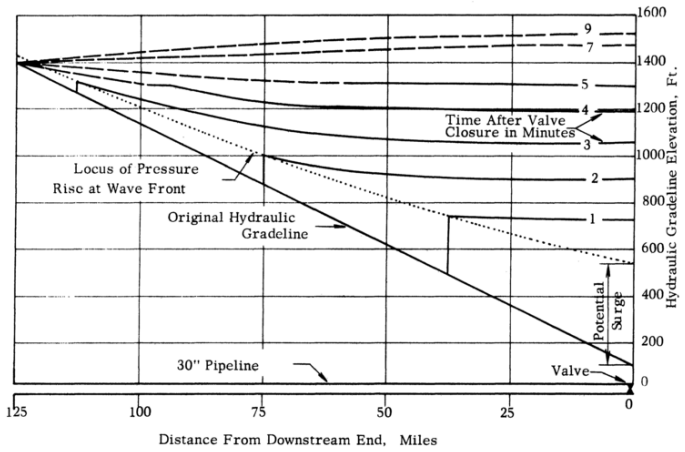

Figure 5. Results of Computer Solution of Valve Closure on Long Pipeline.

View Verification Case 19 Model

Verification Case 19

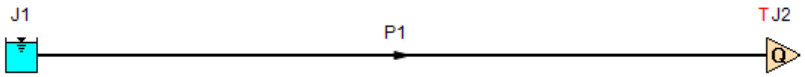

Kaplan M., Streeter V., and Wylie E.B., Oil Pipeline Transients, The University of Michigan, Industry Program of the College of Engineering, August 1966, IP-743, Long Pipeline

Verification Case 20

View Model Problem Statement

PRODUCT: AFT Impulse

TITLE: ImpVerify20.imp

REFERENCE: Karney, Bryan W and McInnis, Duncan, Transient Analysis of Water Distribution Systems, Journal AWWA, July 1990, pp. 62-70, Figures 2 and 3

FLUID: Water

ASSUMPTIONS: N/A

RESULTS:

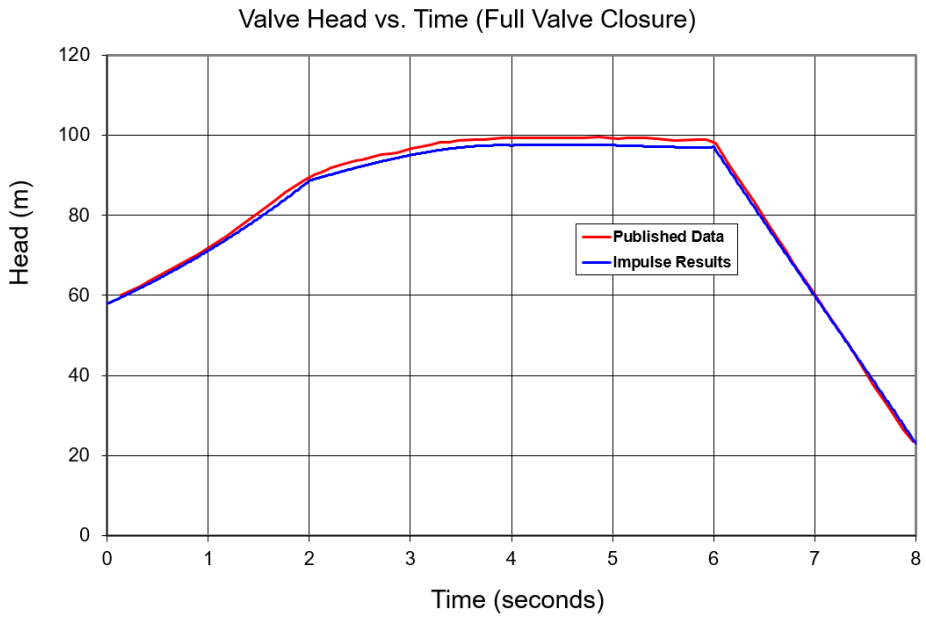

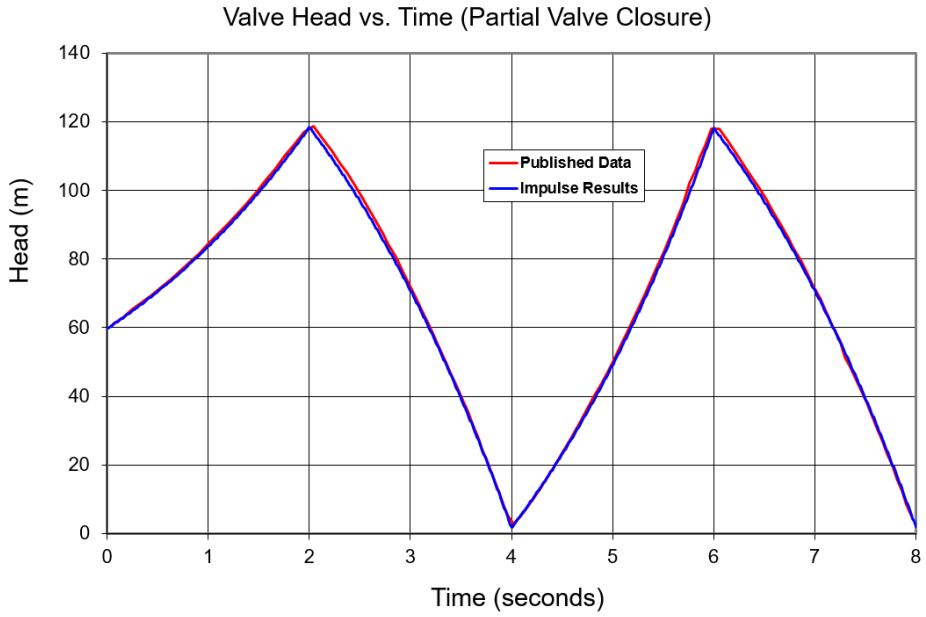
Valve Head vs. Time (Partial Valve Closure)
Head (m)
Time (seconds)
Published Data
Impulse Results
0
20
40
60
80
100
120
140
0
1
2
3
4
5
6
7
8

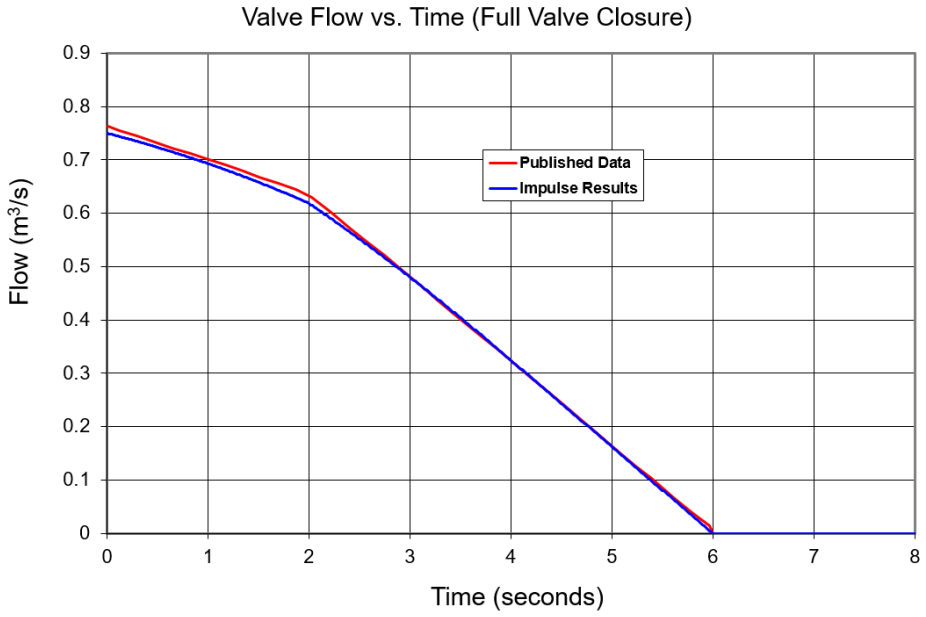
Valve Flow vs. Time (Full Valve Closure)
Flow (m3/s)
Time (seconds)
Published Data
Impulse Results
0
0.1
0.2
0.3
0.4
0.5
0.6
0.7
0.8
0.9
0
1
2
3
4
5
6
7
8

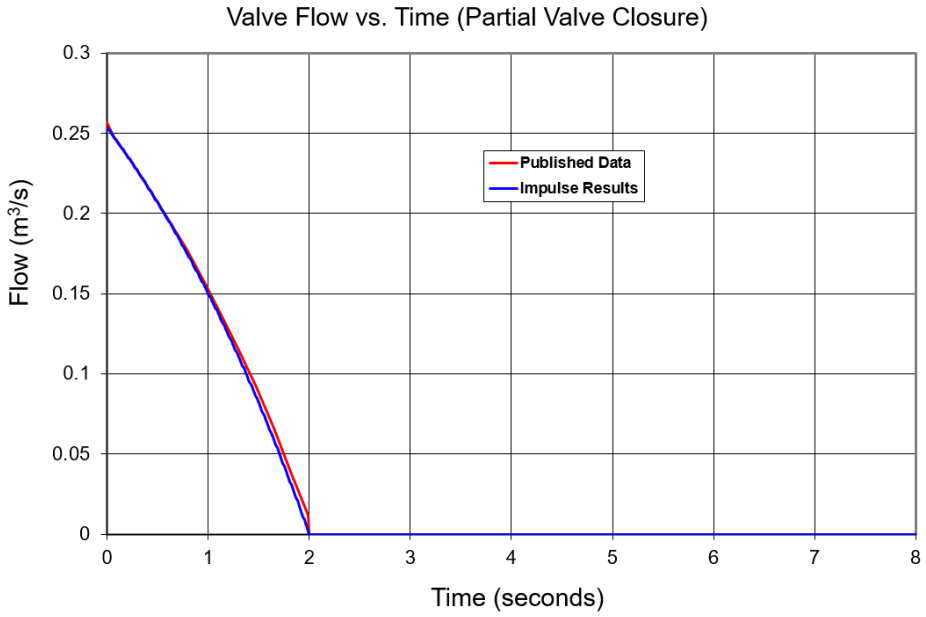

DISCUSSION:

The valve Cv is not given, but was calculated based on flow and pressure drop.

List of All Verification Models

Verification Case 20 Problem Statement

Verification Case 20

Karney, Bryan W and McInnis, Duncan, Transient Analysis of Water Distribution Systems, Journal AWWA, July 1990, pp. 62-70, Figures 2 and 3

Karney Title Page

devices can lead to the most severe transient problems. Yet such issues are central to system design and operation.

This article emphasizes that the details of how a hydraulic system is modeled or represented can have a critical impact on the predicted transient conditions. Examples illustrate the following three points: (1) in some pipeline systems, the maximum transient pressure is quite sensitive to the assumed initial steady-state velocity; (2) transient conditions may sometimes be more severe in branched or looped systems than in simple series pipelines; and (3) oversizing surge-suppression equipment such as relief valves may degrade a system's transient response. The key result is that transient phenomena in a pipeline system can be both surprising and dramatic. Because of the complexity of system response, the transient analyst must learn to think fundamentally and analyze comprehensively.

Transient analysis and design

Unfortunately, transient analysis is not easy. The governing equations describing the flow are of the nonlinear partial differential variety, the hydraulic devices are complex and data on their performance are difficult to obtain, and the pipeline systems themselves are subject to a host of operating conditions and requirements. To make matters worse, the physical character of the pulse wave propagation is frequently hard to visualize or interpret even for the analyst accustomed to transient phenomena.

The complexity of transient phenomena has, at times, induced many analysts to adopt simplified design procedures. The analysis of hydraulic systems is often facilitated in two primary ways: (1) complex components and other complications in the physical system itself may be ignored, or (2) the range of operating and loading conditions to which the system is subjected is greatly reduced. These simplifications are rationalized on the grounds of necessity (the actual physical system cannot be analyzed) and conservatism (the analyzed system performs worse than the real one). Unfortunately, the assumption that some rudimentary and conservative system can be found is questionable. It is difficult to simplify a pipeline system to ensure worst-case performance under all transient conditions, particularly if the simplifications are made before any analysis has been performed.

Traditional wisdom for identifying worst-case scenarios is based on elementary equations, rules of thumb, or common sense; in other words, simple relations that may have little or no bearing on the performance of more complex systems. Several of the most common of these ideas are presented in this article along with counterexamples

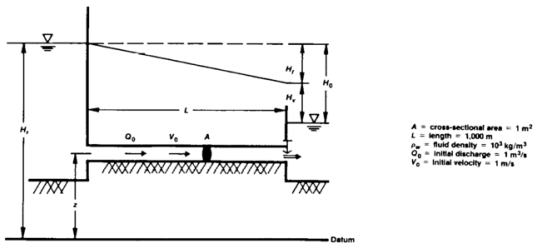

Figure 2. Fluid and pipeline properties of two constant head reservoirs joined by a series pipeline with a downstream valve

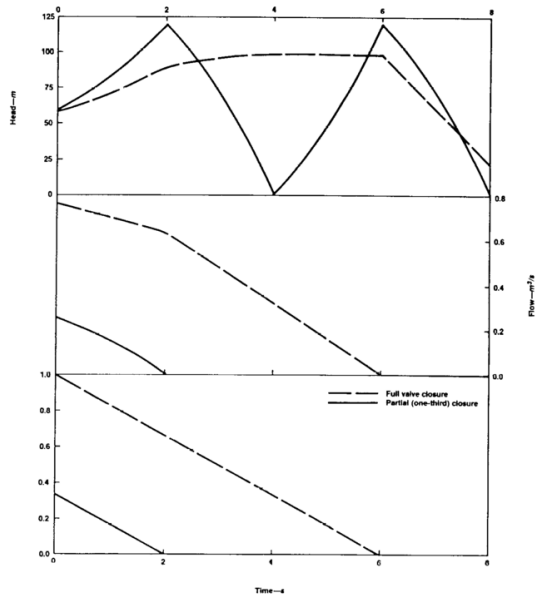

Figure 3. Valve action and transient response of a single-pipe system to valve closure from full and partial (one-third) opening (*head and discharge values are given at the valve end of the pipe;* $H_0 = 60$ *m,* $f = 0.010$)

View Verification Case 20 Model

Verification Case 20

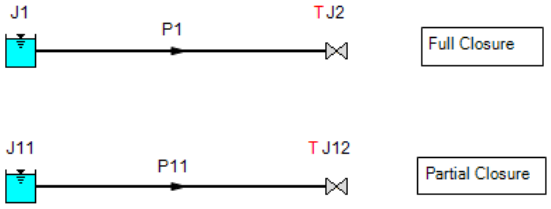

Karney, Bryan W and McInnis, Duncan, Transient Analysis of Water Distribution Systems, Journal AWWA, July 1990, pp. 62-70, Figures 2 and 3

Verification Case 21

View Model Problem Statement

PRODUCT: AFT Impulse

TITLE: ImpVerify21.imp

REFERENCE: Karney, Bryan W and McInnis, Duncan, Transient Analysis of Water Distribution Systems, Journal AWWA, July 1990, pp. 62-70, Figures 5 - 7

FLUID: Water

ASSUMPTIONS: Valve Cv is unknown, but calculated based on flow and pressure drop.

RESULTS:

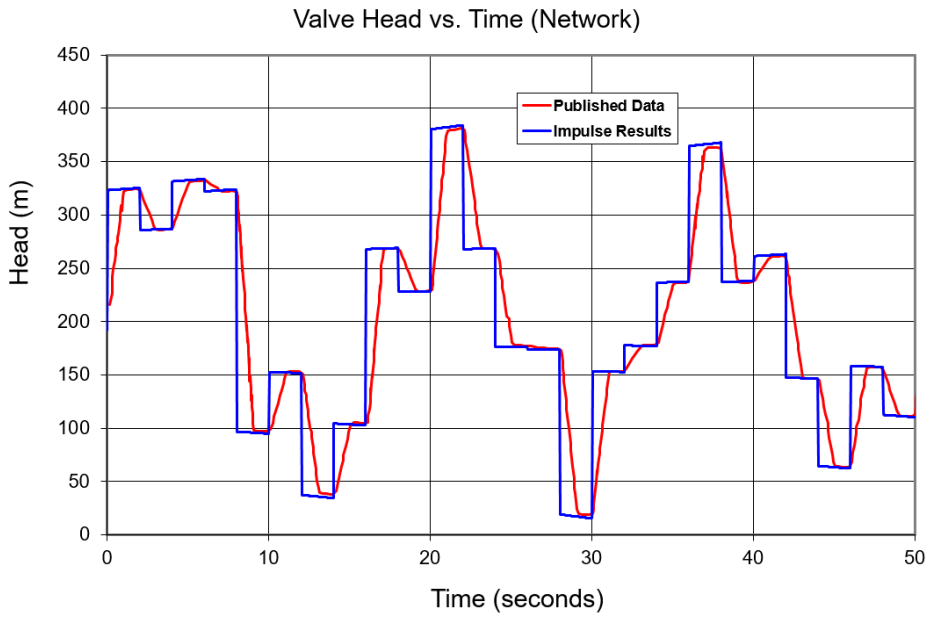

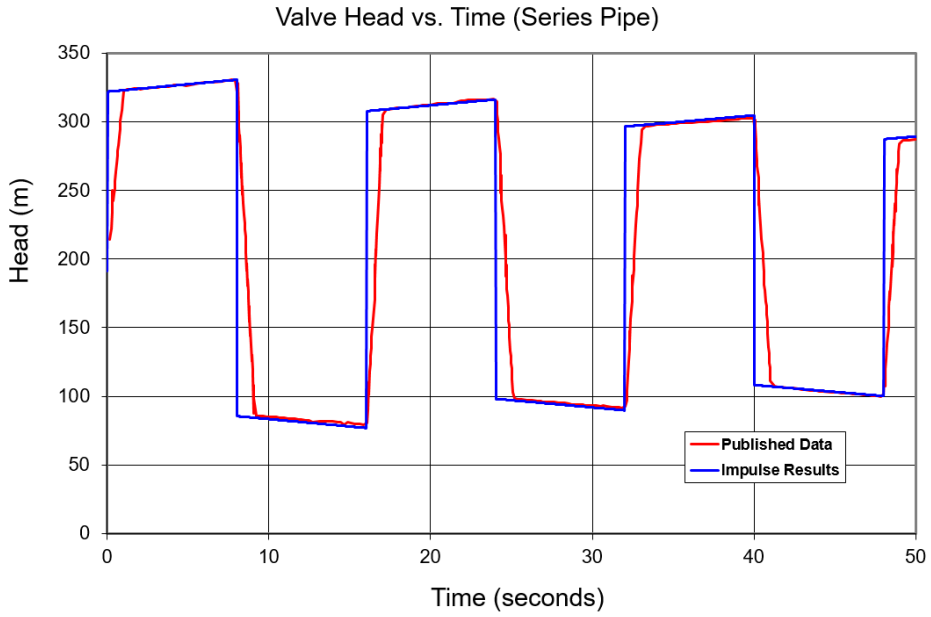

DISCUSSION:

Karney uses very few sections, using fewer in AFT Impulse will result in more similar results to Karney, but using more sections is required to get a better description of the square wave behavior that results from an instantaneous closure.

List of All Verification Models

Verification Case 21 Problem Statement

Verification Case 21

Karney, Bryan W and McInnis, Duncan, Transient Analysis of Water Distribution Systems, Journal AWWA, July 1990, pp. 62-70, Figures 5 - 7

Karney Title Page

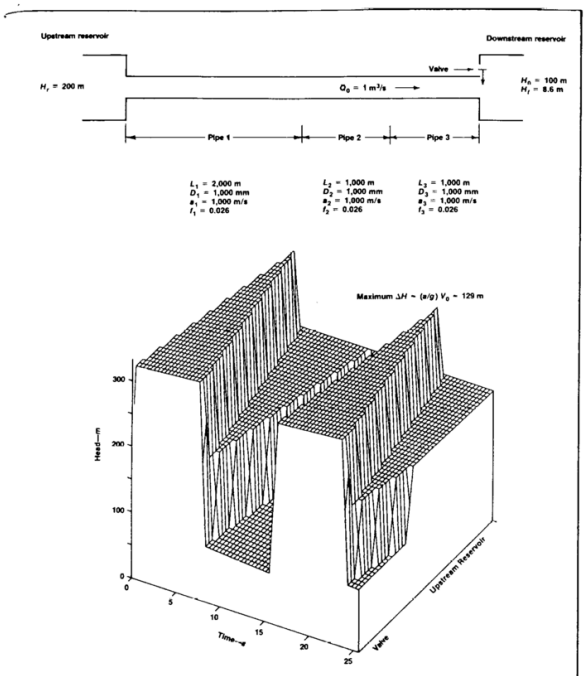

Figure 5. Plan sketch, parameter values, and three-dimensional response surface for instantaneous downstream valve closure in a simple series pipeline

any movement of the piston, no matter how slowly accomplished, will be accompanied by changes in fluid density, conduit dimension, and pressure. Even though the resulting changes in density and dimension are typically small, the changes in fluid pressure can be large and cannot be neglected.

The connections between this simple static compression test and a pipeline transporting fluid are easily made. If the actual conduit length in the static case is taken to be the final value of 1,000 m, what this pipe experiences during the compression can be thought of as a mass imbalance. That is, more fluid is forced to enter the conduit than was originally contained within it. Whenever such an imbalance occurs, compressibility effects must play a role. Thus, whenever flow conditions in a pipeline result in more fluid entering one end than is leaving the other, large pressure changes can be expected. In addition, the greater the mass imbalance, the more severe the resulting pressure changes tend to be. In anticipation of ideas to be broached subsequently, it could be suggested that mass imbalance constitutes a more natural and theoretically satisfying criterion for the severity of a system's transient response than does fluid velocity.

The origin of transient conditions. The connections between fluid properties (density and compressibility) on the one hand and the law of mass conservation on the other are fundamental to an understanding of fluid transients. Suppose, for example, an adjustment is made to a valve at the downstream end of a pipeline carrying fluid at some initial velocity (Figure 2). For simplicity, it is assumed that the valve is suddenly closed. The valve, of course, can only act locally—it specifies a relationship between flow through the valve and the head loss across the valve. In this case, the discharge and velocity of the fluid at the valve become zero the instant the valve is shut. However, in order for the fluid mass as a whole to be stopped, a decelerating force sufficient to eliminate the substantial 10^6 kg m/s of momentum must be applied. The only way to provide the required decelerating force is to compress the fluid, thereby generating an increase in pressure large enough to arrest the fluid flow. Because water is heavy, the required force is large; but because water is only slightly compressible, the wave or disturbance will travel quickly. In a system like the one shown, a pressure wave of approximately 100 m would propagate along the pipeline at roughly 1,000 m/s.

In many ways, this system is typical. Closed-conduit systems frequently carry huge amounts of momentum and kinetic energy, and, in addition, hydraulic conditions are in an almost continual state of change. For such systems, the only available mechanism for controlling or changing the flow conditions is shock wave propagation resulting from fluid and pipeline elasticity. Only if the changes in flow rate take place gradually, such that the mass imbalance in the line is always small, is it possible to go smoothly from one steady condition to another. Under these circumstances, no large fluctuations in pressure head or velocity occur, because the pipeline is always near a state of equilibrium.*

If rapid changes occur, whether caused by standard operating procedures or accidental events, a relatively large mass imbalance may arise. The associated pressure pulses are of great magnitude and are capable of bursting or damaging pipelines. In order to model or predict these rapid transient phenomena, complete equations of motion need to be written and solved, both for the pipeline and for all the devices used to control the flow. Standard texts such as those by Wylie and Streeter[1] and Chaudhry[2] provide the details. The more complete mathematical description should not, however, detract from fundamental insights. Transient conditions arise from local disturbances to the fluid flow that create a mass imbalance. This mass imbalance then acts through the combined effects of fluid and pipeline elasticity to accelerate the flow and, ultimately, create a new steady state.

Special devices that are designed to control or eliminate transient effects should be viewed with caution. It is the physical nature of the control problem that dictates that transient conditions must occur and that frequently deter-

*Even in cases such as this, however, the actual mechanism for maintaining equilibrium in the pipe is still mass imbalance and compressibility effects. The only difference is that the pressure waves are much smaller in magnitude and travel quickly relative to the changes that occur at the ends of the conduit. In such applications, it is often justified to approximate transient behavior by assuming the fluid to be incompressible. Neglecting fluid compressibility leads to the so-called "rigid water column" model.

mines how dramatic transient conditions will be. Often, as in other areas of engineering, no design is superior from all points of view. Instead, there may be compromises that trade off a degree of control under some circumstances for less control under others.

Transient folklore

Much traditional "wisdom" has evolved over time on how to cope with the intricacies of transient phenomena. This wisdom often pertains to design assumptions that simplify the analyst's task by restricting the number and complexity of transient cases that need to be analyzed or specified. In light of modern computer power, however, the rationale for these assumptions needs to be questioned. Indeed, many of the a priori design assumptions are so misleading and so frequently false that they should not be regarded as rational design rules but more as outdated and discredited transient folklore.

In this article, several of these misconceptions are addressed, and, by means of counterexamples, their potential for erroneous application becomes clear.* To avoid misleading the reader, the title of each topic is stated as the converse of the often improperly understood and applied design axiom.

The three most widely revered axioms of transient folklore probably are:

- maximum steady-state velocities (flows) produce maximum transient head change,
- networks fare better (i.e., looped or branched configurations alleviate water hammer), and
- if one surge-protection device is good, then two (or more) are better.

The examples that follow were not difficult to find, nor have they been substantially altered to make the results contradict the aforementioned notions. They simply demonstrate that there are important cases for which these guidelines are either false or, at the very least, misleading.

Like much of what is called folklore in other areas, the previously stated transient rules have some basis in fact. For example, the origin of the first two rules can be traced to the famous fundamental equation of water hammer, which is also called the Joukowski relation. This relation equates changes in head (ΔH) in a pipe to the associated changes in fluid velocity (ΔV):

$$\Delta H = \pm (a/g)\,\Delta V \qquad (1)$$

in which a is the wave speed and g is the acceleration resulting from gravity. Clearly this equation implies that the

*All of the transient simulations presented here were produced using TRANSAM (acronym for Transient Analysis Model), which is a proprietary software product of HydraTek Associates, Toronto, Ont., Canada.

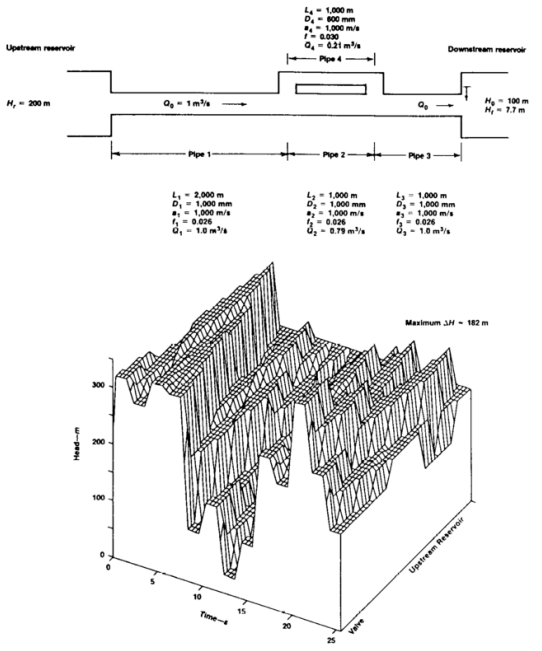

Figure 6. Plan sketch, parameter values, and three-dimensional response surface for instantaneous downstream valve closure in a looped-pipe network

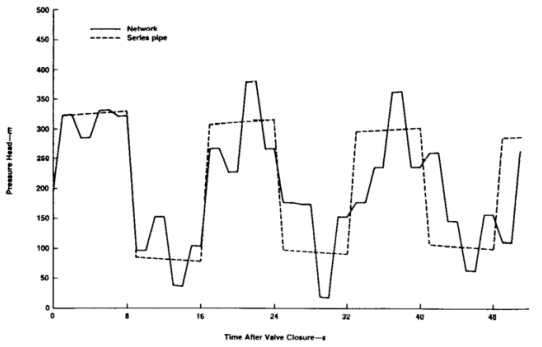

Figure 7. Variation in pressure head at the valve end for a simple series pipeline and a looped network

View Verification Case 21 Model

Verification Case 21

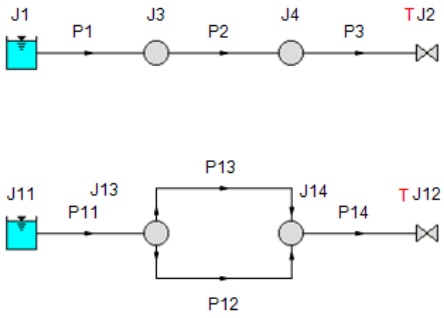

Karney, Bryan W and McInnis, Duncan, Transient Analysis of Water Distribution Systems, Journal AWWA, July 1990, pp. 62-70, Figures 5 -7

Verification Case 22

View Model Problem Statement

PRODUCT: AFT Impulse

TITLE: ImpVerify22.imp

REFERENCE: Liou, Jim C. P., Understanding Line Packing in Frictional Water Hammer, ASME, Journal of Fluids Engineering, August 2016, Vol. 138, Application Example

FLUID: Oil

ASSUMPTIONS: Closure is started at 20 seconds in both cases. Liou states valve Cv vs. time is known, but no curve is provided. It is assumed the valves close linearly over 60 or 180 seconds.

RESULTS:

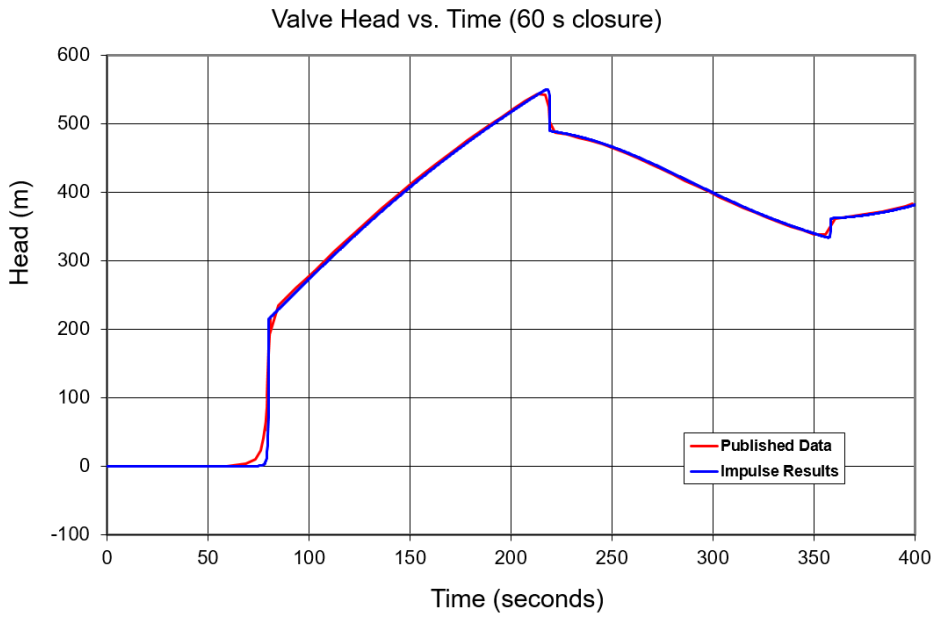

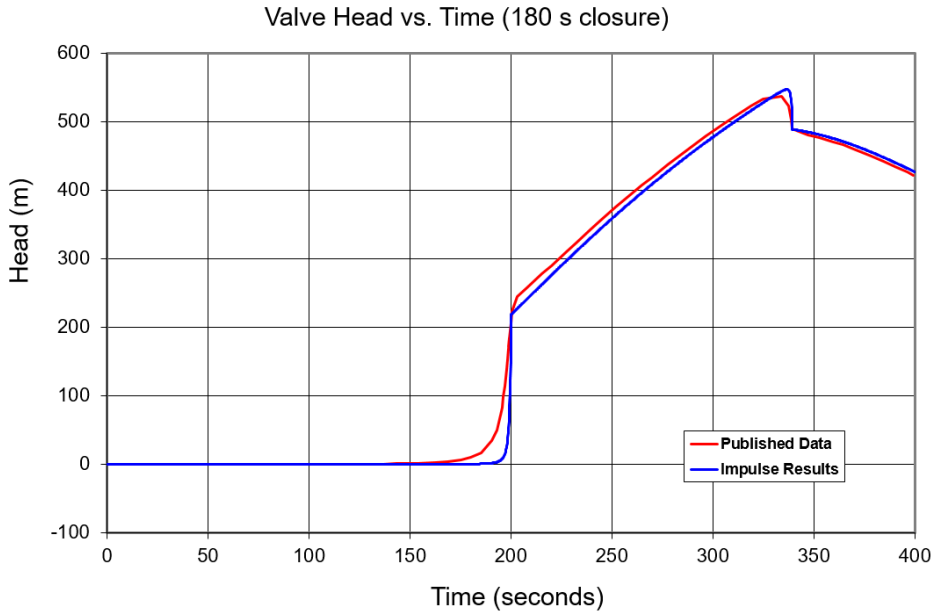

DISCUSSION:

Liou states "Since the valve head loss is negligible relative to the pipe frictional head loss, the effective valve closure time is much shorter than the physical closure times. Therefore, an instantaneous closure of this valve can be assumed". This is essentially correct as an instantaneous closure results in essentially the same maximum head as the longer closure profiles. This is typically true for long pipelines with long communication times and insignificant valve head loss. Cv profiles should not be considered negligible if the closure time is greater than communication time or if the valve has significant head loss compared to pipe friction (major losses).

List of All Verification Models

Verification Case 22 Problem Statement

Verification Case 22

Liou, Jim C. P., Understanding Line Packing in Frictional Water Hammer, ASME, Journal of Fluids Engineering, August 2016, Vol. 138, Application Example

Liou Title Page

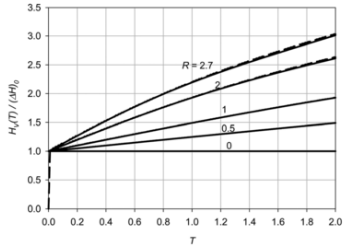

Fig. 8 Comparison between analytical (solid line) and numerical (dashed line) head at the valve after its sudden closure

It is seen that within the range of R of interest, the linear profile is a good approximation, especially for lower R. With this approximation,

$$\int_b^d (U(T'))^2 dT' = V^2(T)\frac{T}{3} \tag{24}$$

Using Eq. (20) for V_b, Eq. (21) for H_b, Eq. (24) for the integral, and setting V_d to zero, H_d can be solved from Eq. (22). After simplification, and denoting H_d as $H_V(2T)$, it can be established that

$$\frac{H_v(2T)}{(\Delta H)_0} = 1 + RT\left(1 - \frac{1}{3}\tanh^2\left(\frac{RT}{2}\right)\right) \quad \text{for} \quad 0 \le T \le 1 \tag{25}$$

Figure 8 compares the head at the closed valve from Eq. (25) with the results from numerical simulations between 0 and $2L/a$ s. It is seen that Eq. (25) yields a close approximation to the head rise at the closed valve.

It should be noted, because no assumption was made on how U vary along the C^+ characteristics, a valid numerical simulation can produce more accurate results than Eq. (25) can. Thus, Eq. (25) is not an alternative to a valid numerical simulation. However, Fig. 8 demonstrates that Eq. (25) is an option to quickly and directly compute the head rise at the valve with acceptable accuracy.

Accuracy of the Analytical Solution for Line Packing

Accurate numerical simulations to Eqs. (3) and (4) for the instantaneous valve closure transients were used to evaluate the accuracy of Eq. (25) and, separately, the strain energy approximation. For each R, subtract $(\Delta H)_0$ from the simulated head at the valve at $2L/a$ s and denote the result by W. The subtraction is needed because $(\Delta H)_0$ is a part of the simulated head at the valve but not a part of line packing. The % error of line packing at $T = 1$ from Eq. (25) is defined as

$$\%\ \text{error} = \frac{(H_v(2) - (\Delta H)_0) - W}{W} \cdot 100 \tag{26}$$

The % error for the strain energy approximation is defined in a similar fashion

$$\%\ \text{error strain energy} = \frac{\frac{1}{\sqrt{2}}\frac{fL}{D}\frac{V_0^2}{2g} - W}{W} \cdot 100 \tag{27}$$

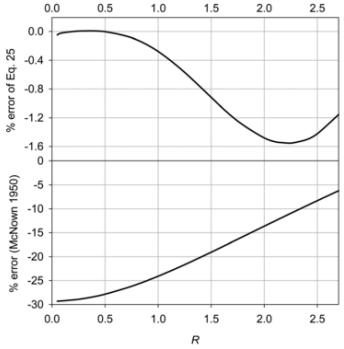

Fig. 9 The error of line packing estimation using Eq. (25) (top panel) and using the strain energy approximation (bottom panel)

Figure 9 shows the errors. The maximum error for Eq. (25) occurs at $R = 2.25$ where the line pack is underestimated by 1.55%. The error is negligible for small R. Equation (25) is quite an improvement of the strain energy approximation. The latter significantly underestimates the line packing.

Application Example

The example below shows how to apply Eq. (25). It also indicates the reasonableness of using an instantaneous valve closure to approximate valve closures with finite physical closure time for pipelines where the initial steady-state frictional head loss far exceeds the valve head loss prior to its closure. This is often the case for cross-country oil pipelines.

A 591 mm inside diameter pipe with a length of 80 km transports oil from a source tank with a fixed head to a delivery tank at 0 m of head. The pipeline system has a water hammer wave speed of 1150 m/s. At the discharge end of the pipeline is a motor operated control valve. The valve is a full-ported ball valve with a flow coefficient of 88,900 gpm at 100% stroke (i.e., wide open). The inherent valve characteristic (the flow coefficient versus % stroke curve) is known and used in the simulations described below.

Prior to its closure, the control valve is wide open, the velocity is 1.82 m/s, and the corresponding Darcy–Weisbach friction factor is 0.018. The control is closed with a constant motor speed in 60 and, separately, in 180 s. (Note that the round-trip travel time for water hammer waves is $2L/a$ or139 s. Thus these closure times are not very fast.) For both cases, the valve closure starts at 20 s. What are the maximum heads just upstream of the control valve?

With the given data, the pipeline frictional head loss at the initial steady state is 411 m and the head loss through the wide-open valve is 0.006 m. This valve head loss is small but realistic. Since the valve head loss is negligible relative to the pipe frictional head loss, the effective valve closure time is much shorter than the physical closure times. Therefore, an instantaneous closure of this valve can be assumed. This simplifies the problem considerably because the valve characteristics become irrelevant.

Using Eq. (5) with $\Delta V = -V_0 = -1.82$ m/s, $(\Delta H)_0 = 213.2$ m. Using Eq. (18), $R = 1.928$. With these values and using $T = 1$, Eq. (25) gives a maximum head of 547.9 m.

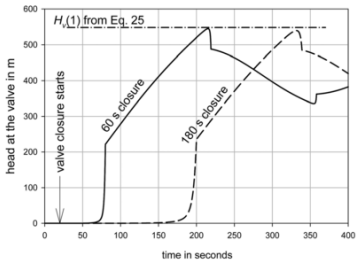

Fig. 10 The maximum head at the valve computed from Eq. (25) and the simulated head traces at the valve for 60 and 180 s closure

This maximum head is compared with the peaks of the simulated head traces at the valve in Fig. 10. The maximum head, which is based on an instantaneous valve closure, matches the simulated peak head for the 60-s valve closure very closely. The maximum head only slightly overpredicted the simulated peak head for the180-s valve closure despite the physical valve closure time is longer than $2L/a$ (139 s) second of the pipeline.

Summary and Conclusion

This study establishes the analytical solution for the attenuated front of velocity and head waves propagating upstream during the L/a s after a sudden valve closure. It also presents an analytical approximation to the head rise at the closed valve during the $2L/a$ s after the valve closure. The accuracy of the approximation is demonstrated. An example illustrates its usage to transients resulted from a discharge valve closure over different times. Although line packing is quantifiable by numerical simulations, the analytical solutions contribute to the understanding of the line packing phenomenon, and offer a simple and direct way to accurately compute the maximum pressure due to line packing without resorting to numerical methods or commercial numerical simulation software.

Acknowledgment

The author would like to thank Dr. E. Benjamin Wylie, Professor Emeritus of Civil and Environmental Engineering at the University of Michigan for several discussions on this subject.

Nomenclature

a = water hammer wave speed
D = pipe diameter
f = Darcy–Weisbach friction factor
g = gravitational acceleration
H = head
H_S = steady state head
H_U = head at the supply reservoir
H_V = head at the valve
L = pipe length
R = friction coefficient
t = time
T = dimensionless time
T' = dimensionless time between T and $2T$
V = discharge velocity
V_0 = steady state discharge velocity
W = accurately simulated line packing at $2L/a$ s
x = distance from the reservoir toward the valve
ΔH = amplitude of the head wave front
$(\Delta H)_0 = (a/g)V_0$
ΔV = amplitude of the velocity wave front

References

[1] Liou, C. P., and Wylie, E. B., 2016, "Water Hammer," *Handbook of Fluid Dynamics*, 2nd ed., R. W. Johnson, ed., CRC Press—Taylor & Francis Group, Boca Raton, FL, Chap. 25.
[2] Roberson, J. A., Crowe, C. T., and Elger, D. F., 2001, *Engineering Fluid Mechanics*, 7th ed., Wiley, New York.
[3] Houghtalen, R. J., Akan, A. O., and Hwang, N. H. C., 2010, *Fundamentals of Hydraulic Engineering Systems*, 4th ed., Pearson Higher Education, Inc., Upper Saddle River, NJ.
[4] Prasuhn, Al. L., 1987, *Fundamentals of Hydraulic Engineering*, Holt, Rinehart and Winston, New York.
[5] Wylie, E. B., and Streeter, V. L., 1993, *Fluid Transients in Systems*, Prentice Hall, Englewood Cliffs, NJ.
[6] Chaudhry, M. H., 1979, *Applied Hydraulic Transients*, Van Nostrand Reinhold Company, New York.
[7] Ziekle, W., 1968, "Frequency-Dependent Friction in Transient Pipe Flow," ASME J. Basic Eng., **90**(1), pp. 109–115.
[8] Szymkiewicz, R., and Mitosek, M., 2014, "Alternative Convolution Approach to Friction in Unsteady Pipe Flow," ASME J. Fluids Eng., **136**(1), p. 011202.
[9] Vardy, A. E., Brown, J. M. B., He, S., Ariyaratne, C., and Gorji, S., 2015, "Applicability of Frozen-Viscosity Models of Unsteady Wall Shear Stress," ASCE J. Hydraulic Eng., **141**(1), p. 04014064.
[10] Wahba, E. M., 2016, "On the Propagation and Attenuation of Turbulent Fluid Transients in Circular Pipes," ASME J. Fluids Eng., **138**(3), p. 031106.
[11] Meniconi, S., Duan, H. F., Brunone, B., Ghidaoui, M. S., Lee, P. J., and Ferrante, M., 2014, "Further Development in Rapidly Decelerating Turbulent Pipe Flow Modeling," ASCE J. Hydraulic Eng., **140**(7), p. 04014028.
[12] Bergant, A., Tijsseling, A. S., Vitkovsky, J. P., Covas, D. I. C., Simpson, A. R., and Lambert, M. F., 2008, "Parameters Affecting Water Hammer Wave Attenuation, Shape, and Timing—Part 2: Case Studies," IAHR J. Hydraulic Res., **46**(3), pp. 382–391.
[13] Brunone, B., Karney, B. W., Mecarelli, M., and Ferrante, M., 2000, "Velocity Profiles and Unsteady Pipe Friction in Transient Flow," J. Water Resour. Plann. Manage., **126**(4), pp. 236–244.
[14] Ghidaoui, M. S., Mansour, S. G. S., and Zhao, M., 2002, "Applicability of Quasi-Steady and Axisymmetric Turbulence Models in Water Hammer," ASCE J. Hydraulic Eng., **128**(10), pp. 917–924.
[15] Brunone, B., Ferrante, M., and Cacciamani, M., 2004, "Decay of Pressure and Energy Dissipation in Laminar Transient Flow," ASME J. Fluids Eng., **126**(11), pp. 928–934.
[16] Jung, B. S., Karney, B. W., Boulos, P. F., and Wood, D. J., 2007, "The Need for Comprehensive Transient Analysis of Distribution Systems," J. AWWA, **99**(1), pp. 112–123.
[17] Wood, D. J., Lingireddy, S., Boulos, P. F., Karney, B. W., and McPherson, D. L., 2005, "Numerical Methods for Modeling Transient Flows in Distribution Systems," J. AWWA, **97**(7), pp. 104–115.
[18] Meniconi, S., Brunone, B., Ferrante, M., Capponi, C., Carrettini, C. A., Chiesa, C., Segalini, D., and Lanfranchi, E. A., 2015, "Anomaly Pre-Localization in Distribution-Transmission Mains by Pump Trip: Preliminary Field Tests in the Milan Pipe System," J. Hydroinf., **17**(3), pp. 377–389.
[19] Ludwig, M., and Johnson, S. P., 1950, "Prediction of Surge Pressures in Long Oil Transmission Lines," Proc. API Div. Transp., **30**(5), pp. 62–70.
[20] Leslie, D. J., and Tijsseling, A. S., 2000, "Traveling Discontinuities in Water-hammer Theory – Attenuation Due to Friction," BHR Group 2000 Pressure Surges, Apr. 12–14, The Hague, The Netherlands, pp. 323–335.
[21] Gibson, A. H., 1948, *Hydraulics and Its Applications*, 4th ed., Constable and Company, Ltd., London.
[22] McNown, J. S., 1950, "Surges and Water Hammer," Proceedings of the Fourth Hydraulic Conference, Iowa Institute of Hydraulic Research, Jun. 12–15, H. Rouse, ed., Wiley, New York, Chapter VII.
[23] Ellis, J., 2008, *Pressure Transients in Water Engineering*, Thomas Telford Publishing, London.
[24] Liou, C. P., 1993, *Pipeline Variable Uncertainties and Their Effects on Leak Detectability*, American Petroleum Institute, Washington, DC.

View Verification Case 22 Model

Verification Case 22

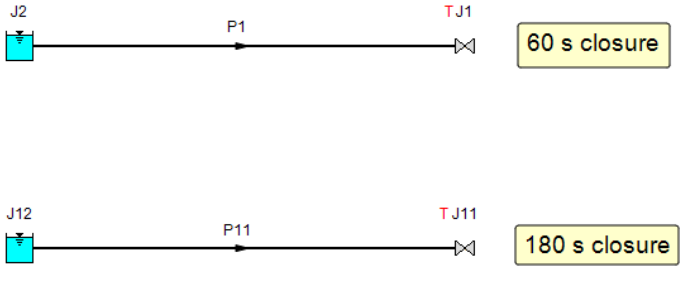

Liou, Jim C. P., Understanding Line Packing in Frictional Water Hammer, ASME, Journal of Fluids Engineering, August 2016, Vol. 138, Application Example